

# Meson-antimeson mixing

Ulrich Nierste<sup>a</sup>

<sup>a</sup>Karlsruhe Institute of Technology (KIT), Institute for Theoretical Particle Physics (TTP), Wolfgang-Gaede-Straße 1, 76131 Karlsruhe, Germany

© 20xx Elsevier Ltd. All rights reserved.

## Contents

Nomenclature	2
Objectives	2
1 Introduction	2
2 $K-\bar{K}$ mixing, discrete symmetries, and the Cabibbo-Kobayashi-Maskawa matrix	4
3 $B-\bar{B}$ mixing, flavor oscillations, $CP$ asymmetries, and the unitarity triangle	8
4 $D-\bar{D}$ mixing	15
5 Time evolution of neutral mesons and associated $CP$ -violating quantities	16
5.1 Time evolution	16
5.2 $\Delta M$ , $\Delta\Gamma$ , and $CP$ violation in mixing	20
5.3 Mixing-induced $CP$ asymmetries, $CP$ violation in $K-\bar{K}$ mixing, and time-dependence of exclusive decays	24
6 Meson-antimeson mixing in the Standard Model and beyond	29
6.1 Yukawa interaction as the origin of flavor violation	29
6.2 Effective $ \Delta B  = 2$ hamiltonian and Standard-Model prediction for $\Delta M_{d,s}$	31
6.3 Effective $ \Delta B  = 1$ hamiltonian and Standard-Model predictions for $\Delta\Gamma_{d,s}$ and $a_{fs}^{d,s}$	35
6.4 Effective hamiltonians for $K-\bar{K}$ mixing with predictions for $\epsilon_K$ and $\Delta M_K$ , overall picture of the UT	40
7 Conclusions	44
Acknowledgments	44
References	44

## Abstract

Meson-antimeson transitions are flavor-changing neutral current processes in which the strangeness, charm, or beauty quantum number changes by two units. In the Standard Model (SM) these transitions originate from box diagrams with two W bosons. They permit the preparation of time-dependent, oscillating quantum states which are superpositions of a meson and its antimeson. By studying their decays one gains information on both the meson-antimeson mixing amplitude itself and the decay amplitude involved, in particular one can measure complex phases quantifying the violation of charge-parity ( $CP$ ) violation. I present a comprehensive overview on the topic, starting with phenomenological presentations of  $K-\bar{K}$ ,  $B_d-\bar{B}_d$ ,  $B_s-\bar{B}_s$ , and  $D-\bar{D}$  mixing and their impact on the formulation of the SM. Highlights are the discovery of the violation of  $CP$  and other discrete symmetries, the prediction of the charm quark and its mass, the prediction of a heavy top quark, and the confirmation of the Kobayashi-Maskawa mechanism of  $CP$  violation. Further sections cover the theoretical formalism needed to describe meson-antimeson mixing and to calculate observables in terms of the fundamental parameters of the SM or hypothetical theories of new physics. I discuss the unitarity triangle of the Cabibbo-Kobayashi-Maskawa matrix, which is used to visualize how various  $CP$ -violating and  $CP$ -conserving quantities combine to probe the SM. I describe the emergence of precision flavor physics and the role of reliable theory calculations to link  $K-\bar{K}$  mixing to  $B_d-\bar{B}_d$  mixing, which was essential to confirm the Kobayashi-Maskawa mechanism, and present the current status of theory predictions. Today, the focus of the field is on physics beyond the SM, because meson-antimeson mixing amplitudes are sensitive to virtual effects of heavy particles with masses which are several orders of magnitude above the reach of current particle colliders.

**Keywords:** weak interaction, flavor physics, meson-antimeson mixing,  $CP$  violation, BSM physics

## 2 Meson-antimeson mixing

### Nomenclature

$\alpha, \beta, \gamma$	angles of the unitarity triangle
$a_{fs}$	$CP$ asymmetry in flavor-specific decays
$A_{CP}^{\text{dir}}(M \rightarrow f)$	direct $CP$ asymmetry in $M \rightarrow f$
$A_{CP}^{\text{mix}}(M \rightarrow f)$	mixing-induced $CP$ asymmetry in $M \rightarrow f$
$B$	neutral $b$ -flavored meson $B_d$ or $B_s$ , beauty (a.k.a. bottom) quantum number
BSM	beyond Standard Model
C	charm quantum number, charge conjugation
CKM	Cabibbo-Kobayashi-Maskawa
$CP$	charge-parity conjugation
$D$	neutral $D$ meson
$\delta_{KM}$	Kobayashi-Maskawa phase
$\Delta\Gamma$	width difference between the two mass eigenstates
$\Delta M$	mass difference between the two mass eigenstates
$F$	flavor quantum number, $F = B, C, S, U, D$
$G_F$	Fermi constant
$\Gamma_{12}$	off-diagonal matrix element of the meson-antimeson decay matrix
$g_w$	weak coupling constant
HQE	Heavy Quark Expansion
K	neutral Kaon
$\lambda, A, \rho, \eta$	Wolfenstein parameters
M	any of $K, D, B_d$ , or $B_s$
$M_{12}$	off-diagonal matrix element of the meson-antimeson mass matrix
OPE	Operator Product Expansion
P	parity
QCD	quantum chromodynamics
$(\bar{\rho}, \bar{\eta})$	apex of the standard unitarity triangle
S	strangeness quantum number
SM	Standard Model
T	time reversal
$\tau$	lifetime
UT	unitarity triangle
$V$	CKM matrix
$V_C$	Cabibbo matrix
QFT	quantum field theory

### Objectives

1. The text intends to be a comprehensive introduction into  $K-\bar{K}$ ,  $B_d-\bar{B}_d$ ,  $B_s-\bar{B}_s$ , and  $D-\bar{D}$  mixing for people studying any of these topics in experiment or theory. It shall convey the special knowledge needed to interpret an experimental analysis or to understand the concepts of a theoretical calculation.
2. Furthermore, the text comprises an overview from a larger perspective and is self-contained, so that it may serve as a basis for a topical course or as material for the preparation for a PhD exam.
3. In addition, the text aims at giving a detailed and accurate presentation of the historical developments of the field, from the understanding of  $K-\bar{K}$  mixing in the 1950s to the study of  $B-\bar{B}$  and  $D-\bar{D}$  mixing in modern high-statistics flavor experiments. I show how the interplay of excellent experimental achievements and innovative theoretical ideas lead to landmark results which shaped the Standard Model of Elementary Particle Physics.
4. Finally, I elucidate the importance of the precision calculations which were needed to link  $K-\bar{K}$  mixing to  $B_d-\bar{B}_d$  mixing to confirm the Kobayashi-Maskawa interpretation of  $CP$  violation and, today, allow us to precisely determine fundamental parameters of the Standard Model's Yukawa sector and to constrain the parameter spaces of new-physics models.

## 1 Introduction

In this introductory section the basic notation and the fundamental concepts of meson-antimeson mixing are introduced, mostly in a qualitative way, with quantitative details relegated to later sections.

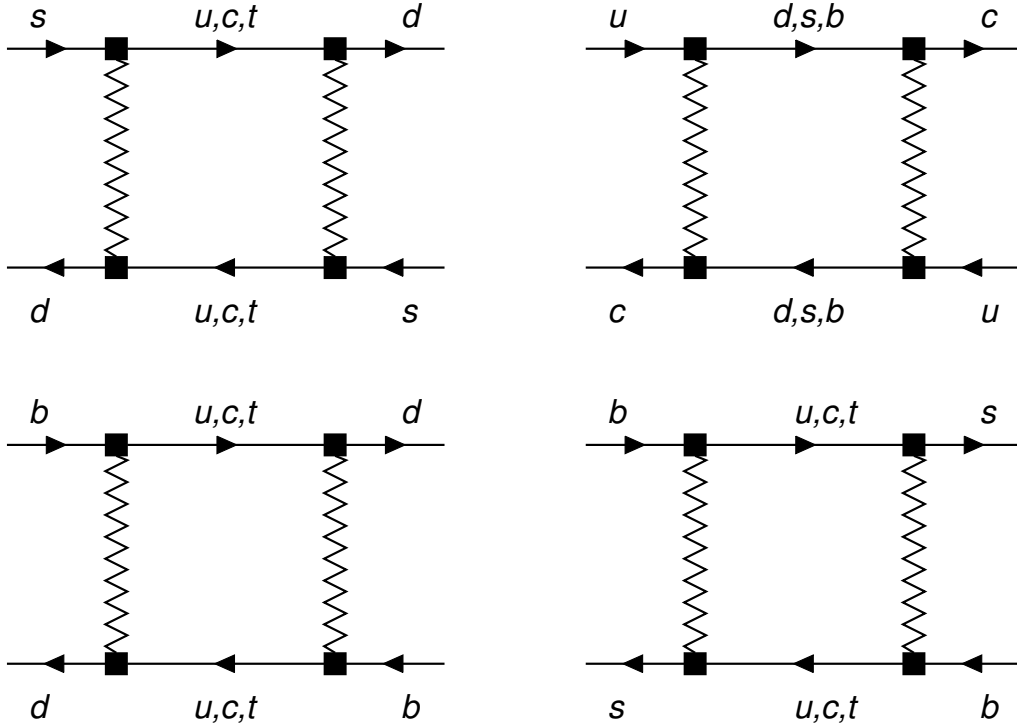


**Fig. 1** Box diagrams for  $K-\bar{K}$ ,  $D-\bar{D}$ ,  $B_d-\bar{B}_d$  and  $B_s-\bar{B}_s$  mixing with zigzag lines representing W bosons. The diagrams show the transition from antimeson  $\bar{M}$  meson entering the diagram from the left into meson  $M$  leaving the diagram to the right. For each process there is also a second box diagram, obtained by a  $90^\circ$  rotation.

Mesons can be labeled by flavor quantum numbers, which characterize the quark-antiquark pair from which they are formed. For example, a  $D_s^+$  meson has the flavor quantum numbers  $C = 1$  and  $S = 1$ , which denote charm and strangeness, respectively. One shortly writes  $D_s^+ \sim c\bar{s}$  to indicate that  $D_s^+$  has the same flavor quantum numbers as the indicated quark-antiquark pair. We further need the beauty quantum number  $B$  and, for completeness, also introduce  $D$  and  $U$  for  $\bar{d}$  and  $u$  quark. The flavor quantum numbers are +1 for up-type quarks and -1 for down-type quarks, with opposite signs for the antiquarks. When referring to a generic flavor quantum number we write  $F$ , i.e.  $F = B, C, S, U$ , or  $D$ . While the strong interaction, described by quantum chromodynamics (QCD), respects the flavor quantum numbers, the weak interaction can change them. The most prominent examples for flavor-changing transitions are weak decays like  $D_s^+ \rightarrow K^+\pi^0$ ; in this example the  $C$  quantum number changes from  $C = 1$  to  $C = 0$  while  $U$  increases by one unit. Weak decays are  $|\Delta F| = 1$  processes mediated by the exchange of one  $W$  boson. But the Standard Model (SM) of Elementary Particle Physics also permits  $|\Delta F| = 2$  transitions, through Feynman diagrams with two  $W$  bosons. This feature makes any of the following four neutral mesons,

$$K \sim \bar{s}d, \quad D \sim \bar{c}u, \quad B_d \sim \bar{b}d, \quad B_s \sim \bar{b}s, \quad (1)$$

mix with its respective antimeson,

$$\bar{K} \sim s\bar{d}, \quad \bar{D} \sim \bar{c}\bar{u}, \quad \bar{B}_d \sim b\bar{d}, \quad \bar{B}_s \sim b\bar{s}. \quad (2)$$

The Feynman diagrams for the four possible meson-antimeson mixing amplitudes are shown in Fig. 1. Meson-antimeson mixing are examples of *flavor-changing neutral current (FCNC)* processes, in which a quark morphs into another quark with the same electric charge but different flavor. In the SM FCNC processes are rare, because they are forbidden at tree-level. Meson-antimeson mixing has two important implications:

- i. The flavor eigenstates  $|M\rangle$  and  $|\bar{M}\rangle$  corresponding to the mesons in Eqs. (1) and (2) are not the physical mass eigenstates and do not obey exponential decay laws. Instead the mass eigenstates are linear combinations of  $|M\rangle$  and  $|\bar{M}\rangle$ . For  $K$ ,  $\bar{K}$  the mass eigenstates are  $|K_{\text{short}}\rangle$  and  $|K_{\text{long}}\rangle$ , with the subscript referring to their lifetime  $\tau$ . Since  $\tau_{K_{\text{long}}} \gg \tau_{K_{\text{short}}}$  it is natural to use the mass eigenstates to describe observables in Kaon physics: For sufficiently large times the  $K_{\text{short}}$  component of a neutral Kaon has decayed away and one can study  $K_{\text{long}}$  decays, while for times  $t \sim \tau_{K_{\text{short}}}$  decays of the  $K_{\text{short}}$  component of the Kaon are dominant.
- ii. If we produce a meson  $M$  at some time  $t = 0$ , the corresponding state will evolve into a superposition of  $M$  and  $\bar{M}$  at later times  $t > 0$ , leading to meson-antimeson oscillations. This property is used in  $D$ ,  $B_d$ , and  $B_s$  physics, where the lifetime differences of the mass eigenstates is small.

## 4 Meson-antimeson mixing

As an important consequence, meson-antimeson mixing permits the study of a *quantum-mechanical superposition of a particle with its antiparticle*. This feature gives access to the relative complex phase between the  $M \rightarrow f$  and  $\bar{M} \rightarrow f$  decay amplitudes for final states  $f$  into which both  $M$  and  $\bar{M}$  can decay.

To calculate the two mass eigenstates in terms of the flavor eigenstates  $M$  and  $\bar{M}$  one must solve a quantum-mechanical two-state system by diagonalising a  $2 \times 2$  matrix. The off-diagonal elements of this matrix are calculated from the box diagrams in Fig. 1; this calculation will be explained in detail in this chapter. As a consequence of meson-antimeson mixing, the eigenstates differ in their masses and decay width. One may label the eigenstates by their lifetimes, as we did above in (i) for the neutral Kaons. While  $\Gamma(K_{\text{short}}) = 1/\tau(K_{\text{short}}) > \Gamma(K_{\text{long}}) = 1/\tau(K_{\text{long}})$  by definition, the sign of the  $K_{\text{long}} - K_{\text{short}}$  mass difference is not fixed and must be determined by measurement. In  $B_{d,s}$  and  $D$  physics one commonly labels the eigenstates by their masses as  $|M_H\rangle$  and  $|M_L\rangle$  with the labels referring to “heavy” and “light”. With this definition

$$\Delta M \equiv M_H - M_L > 0, \quad \text{while} \quad \Delta\Gamma \equiv \Gamma_L - \Gamma_H \quad (3)$$

can have either sign. Here  $M_{H,L}$  and  $\Gamma_{H,L}$  denote masses and width of the eigenstates.<sup>1</sup> For neutral Kaons the sign of  $\Delta\Gamma/\Delta M$  is firmly established, so that today we know that

$$|K_H\rangle = |K_{\text{long}}\rangle, \quad |K_L\rangle = |K_{\text{short}}\rangle. \quad (4)$$

(I refrain from employing the usual notation  $K_{L,S}$  for  $K_{\text{long,short}}$ , because I use “L” for “light” and the lighter Kaon happens to be  $K_L = K_{\text{short}}$ .) Note the choice of the sign of  $\Delta\Gamma$  in Eq. (3). This choice is motivated by aiming at positive numbers for both  $\Delta M$  and  $\Delta\Gamma$  for neutral Kaons. With this definition also the SM expectation for  $\Delta\Gamma$  for the  $B - \bar{B}$  systems is positive and this is experimentally confirmed for  $B = B_s$ , while no data are yet available for  $B = B_d$ .

We will also need the average mass and average width,

$$M = \frac{M_H + M_L}{2}, \quad \Gamma = \frac{\Gamma_H + \Gamma_L}{2} \quad (5)$$

and note that the *average lifetime* is defined as  $\tau \equiv 1/\Gamma$ , that is, it is *not* the average of  $\tau(M_H)$  and  $\tau(M_L)$ . The Particle Data Table lists the such defined average masses and lifetimes for the neutral mesons except for  $K_{\text{long}}$  and  $K_{\text{short}}$ , for which the individual lifetimes are quoted [1].

The mass eigenstates follow exponential decay laws,

$$|M_{L,H}(t)\rangle = e^{-iM_{L,H}t - \Gamma_{L,H}t/2} |M_{L,H}\rangle \quad \text{with} \quad |M_{L,H}(0)\rangle = |M_{L,H}\rangle. \quad (6)$$

Here the oscillatory term in the exponent with the meson mass  $M_{L,H}$  is the usual factor time-evolution factor  $\exp(-iEt)$  with  $E = M_{L,H}$  in the meson rest frame; here and throughout this chapter I use natural units with  $\hbar = c = 1$ . We can use  $|M_H(t)\rangle, |M_L(t)\rangle$  as a basis to express any neutral meson state (i.e. any chosen superposition of  $|M\rangle$  and  $|\bar{M}\rangle$ ),

$$|M_{\text{any}}\rangle = \alpha|M_L(t)\rangle + \beta|M_H(t)\rangle = e^{-iMt - \Gamma t/2} [\alpha e^{i\Delta Mt/2 - \Delta\Gamma t/4} |M_L\rangle + \beta e^{-i\Delta Mt/2 + \Delta\Gamma t/4} |M_H\rangle], \quad (7)$$

where I have used Eqs. (3) and (5) as  $M_{H,L} = M \pm \Delta M/2$  and  $\Gamma_{H,L} = \Gamma \mp \Delta\Gamma/2$ . The first factor in Eq. (7) is just the time evolution of a particle state which does not mix, such as a charged-meson state. The term in square brackets shows that  $\Delta M \neq 0$  introduces oscillatory terms and that further  $\Delta\Gamma \neq 0$  changes the familiar exponential decay law to a two-exponential formula. For the cases that  $|M_{\text{any}}\rangle = |M\rangle$  or  $|M_{\text{any}}\rangle = |\bar{M}\rangle$  we will learn that  $|\alpha| \simeq |\beta| \simeq 1/\sqrt{2}$ . Now the probability to observe  $M_{\text{any}}$  as  $M$  at time  $t$  is given by  $|\langle M | M_{\text{any}} \rangle|^2$  which involves oscillatory terms like  $\sin^2(\Delta Mt/2) = (1 - \cos(\Delta Mt))/2$  and  $\sin(\Delta Mt/2) \cos(\Delta Mt/2) = (\sin(\Delta Mt))/2$ , so that the oscillation frequency in observable quantities is  $\Delta M$  and not  $\Delta M/2$ . Likewise  $|\langle M | M_{\text{any}} \rangle|^2$  and other observables involve  $\sinh(\Delta\Gamma t/2)$  and  $\cosh(\Delta\Gamma t/2)$ . The detailed expressions for the time evolution of states and observables will be derived later in Sec. 5.

This chapter is organized as follows: In Secs. 2–4 I will discuss  $K - \bar{K}$ ,  $B - \bar{B}$ , and  $D - \bar{D}$  mixing with emphasis on the phenomenology and the historical evolution of the field. This includes the presentation of theoretical and experimental landmark results. In the context of these discussions I will derive the necessary theoretical formulae avoiding lengthy derivations as much as possible. Technical details are relegated to Secs. 5 and 6. In Sec. 5 I derive the formulae for the time evolution of the neutral mesons, the relation between flavor and mass eigenstates, and expressions linking these to physical observables. Sec. 6 presents the origin of flavor mixing in the SM and beyond, and discusses how meson-antimeson mixing contributes to constrain—or eventually discover—new physics. Finally, Sec. 7 contains the Conclusions.

## 2 $K - \bar{K}$ mixing, discrete symmetries, and the Cabibbo-Kobayashi-Maskawa matrix

In this section I describe  $K - \bar{K}$  mixing and the historical role which this process played to shape the SM, with emphasis on the discrete symmetries parity, charge conjugation, and time reversal. I use  $K - \bar{K}$  mixing to exemplify general concepts of meson-antimeson mixing and to introduce basic concepts of flavor violation in the SM.

---

<sup>1</sup>Using the same notation for a generic meson  $M$  and its mass should not lead to confusion.

Historically, for three decades  $K - \bar{K}$  mixing was the only known meson-antimeson mixing process.  $K - \bar{K}$  mixing was predicted in 1955 by Gell-Mann and Pais from the following observations [2]:

- i. The decays  $K \rightarrow \pi^- e^+ \nu_e$  and  $\bar{K} \rightarrow \pi^+ e^- \bar{\nu}_e$  have shown that there are two neutral Kaons. There was confidence in a  $\Delta S = \Delta Q$  rule linking the changes in strangeness  $S$  and electric charge  $Q$  of the hadron in semileptonic decays. (In modern language: It was (correctly) assumed that the lepton charge *tags*  $S$ .) Thus it was clear that  $K$  and  $\bar{K}$  are distinct particles characterized by  $S = 1$  and  $S = -1$ , respectively.
- ii. The observation that neutral Kaons decay to  $\pi\pi$  states implies the possibility of  $K \leftrightarrow \pi\pi \leftrightarrow \bar{K}$  transitions, and the principles of quantum physics dictate that  $|K\rangle$  and  $|\bar{K}\rangle$  must mix. (In modern language: A virtual  $\pi\pi$  loop permits a non-zero  $K \rightarrow \bar{K}$  transition amplitude.) With a symmetry argument Gell-Mann and Pais concluded that the mass eigenstates are not close to  $|K\rangle$  or  $|\bar{K}\rangle$ , but instead coincide with maximally mixed states  $(|K\rangle \pm |\bar{K}\rangle)/\sqrt{2}$ . I discuss their arguments a few paragraphs below in the context of discrete symmetries. An important prediction of Ref. [2] was the existence of  $K_{\text{long}}$ , for which soon after evidence [3] and observation [4] were reported. To facilitate the study of the original literature I remark that an early notation was  $\theta^0 \equiv K$ ; later  $K_1^0$  and  $K_2^0$  were introduced to denote  $K_{\text{short}}$  and  $K_{\text{long}}$ , respectively.

Both meson-antimeson mixing and the  $M$  decays involve the weak interaction mediated by the  $W$  boson, which is the only SM particle with flavor-violating couplings. The corresponding piece of the SM Lagrangian for quarks reads

$$L_W = \frac{g_w}{\sqrt{2}} \sum_{j,k=1,2,3} \left[ V_{jk} \bar{u}_{jL} \gamma^\mu d_{kL} W_\mu^+ + V_{jk}^* \bar{d}_{kL} \gamma^\mu u_{jL} W_\mu^- \right]. \quad (8)$$

Here  $g_w$  is the weak coupling constant and I have used the notations  $(d_1, d_2, d_3) = (d, s, b)$  and  $(u_1, u_2, u_3) = (u, c, t)$ .  $V$  is a unitary  $3 \times 3$  matrix,

$$V = \begin{pmatrix} V_{ud} & V_{us} & V_{ub} \\ V_{cd} & V_{cs} & V_{cb} \\ V_{td} & V_{ts} & V_{tb} \end{pmatrix}, \quad (9)$$

the *Cabibbo-Kobayashi-Maskawa (CKM) matrix*. We can decompose any four-component Dirac spinor field  $\psi(x)$  as  $\psi(x) = \psi_L(x) + \psi_R(x)$  with the subscripts ‘‘L’’ and ‘‘R’’ referring to left and right chirality, respectively. The parity transform  $P$  flips the signs of the spatial components of the four-vector  $x$  as  $\vec{x} \rightarrow -\vec{x}$  and maps Nature onto a fictitious mirror-world.  $P$  also exchanges  $\psi_L(x) \leftrightarrow \psi_R(x)$  and the  $W$  interactions in Eq. (8) do not involve the right-handed components of the quark spinor fields  $u_{jL}(x)$  and  $d_{kL}(x)$  at all. This feature is called *maximal parity violation*. Until 1956 it was believed that  $P$  is a good symmetry of Nature, but the observation that a Kaon can decay into two-pion states with parity quantum number  $P = +1$  as well as three-pion states with parity quantum number  $P = -1$  lead Lee and Yang to the conclusion that the weak interaction violates parity [5]. By contrast, the strong and electromagnetic interactions obey parity symmetry.

There are three fundamental discrete symmetries which are useful to characterize interactions within and beyond the SM; apart from  $P$  these are the *charge conjugation* ( $C$ ) and *time reversal* ( $T$ ) symmetries.  $C$  maps particles onto antiparticles and vice versa or Nature onto a fictitious antiworld. More precisely,  $C$  maps a spinor field  $\psi(x)$  which destroys a fermion and creates an antifermion onto the field  $\psi^c(x)$  which instead destroys an antifermion and creates a fermion.  $\psi^c(x)$  is calculated from the adjoint spinor field  $\bar{\psi} = \psi^\dagger \gamma^0$  (with the Dirac matrix  $\gamma^0$ ), but we do not need the explicit form of  $\psi^c(x)$  in this chapter. As an important feature,  $C$  also flips the chirality, e.g. if  $\psi = \psi_L$  is left-handed, then  $\psi^c = \psi_L^c = (\psi^c)_R$  is right-handed. Thus the maximal  $P$  violation in Eq. (8) implies also maximal  $C$  violation. In 1956 nothing was known about quarks and the role of quark currents in meson decays, but it was clear that in (semi-)leptonic decays  $P$  violation implies  $C$  violation [6].<sup>2</sup> Still no conclusion was drawn on  $C$  violation in hadronic weak decays or  $K - \bar{K}$  mixing and there was no consensus on the question for a long time.

Since more than five decades studies of meson-antimeson mixing are instrumental to explore  $CP$  violation. The  $CP$  transformation is a consecutive application of  $C$  and  $P$ . The order in which the operations are carried out does not matter, i.e.  $C$  and  $P$  commute.  $CP$  is intimately related to the time reversal operation  $T$  which maps Nature onto a fictitious world in which time goes backwards.  $T$  is better described as a reversal of particle motion, to study  $T$  one could compare a scattering process  $A + B \rightarrow C + D$  with  $C + D \rightarrow A + B$ , but in practice one studies the violation of the associated quantum number  $T = \pm 1$  in a suitable process or identifies  $T$ -odd observables, just as one does in the study of  $P$  violation. The famous CPT theorem, states that any local Poincaré-invariant quantum field theory (QFT) is invariant under the successive application of  $C$ ,  $P$ , and  $T$  (in any order) [8–10]. That is, if we take a video of some physical process, it will be indistinguishable from the video of the corresponding process with all particles exchanged by their antiparticles shown backwards in a mirror. Thus under the very wide prerequisites of the CPT theorem  $CP$  violation is identical to  $T$  violation. It is easier to work with  $CP$  rather than  $T$ , because  $CP$  is a unitary operation on quantum fields and states, while  $T$  is anti-unitary, meaning that it combines a unitary transformation with a complex conjugation.

In their prediction of  $K - \bar{K}$  mixing and the existence of  $K_{\text{long}}$  in Ref. [2] Gell-Mann and Pais assumed that  $C$  is a good symmetry and concluded that  $|K_{\text{short}}\rangle$  and  $|K_{\text{long}}\rangle$  must be eigenstates of  $C$  with opposite quantum numbers, because the hamiltonian  $H$  and the  $C$  operator must have common eigenstates if  $[H, C] = 0$ . Ironically, today we know that  $C$  is maximally broken, but their argument applies as well for  $CP$  which is almost a good symmetry for the  $K - \bar{K}$  system: If we assume that  $K_{\text{long}}$  is  $CP$ -odd and that further the weak decay process obeys the  $CP$  symmetry, the decay  $K_{\text{long}} \rightarrow \pi\pi$  (with a pair of neutral or charged pions) into a  $CP$ -even final state is forbidden. Instead the dominant  $K_{\text{long}}$  decay modes involve three pions and the small phase space suppresses the decay rate to a level that  $\tau_{K_{\text{long}}} \sim 500 \times \tau_{K_{\text{short}}}$ .

<sup>2</sup>The seminal paper by Wu et al. [7] mentions the observation of both  $P$  and  $C$  violation in an angular asymmetry in  $\beta$  decay and Ref. [7] does so for  $\pi^+ \rightarrow \mu^+ [\rightarrow e^+ 2\nu] \nu$ .

## 6 Meson-antimeson mixing

The width difference  $\Delta\Gamma_K$  in the  $K - \bar{K}$  system is an unspectacular quantity, it is essentially equal to  $\Gamma_{\text{short}}$ , which in turn is completely dominated by  $K_{\text{short}} \rightarrow \pi\pi$  decays. The decay rates of  $K_{\text{short}} \rightarrow \pi^+\pi^-$  and  $K_{\text{short}} \rightarrow \pi^0\pi^0$  cannot be reliably calculated from first principles. Experimentally we have [1]

$$\Delta\Gamma_K^{\text{exp}} = (7.338 \pm 0.003) \mu\text{eV} = (11.149 \pm 0.005) \cdot 10^{-3} \text{ ps}^{-1}. \quad (10)$$

Already in 1958 the time evolution of neutral kaons was used for a measurement of  $|\Delta M_K|$  [11] to find  $|\Delta M_K/\Gamma_{\text{short}}| \sim 1$  [11]. This reference plots a likelihood function, but does not quote an error on the measurement. A later measurement employing the idea to regenerate  $K_{\text{short}}$ 's from a  $K_{\text{long}}$  beam passing through matter found [12] found  $|\Delta M_K/\Gamma_{K_{\text{short}}}| < 1.1$  at 95% C.L., preferring values smaller than 1. Today we know [1]

$$\Delta M_K = (3.476 \pm 0.006) \mu\text{eV} = (5.281 \pm 0.009) \cdot 10^{-3} \text{ ps}^{-1}. \quad (11)$$

The regenerator method also permitted to determine the sign of  $\Delta M_K/\Delta\Gamma_K$ .

Already in 1958 S. Weinberg estimated that  $CP$  violation in  $K_{\text{long}}$  decays must be smaller than 1% and concluded “Probably it will be some time before experiments are performed which are capable of detecting such small charge asymmetries.” [13]. The discovery of  $CP$  violation had to wait until 1964, when Christenson, Cronin, Fitch, and Turlay discovered the decay  $K_{\text{long}} \rightarrow \pi^+\pi^-$  and concluded that  $CP$  is violated at the permille level in  $K - \bar{K}$  mixing [14]. Their grant proposal was primarily aiming at a better measurement of  $K_{\text{short}}$  regeneration, but further mentions “Other results to be obtained will be a new and much better limit for the partial rate of  $K_2^0 \rightarrow \pi^+\pi^-$ ” and the authors expect their apparatus to “set a limit of about one in a thousand for the partial rate of  $K_2 \rightarrow \pi\pi$  in one hour of operation.” The experimental result—a discovery rather than a limit—was interpreted as the discovery of  $CP$  violation in the  $K - \bar{K}$  mixing amplitude, i.e. in a  $|\Delta S| = 2$  process, and subsequent theory papers shared that view, because models attempting to explain the measurement with *direct CP violation*, i.e.  $K \rightarrow \pi^+\pi^-$  and  $\bar{K} \rightarrow \pi^+\pi^-$  amplitudes of different magnitude, were considered disfavoured by other measurements [15]. Nevertheless, Refs. [16, 17] ascribed the  $CP$  violation to the weak  $|\Delta S| = 1$  amplitudes with Ref. [17] exploiting the  $K \leftrightarrow \pi\pi \leftrightarrow \bar{K}$  mechanism of Ref. [2] to generate  $CP$  violation in the  $|\Delta S| = 2$   $K - \bar{K}$  mixing amplitude. Yet the connection to the weak interaction was not obvious at all at the time, recall that there was no SM yet (and clearly nothing was known about box diagrams). In Ref. [18] it was speculated that instead the electromagnetic interaction of hadrons violates  $C$  and  $T$ . Furthermore, the authors of Ref. [19] decomposed the hamiltonian as  $H_G + H_F$  with  $H_G$  comprising “the usual weak interaction which ... is invariant under  $CP$ ” and further describing  $H_F$  as “a new interaction which does not conserve  $CP$ ”. The paper discusses the three cases that  $H_F$  contains  $\Delta S = 0$ ,  $|\Delta S| = 1$ , and  $|\Delta S| = 2$  interactions, and the third possibility, called *superweak* model has been a benchmark model which the SM was compared to for a long time.<sup>3</sup> The 1965 status of the field is well-described in the talk by Prentki in Ref. [23]. This talk and the summary talk by Salam also show that the situation with  $C$  violation was not clear at the time.

The landmark result of Ref. [14] was the branching ratio

$$B(K_{\text{long}} \rightarrow \pi^+\pi^-) = (2.0 \pm 0.4) \cdot 10^{-3}. \quad (12)$$

Today's world average is [1]

$$B(K_{\text{long}} \rightarrow \pi^+\pi^-) = (1.967 \pm 0.010) \cdot 10^{-3}. \quad (13)$$

The further interpretation of this result needs the theoretical machinery of Sec. 5 and is relegated to later sections of this chapter.

In the SM FCNC processes can only be studied in a meaningful way since the introduction of the charm quark field by Glashow, Iliopoulos, and Maiani in 1970 [24]. The old three-quark version of the SM involved the FCNC coupling  $\bar{s}_L \gamma^\mu d_L Z_\mu$  of the  $Z$  boson, while the new four-quark model, treating two SU(2) doublets  $(u_L, d_L)^T$  and  $(c_L, s_L)^T$  equally, lead to flavor-conserving  $Z$  couplings. This feature is called *tree-level GIM mechanism*. The authors were guided by the three-flavor-SM prediction of an unduly large  $K - \bar{K}$  mixing as well as  $K_{\text{long}} \rightarrow \mu^+\mu^-$  and  $K^+ \rightarrow \pi^+ e^+ e^-$  decay amplitudes, in contradiction to experiment. In the four-quark model  $K - \bar{K}$  mixing involves the box diagram of Fig. 1 with all four combinations of  $u$  and  $c$  quarks on the two internal quark lines. In the four-quark model,  $V$  in Eq. (9) reduces to the  $2 \times 2$  Cabibbo matrix  $V_C$  which is the upper left sub-matrix of  $V$ . The unitarity of  $V_C$  makes the  $K - \bar{K}$  mixing amplitude vanish exactly in the limit  $m_c = m_u$  of equal up and charm quark masses. In this limit the box diagram is identical for all four combinations of  $u$  and  $c$  quarks on the internal lines and the CKM elements combine to  $(V_{us} V_{ud}^* + V_{cs} V_{cd}^*)^2$ , which vanishes because a unitary  $2 \times 2$  matrix satisfies  $V_{us} V_{ud}^* = -V_{cs} V_{cd}^*$ . Setting  $m_u = 0$  and keeping  $m_c \neq 0$  one finds that the  $K - \bar{K}$  mixing amplitude is *GIM-suppressed* by a factor of  $m_c^2/M_W^2 \sim 10^{-4}$ , where  $M_W$  is the  $W$  boson mass. Details on the calculation will be presented in Sec. 6. The suppression by factors  $m_c^2/M_W^2$  or  $m_c^2/M_W^2 \ln(m_c^2/M_W^2)$  is a common feature of Kaon FCNC processes called *loop-level GIM mechanism*. In summary, the GIM mechanisms have a dramatic effect on the  $K - \bar{K}$  mixing, reducing the prediction of the tree amplitude of the three-quark model (involving  $Z$  exchange) by a factor of roughly  $m_c^2/(4\pi^2 M_W^2)$ . Gaillard and Lee have estimated  $m_c \approx 1.5 \text{ GeV}$  from  $K - \bar{K}$  mixing [25] which is surprisingly close to the value inferred from the  $c - \bar{c}$  bound state  $J/\psi$  after its discovery [26, 27].

---

<sup>3</sup>The superweak model constrains  $CP$  violation to  $K - \bar{K}$  mixing and was disproven, when  $|\Delta S| = 1$   $CP$  violation was discovered by the CERN NA31 and NA48 as well as the Fermilab KTeV collaborations [20–22].

What did the four-quark model say about  $CP$  violation?  $CP$  maps  $W^+$  onto  $W^-$  and exchanges quark and antiquark fields in Eq. (8). Picking out the  $CP$  transformation of the  $s$  decay vertex one finds

$$L_W \supset \frac{g_w}{\sqrt{2}} \left[ V_{us} \bar{u} \gamma^\mu s W_\mu^+ + V_{us}^* \bar{s} \gamma^\mu u W_\mu^- \right] \quad (14)$$

$$\begin{array}{ccc} \downarrow CP & & \downarrow CP \\ V_{us} \bar{s} \gamma^\mu u W_\mu^- + V_{us}^* \bar{u} \gamma^\mu s W_\mu^+ \end{array} \quad (15)$$

While owing to  $V_{us} \neq V_{us}^*$  Eq. (15) looks different from Eq. (14) these two expressions are nevertheless physically equivalent, because we can rephase any quark field as

$$d_j \rightarrow e^{i\phi_j^d} d_j, \quad u_k \rightarrow e^{i\phi_k^u} u_k. \quad (16)$$

without changing the physics. This rephasing affects  $V_{jk}$  as  $V_{jk} \rightarrow V_{jk} e^{i(\phi_j^d - \phi_k^u)}$  entailing that we are free to multiply any row or any column of  $V$  by a common phase factor. We can do such a rephasing in Eq. (15) and arrange the phase  $\phi_s - \phi_u \equiv \phi_2^d - \phi_1^u$  to bring the result into agreement with Eq. (14). Of course, in the four-quark model, Eq. (16) has been conventionally applied already in Eq. (8) to obtain a real  $V_C$  with  $V_{ud} = V_{cs} = \cos \theta_C$  and  $V_{us} = -V_{cd} = \sin \theta_C$  in terms of the Cabibbo angle  $\theta_c$  [28]. For this standard choice of the  $V_C$  phase convention the  $CP$  invariance of Eq. (14) and all other  $W$  couplings to quarks is manifest. Thus in 1970 the origin of  $CP$  violation, discovered six years before, was not clear. In 1973 Kobayashi and Maskawa proposed three possibilities to accommodate  $CP$  violation [29]. One of these was based on the observation that the  $n^2$  parameters characterising a unitary  $n \times n$  matrix involve  $n(n-1)/2$  angles (which would suffice for a real orthogonal matrix) and  $n(n+1)/2$  complex phases. With Eq. (16) we can rephase the  $n$  rows and  $n$  columns with  $2n-1$  phase differences  $\phi_j^d - \phi_k^u$  at our disposal to render  $2n-1$  elements of  $V$  real. This leaves  $n(n+1)/2 - 2n+1 = (n-1)(n-2)/2$  complex phases as physical parameters and for the case of  $n=3$  there is exactly one physical phase in  $V$ . Applying our  $CP$  transformation in Eq. (15) to Eq. (8) will not leave  $L_W$  invariant. The mentioned physical phase is the only  $CP$ -violating parameter appearing in the weak interaction of quarks and is called *Kobayashi-Maskawa (KM) phase*  $\delta_{KM}$ . Our exercise further tells us that one cannot locate  $CP$  violation in a particular term in Eq. (8), because by rephasing our quark fields we can render chosen CKM elements real and transfer  $\delta_{KM}$  to other elements.  $CP$ -violating observables always involve CKM elements in combinations which are independent of phase conventions such as  $V_{us} V_{ud}^* V_{ts} V_{td}^*$ , which originate from two interfering amplitudes governed by different combinations of CKM elements.

The standard phase convention of the CKM matrix [30] adopted by the Particle Data Group chooses  $V_{ud}$ ,  $V_{us}$ ,  $V_{cb}$ , and  $V_{tb}$  real and positive. The KM phase appears in  $V_{ub}$  as  $|V_{ub}|e^{-i\delta_{KM}}$  and apart from  $V_{td}$  all remaining CKM elements have phases close to 0 or  $\pi$ . The structure of this matrix is best seen in the approximate *Wolfenstein parametrization* [31],

$$V = \begin{pmatrix} 1 - \frac{1}{2}\lambda^2 & \lambda & A\lambda^3(\rho - i\eta) \\ -\lambda & 1 - \frac{1}{2}\lambda^2 & A\lambda^2 \\ A\lambda^3(1 - \rho - i\eta) & -A\lambda^2 & 1 \end{pmatrix} + O(\lambda^4), \quad (17)$$

which employs an expansion in the small parameter  $\lambda \simeq |V_{us}|$  with three more positive parameters  $A, \rho, \eta$  targeted to be of order 1. Eq. (17) nicely exhibits the hierarchy of the CKM matrix, with diagonal elements close to 1 and the smallest elements in the upper right and lower left corner. The origin of this hierarchy is part of the “flavor puzzle” of the SM and not understood.  $CP$  violation is implemented through  $\eta \neq 0$ . Today we know that  $\lambda = 0.225$ ,  $A = 0.82$ ,  $\rho = 0.16^{+0.01}_{-0.00}$ , and  $\eta = 0.36^{+0.01}_{-0.00}$  if there are no BSM contributions to flavour-changing decays [32]. At this level of experimental precision, the approximation in Eq. (17) is too crude and one better works with exact expressions (see Sec. 6).

Ref. [29] can be viewed as the paper predicting the third fermion generation, but did not receive much attention at first, with only six citations by the end of 1975. At the time the alternative explanation in terms of spontaneous  $CP$  violation with a second Higgs doublet was more popular [33]. In the six-quark model the prediction of the  $K_{\text{long}} \rightarrow \pi^+ \pi^-$  decay rate involves  $\text{Im} \left( V_{ts} V_{td}^* / (V_{us} V_{ud}^*) \right)$ , which apart from  $\delta_{KM}$  depends on other—at the time—poorly known CKM parameters (namely  $A$  and  $\rho$  in Eq. (17)) as well as the unknown top mass. Moreover, the hadronic, non-perturbative piece of the prediction could only be roughly estimated. Thus the confirmation of the KM mechanism had to wait for more data on flavor-changing processes and better theory predictions.

While the third fermion generation is essential for Eq. (13), the impact of tops in the loop is negligible in  $\Delta M_K$ , which scales like  $G_F^2 / (4\pi^2 m_c^2)$ , where the dependence on  $M_W$  is contained in the Fermi constant  $G_F \propto 1/M_W^2$  and  $1/(4\pi^2)$  is the loop suppression factor found from calculating the box diagram.

In retrospective, the 1964 discovery of  $CP$  violation [14] revealed the virtual effect of a very heavy particle, the top quark, with mass  $m_t \sim 350 M_K$ . The box diagram with two top quarks does not suffer from GIM suppression, which partly offsets the smallness of the CKM factor  $(V_{ts} V_{td}^*)^2$ . Thus the absence of GIM suppression enhances the sensitivity to top effects. As a general feature, FCNC processes, and especially meson-antimeson mixing observables, probe mass scales far above the energy of the experiment at which they are carried out. Today, FCNC processes serve as efficient probes of physics beyond the SM (BSM physics). Ref. [34] finds a reach of  $K - \bar{K}$  mixing to BSM particle masses up to 9000 TeV, if they contribute to  $K - \bar{K}$  mixing at tree level with  $O(1)$  couplings.

We close this section by mentioning two important consequences of the CPT theorem: Any particle and its antiparticle have the same mass and lifetime. In the context of meson-antimeson mixing the equalities  $M_K = M_{\bar{K}}$  and  $\Gamma_K = \Gamma_{\bar{K}}$  are essential to correctly relate the tiny mass and width differences of the mass eigenstates as well as the size of  $CP$ -violation to the box diagrams in Fig. 1. In  $K - \bar{K}$  mixing even  $CPT$ -violating quantities have been analyzed and measured to be consistent with zero. One may speculate that CPT symmetry is violated

by the dynamics of quantum gravity associated with the energy scale of the Planck mass  $M_{\text{Planck}} \sim 10^{18} \text{ GeV}$ . The current experimental accuracy is  $|M_K - M_{\bar{K}}|/M_K < 8 \cdot 10^{-19}$  [1], which is of order  $M_K/M_{\text{Planck}}$ , but CPT breaking—if it exists at all—needs not be linear in this parameter.

### 3 $B - \bar{B}$ mixing, flavor oscillations, $CP$ asymmetries, and the unitarity triangle

The mass eigenstates of the  $B_d$  mesons have almost identical lifetimes, so that one needs different methods to study  $B_d - \bar{B}_d$  mixing compared to  $K - \bar{K}$  mixing. The DESY laboratory had operated the DORIS collider with the ARGUS experiment, which was used as a  $B$  factory, which is an  $e^+ - e^-$  collider with the center-of-mass energy of the  $\Upsilon(4S)$  resonance. This resonance essentially only decays to  $(B^+, B^-)$  or  $(B_d, \bar{B}_d)$  pairs. ARGUS had studied dilepton events, i.e. decays in which both  $B^\pm$  or  $\bar{B}_d$  mesons decay semileptonically (into final states with electron/positron  $e^\mp$  or (anti-)muon  $\mu^\mp$ ). In the case of  $B^\pm$  mesons the lepton charges have necessarily opposite signs, since the lepton charge tags the beauty quantum number. ARGUS also observed like-sign dilepton events and concluded that they originate from a  $(B_d, \bar{B}_d)$  pair in which one of the  $\bar{B}_d$  mesons has oscillated into its antimeson. In addition, ARGUS has used events with fully reconstructed kinematics such as  $B_d \rightarrow D^{*-} \pi^+$  (and also decays with more than one pion) in which the charged pion serves as the tag: The up quark in  $\bar{b} \rightarrow \bar{c} u \bar{d}$  ends up in the  $\pi^+$  while the charge-conjugate mode will give a  $\bar{u}$  hadronizing into a  $\pi^-$ . Tagging modes are also called *flavor-specific*, characterized by the property that a decay  $B_d \rightarrow f$  and its  $CP$ -conjugate decay  $\bar{B}_d \rightarrow \bar{f}$  is allowed while  $\bar{B}_d \rightarrow f$  and  $B_d \rightarrow \bar{f}$  are forbidden. Here I have used the definition

$$|\tilde{f}\rangle \equiv CP|f\rangle. \quad (18)$$

which I use for all final multi-particle states, while the  $CP$  transformation of the one-particle states of our four neutral mesons  $K$ ,  $D$ , and  $B_{d,s}$  is given in Eq. (23). It is understood that  $CP$  is applied in the rest frame of the decaying particle where  $\vec{p}_M = 0$ . Thus  $CP$  reverses the momenta of the particles in  $|f\rangle$ , but in two-body final states we can bring  $|\bar{h}_1(\vec{p})\bar{h}_2(-\vec{p})\rangle$  to  $|\bar{h}_1(-\vec{p})\bar{h}_2(\vec{p})\rangle$  by a  $180^\circ$  rotation. This feature is crucial for the  $CP$  physics discussed below, because otherwise we could not define two-body  $CP$  eigenstates in a useful way.

For example,  $B_d \rightarrow \pi^+ \pi^-$  is *not* flavor-specific. Strictly speaking, the decay  $B_d \rightarrow D^{*-} \pi^+$  used by ARGUS is not exactly flavor-specific, because  $\bar{B}_d \rightarrow D^{*-} \pi^+$  is allowed via  $b \rightarrow u \bar{c} d$ , but this amplitude is suppressed by a factor of  $\lambda^2$  compared to  $b \rightarrow c \bar{u} d$  (see Eq. (17)) and could be neglected in 1987.

We will see in Sec. 5 that the oscillation frequency is equal to the difference  $\Delta M_d$  of the masses of the two eigenstates of the  $B_d - \bar{B}_d$  system and is proportional to the absolute value of the box diagram in Fig. 1. Recalling our use of natural units with  $\hbar = c = 1$ , we realize that energy, mass, and frequency have the same dimension. One usually quotes  $\Delta M_d$  in units of inverse picoseconds, because it is measured as the mentioned oscillations frequency and the relevant time scale is the  $B_d$  lifetime of 1.5 ps.  $\Delta M_d$  is proportional to the magnitude of the  $B - \bar{B}$  mixing amplitude, which one can calculate in terms of  $|V_{tb} V_{td}^*|^2$  and  $m_t$ . Contrary to  $K - \bar{K}$  mixing, box diagrams with other CKM elements are negligible. To verify this, we observe from Eq. (17) that all three CKM combinations  $V_{tb} V_{td}^*$ ,  $V_{cb} V_{cd}^*$ , and  $V_{ub} V_{ud}^*$  are quadratic in  $\lambda$  and thus of similar size and recall the GIM mechanism suppressing contributions with light quarks. ARGUS could not track the time evolution of the mesons, but did a time-integrated measurement yielding [35]

$$x_d \equiv \Delta M_d \tau_{B_d} = 0.73^{+0.17}_{-0.18} \quad \text{ARGUS 1987.} \quad (19)$$

Confronting this with the theory prediction, ARGUS concluded that  $m_t$  must be larger than 50 GeV, which was the first evidence for a heavy top quark. Shortly before, the UA1 collaboration had reported evidence for an excess of dilepton events stemming from  $B$  mesons produced in  $p\bar{p}$  collisions, in which all  $b$ -flavored hadrons are produced, and erroneously ascribed the effect to  $B_s - \bar{B}_s$  mixing [36]. This interpretation is compatible with a roughly five times lighter top, because  $|V_{ts}|$  in Eq. (17) is larger than  $|V_{td}|$  and the box diagram roughly grows as  $m_t^2$ .

Using the 2025 value  $\tau_{B_d} = (1.517 \pm 0.004)$  ps, the ARGUS measurement in Eq. (19) implies  $\Delta M_d = 0.48^{+0.11}_{-0.12} \text{ ps}^{-1}$  which perfectly complies with the actual number found from the world average of the oscillation frequency in time-dependent studies,

$$\Delta M_d = (0.5069 \pm 0.0016_{\text{stat}} \pm 0.00116_{\text{syst}}) \text{ ps}^{-1} \quad \text{HFLAV 2025 [37],} \quad (20)$$

which involves data from LEP, Tevatron, BaBar, Belle-II, LHCb, but is dominated by LHCb measurements [38].

The proximity of  $x_d$  to 1 and the smallness of  $|V_{cb}|$  and  $|V_{ub}|$  constitute the  *$B$  physics miracle*: The latter property makes the  $B$  meson long-lived, since only  $b \rightarrow c$  and  $b \rightarrow u$  decay channels are open and suppressed by the small CKM elements, so that the sizable  $B_d$  lifetime around 1.5 ps permits the study of time-dependent observables. The former property means that the oscillation frequency is in the right range to analyze observables governed by  $\sin(\Delta M_d t)$  and  $\cos(\Delta M_d t)$ , i.e. after two lifetimes a meson produced as  $B_d$  has oscillated into a  $\bar{B}_d$ . To study such time-dependent quantities one must produce the  $B$  mesons with a sufficiently large boost. This was the case at the LEP I collider at CERN, where  $b$ -flavored hadrons were produced from  $Z$  decays. The *asymmetric  $B$  factories* Super KEK-B (KEK, Tsukuba, Japan) and PEP-II (SLAC, Menlo Park, USA) with the experiments *Belle* and *BaBar*, respectively, have been built to study time-dependent observables in decays of  $(B_d, \bar{B}_d)$  pairs originating from the  $\Upsilon(4S)$  resonance. The different energies of the  $e^+$  and  $e^-$  beams boosted the center-of-mass of the  $(B_d, \bar{B}_d)$  pair in the detector permitting to measure the difference of the times at which the mesons decay. Currently the upgraded experiment *Belle II* is running. Hadron colliders also provide sufficiently energetic  $B$  mesons and there was a rich  $b$  physics program at the  $p\bar{p}$  collider *Tevatron* at Fermilab (Batavia, USA) with the experiments CDF and DØ. One of the four major experiments

at the  $p\bar{p}$  collider LHC at CERN is LHCb, which is a dedicated forward-spectrometer experiment optimized for studies in  $b$  (as well as  $c$ ) physics. Furthermore, the high- $p_T$  LHC experiments CMS and ATLAS contribute to the field as well.

$B$  factories produce the  $(B_d, \bar{B}_d)$  pair in a coherent state with the quantum numbers of the  $\Upsilon(4S)$ . At any given time  $t$  each of the two involved mesons is a quantum-mechanical superposition of  $B_d$  and  $\bar{B}_d$ , but their correlation is such that the overall beauty quantum number is 0, as that of  $\Upsilon(4S)$ .<sup>4</sup> If we observe at some time  $t_1$  a flavor-specific decay  $B_d \rightarrow f_{fs}$ , the coherent wave function collapses such that the other meson is in a  $|\bar{B}_d\rangle$  state as this time. This “starts the clock” for the time evolution of  $|\bar{B}_d\rangle$ ; one defines the time-dependent state  $|\bar{B}_d(t)\rangle$  which satisfies  $|\bar{B}_d(t_1)\rangle = |\bar{B}_d\rangle$ . For  $t > t_1$  this state  $|\bar{B}_d(t_1)\rangle$  is a calculable superposition of  $|B_d\rangle$  and  $|\bar{B}_d\rangle$  and the decay  $\bar{B}_d(t_2) \rightarrow f$  observed at time  $t_2 > t_1$  provides information on  $B-\bar{B}$  mixing and, if the decay is *not* flavor-specific, on the interference of the  $B_d \rightarrow f$  and  $\bar{B}_d \rightarrow f$  decay amplitudes. The latter feature is heavily used to explore  $CP$  violation.  $(b, \bar{b})$  pairs produced at hadron colliders hadronize into multi-particle states containing many light hadrons in addition to the pair of  $b$ -flavored hadrons. A  $B_d$  can be produced together with a  $B^-$  or  $\Lambda_b$ , so that we cannot expect an entangled  $(B_d, \bar{B}_d)$  pair as in a  $B$  factory. Still the overall beauty quantum number is zero, thus the observation of a  $B^-$  or  $\Lambda_b$  (which contain a  $b$  quark) tags the  $B_d$  and studies of time-dependent  $CP$  asymmetries are possible as well. Here the “clock starts” at the time the  $B_d$  is produced. Hadron colliders produce substantially more  $B_d$  mesons than  $B$  factories, which in turn have a better tagging efficiency. Unlike hadron colliders the entanglement at  $B$  factories can also be used to do  $CP$  tagging, in which one of the  $B$ 's is tagged through a decay into a  $CP$  eigenstate, so that the other  $B$  collapses into the orthogonal state.

To study time-dependent effects one defines the *time-dependent decay rate* of a meson tagged at  $t = 0$  as  $M$ :

$$\Gamma(M(t) \rightarrow f) = \frac{1}{N_M} \frac{d N(M(t) \rightarrow f)}{dt}, \quad (21)$$

where  $d N(M(t) \rightarrow f)$  denotes the number of decays into the final state  $f$  occurring within the time interval between  $t$  and  $t + dt$ .  $N_M$  is the total number of  $M$ 's produced at time  $t = 0$ . An analogous definition holds for  $\Gamma(\bar{M}(t) \rightarrow f)$ . We consider a decay into a  $CP$  eigenstate  $f_{CP}$ ,

$$CP|f_{CP}\rangle = \eta_{CP,f}|f_{CP}\rangle \quad (22)$$

with the  $CP$  quantum number  $\eta_{CP,f} = \pm 1$ . For example,  $D^+D^-$  and  $\pi^+\pi^-$  are  $CP$ -even eigenstates with  $\eta_{CP,D^+D^-} = \eta_{CP,\pi^+\pi^-} = 1$ .

We also need the  $C$  and  $CP$  transformations for the state of the decaying meson, which I choose as

$$C|M(\vec{p})\rangle = |\bar{M}(\vec{p})\rangle, \quad C|\bar{M}(\vec{p})\rangle = |M(\vec{p})\rangle, \quad CP|M(\vec{p})\rangle = -|\bar{M}(-\vec{p})\rangle, \quad CP|\bar{M}(\vec{p})\rangle = -|M(-\vec{p})\rangle, \quad (23)$$

where it is used that  $M = K, D, B_d, B_s$  are all  $P$ -odd. One can put arbitrary phase factors into these definitions like  $C|M(\vec{p})\rangle = \exp(i\phi_C)|\bar{M}(\vec{p})\rangle$  with  $C|\bar{M}(\vec{p})\rangle = \exp(-i\phi_C)|M(\vec{p})\rangle$ , because the phase of any state vector is arbitrary: Changing from  $|M\rangle$  to  $|M'\rangle \equiv \exp(i\phi_C/2)|M\rangle$  with  $|\bar{M}'\rangle \equiv \exp(-i\phi_C/2)|\bar{M}\rangle$  and applying  $C$  of Eq. (23) leads to  $C|M'(\vec{p})\rangle = \exp(i\phi_C)|\bar{M}'(\vec{p})\rangle$ . Similarly, such a freedom exists for the definition of the  $CP$  transform of the fields in  $L_W$  in Eqs. (14) and (15). One does not need to carry these arbitrary phases through the calculations, instead one can stick to Eq. (23) and e.g. confirm  $CP$  invariance by checking that the  $CP$ -transformed quantity can be brought into agreement with the original expression by changing unphysical phases of fields and states, just as we did in the discussion of Eqs. (14) and (15). However, sometimes one checks the (non-)dependence on  $\phi_C$  to identify physical quantities and to perform a “sanity check” of a calculation by confirming that some calculated observable is independent of the choices for unphysical phases.

Needless to say, the ambiguity of  $\phi_C$  leads to the fact that you can find different “standard definitions” of  $C$  and  $CP$  in the literature, corresponding to  $\phi_C = 0$  and  $\phi_C = \pi$ , so that the signs are flipped compared to Eq. (23). There is, however, a good reason for my choice: While there are many phase conventions involved in a quantum field theory, several of these conventions are related to each other. A standard convention for the definition of the light meson states in terms of (anti-)quark fields uses the standard Gell-Mann matrices  $\lambda^a$ ,  $a = 1, \dots, 8$ , in the meson octet as  $M^a = (\bar{u}, \bar{d}, \bar{s})\lambda^a(u, d, s)^T$ , so that  $K \sim d\bar{s}$  and  $\bar{K} \sim s\bar{d}$  in Eqs. (1) and (2), without any “ $-$ ” signs (or, more generally, without phase factors). Now we can employ the  $SU(3)_F$  symmetry to rotate  $|K(\vec{p})\rangle$  into  $|\bar{K}(\vec{p})\rangle$ ; this is a so-called U-spin  $SU(2)$  rotation of  $(s, d)^T$ , the analogue of an isospin rotation of the isodoublet  $(u, d)^T$ . Thus we can get from  $|K(\vec{p})\rangle$  to  $|\bar{K}(\vec{p})\rangle$  in two ways, by a U-spin rotation or by applying  $C$ , and these two operations must be consistent with each other. A rotation by  $\pi$  around the  $y$ -axis in U-spin space leads to  $|K(\vec{p})\rangle \rightarrow -|\bar{K}(\vec{p})\rangle$  and, by convention, the combination of this rotation and  $C$  is the  $G_U$  parity transformation which maps the three members of the U-spin triplet onto themselves [40–43].  $G_U$  parity is the analogue of the famous  $G$  parity which combines  $C$  with an isospin rotation and has the property that  $G|\pi^\pm\rangle = -|\pi^\pm\rangle$  and  $G|\pi^0\rangle = -|\pi^0\rangle$ , with the “ $-$ ” sign fixed from the  $G$  parity of  $\pi^0$ , for which no choice of phase of the  $C$  transformation is possible, because it is a  $C$  eigenstate [44]. Thus the definitions of  $G_U$  and  $G$  parities require the choice for  $C$  in Eq. (23) for neutral Kaons and  $C|\pi^+\rangle = |\pi^-\rangle$  for charged pions. In decays of  $D$  or  $B$  into final states with one or more neutral Kaons, this subtlety indeed matters in analyses using  $SU(3)_F$  symmetry and leads to mistakes if ignored as shown in Refs. [43, 45]. For the heavy  $D$  and  $B$  mesons the argument presented above does not apply, because nobody uses flavor symmetries rotating heavy mesons into their antimesons. Nevertheless, I use the same phase conventions for  $C$  and  $CP$  for all neutral mesons.

The *time-dependent  $CP$  asymmetry* for  $M \rightarrow f_{CP}$  is defined as

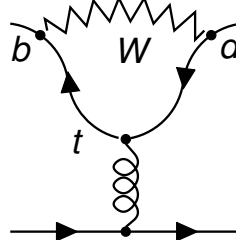
$$a_{CP}(M(t) \rightarrow f_{CP}) \equiv \frac{\Gamma(\bar{M}(t) \rightarrow f_{CP}) - \Gamma(M(t) \rightarrow f_{CP})}{\Gamma(\bar{M}(t) \rightarrow f_{CP}) + \Gamma(M(t) \rightarrow f_{CP})}. \quad (24)$$

Specifying to  $M = B_d$  one finds

$$a_{CP}(B_d(t) \rightarrow f_{CP}) = -A_{CP}^{\text{dir}} \cos(\Delta M_d t) - A_{CP}^{\text{mix}} \sin(\Delta M_d t). \quad (25)$$

---

<sup>4</sup>The time evolution of a coherent  $(B_d, \bar{B}_d)$  pair is discussed e.g. in Ref. [39].

Fig. 2 Penguin diagram contributing to a  $\Delta S = 0$  decay of a  $b$ -flavored hadron.

We will derive Eq. (25) in Sec. 5 and note that in Eq. (25) some sub-percent corrections are set to zero. The first term is non-zero already for  $t = 0$ , when  $|B_d(t)\rangle = |B_d\rangle$ .  $a_{CP}(B_d(0) \rightarrow f_{CP})$  simply quantifies the amount by which the decay rates  $\Gamma(\bar{B}_d \rightarrow f_{CP})$  and  $\Gamma(B_d \rightarrow f_{CP})$  differ from each other. This feature is called *direct CP violation* and motivates the notation  $A_{CP}^{\text{dir}}$  in Eq. (25). As time elapses, the initially produced  $(\bar{B}_d)$  oscillates into a superposition of  $B_d$  and  $\bar{B}_d$  which makes  $a_{CP}(B_d(t) \rightarrow f_{CP})$  sensitive to the interference of  $B_d \rightarrow f_{CP}$  and  $\bar{B}_d \rightarrow f_{CP}$  and the size of this effect is encoded in  $A_{CP}^{\text{mix}}$ , the *mixing-induced CP asymmetry*. Thus  $A_{CP}^{\text{mix}} \sin(\Delta M t)$  quantifies *CP violation in the interference of mixing and decay*. Of course,  $A_{CP}^{\text{dir/mix}} = A_{CP}^{\text{dir/mix}}(B_d \rightarrow f_{CP})$  depends on the decay mode, but to keep the notation short I omit this dependence wherever this does not lead to confusion.

For a non-zero *CP* asymmetry we need two interfering amplitudes. In the case of  $A_{CP}^{\text{dir}}$  these are two decay amplitudes governed by different CKM elements. For example,  $\bar{B}_d \rightarrow D^+ D^-$  is dominated by the tree-level  $W$ -mediated  $b \rightarrow c\bar{c}$  amplitude but also receives a contribution from the top penguin depicted in Fig. 2 and a similar diagram with internal up quark. These three contributions are proportional to  $V_{cb} V_{cd}^*$ ,  $V_{tb} V_{td}^*$ , and  $V_{ub} V_{ud}^*$ , respectively. There is further a charm penguin diagram which comes with the same CKM structure as the tree contribution.

Using unitarity we can eliminate one of these CKM combinations, e.g.  $V_{tb} V_{td}^* = -V_{cb} V_{cd}^* - V_{ub} V_{ud}^*$ , so we are left with a decay amplitude of the form  $A(\bar{B}_d \rightarrow D^+ D^-) = V_{cb} V_{cd}^* A_T + V_{ub} V_{ud}^* A_P$  with complex  $A_{T,P}$ . This (commonly used) notation is reminiscent of “tree” and “penguin”, although  $A_T$  also comprises the charm penguin and a part of the top penguin. The *CP*-conjugate mode has the amplitude  $A(B_d \rightarrow D^+ D^-) = -V_{cb}^* V_{cd} A_T - V_{ub}^* V_{ud} A_P$ , with the “ $-$ ” sign stemming from  $CP|B_d\rangle = -|\bar{B}_d\rangle$  in Eq. (23). The phases of the CKM elements flip their signs, because the quarks flow in the opposite direction and the corresponding vertex Feynman rules in Eq. (8) involve the complex conjugate of the CKM element entering  $A(\bar{B} \rightarrow D^+ D^-)$ . That is, *CP-violating* phases flip signs when going from a process to its *CP*-conjugate one. The remainder stays the same,  $A(\bar{B} \rightarrow D^+ D^-)$  and  $A(B \rightarrow D^+ D^-)$  involve the same  $A_T$  and  $A_P$ , because the SM has no other *CP*-violating parameters beyond the elements of  $V$ .<sup>5</sup> While the hadronic dynamics in  $A_{T,P}$  is complicated and uncalculable, the *CP* invariance of QCD ensures that these quantities are equal in  $A(\bar{B} \rightarrow D^+ D^-)$  and  $A(B \rightarrow D^+ D^-)$ . The phases of  $A_{T,P}$  are dubbed *CP-conserving* or *strong phases*. In decays in which the strong phases of  $A_T$  and  $A_P$  are the same, one readily finds  $|A(\bar{B} \rightarrow D^+ D^-)| = |A(B \rightarrow D^+ D^-)|$ , so that a non-zero  $A_{CP}^{\text{dir}}$  needs  $\arg A_T \neq \arg A_P$ . It is impossible to calculate these phases from first principles, making predictions for  $A_{CP}^{\text{dir}}$  impossible and rendering essentially all direct *CP* asymmetries useless for the determination of  $\delta_{KM}$  or potential BSM *CP* phases.<sup>6</sup>

Whenever two amplitudes  $A_T$  and  $A_P$  contribute to the decay, also  $A_{CP}^{\text{mix}}$  cannot be calculated. However, there are cases in which one of the two amplitudes is highly suppressed or even absent. Such decays are called *gold-plated modes*. Thus gold-plated modes have necessarily  $A_{CP}^{\text{dir}} = 0$ . (The converse is not true,  $A_T$  and  $A_P$  could have the same strong phase leading to  $A_{CP}^{\text{dir}} = 0$ . Therefore by measuring  $A_{CP}^{\text{dir}} = 0$  one cannot conclude that the mode is gold-plated.) The prime example of a gold-plated mode is  $B_d \rightarrow J/\psi K_{\text{short}}$ , proposed by Bigi and Sanda [49], in which the tree amplitude  $A_T$  is multiplied by  $V_{cs} V_{cb}^*$  which is proportional to two powers of the Wolfenstein parameter  $\lambda$ , while  $A_P$  instead involves  $V_{us} V_{ub}^* \propto \lambda^4$ . In this context  $A_P$  is dubbed “penguin pollution”, as it inflicts an uncertainty of a few percent on the value of the *CP* phase extracted from a measurement of  $A_{CP}^{\text{mix}}(B_d \rightarrow J/\psi K_{\text{short}})$ . Experimentally one detects the lepton pair from the  $J/\psi$  decay and a  $\pi^+ \pi^-$  pair with the invariant mass of the neutral Kaon. Thus really  $a_{CP}(B_d(0) \rightarrow J/\psi [\pi^+ \pi^-]_{M_K})$  is measured. This feature is important, because the  $\bar{b} \rightarrow \bar{c}c\bar{s}$  transition in the  $B_d$  decay produces a  $K$  meson while  $b \rightarrow c\bar{c}s$  triggering the  $\bar{B}_d$  decay produces a  $\bar{K}$ . The interference of the  $K \rightarrow \pi^+ \pi^-$  and  $\bar{K} \rightarrow \pi^+ \pi^-$  decays is needed to obtain a meaningful  $A_{CP}^{\text{mix}}$ .

Interestingly, we can deduce which *CP* phase is measured from  $A_{CP}^{\text{mix}}$  without performing the detailed calculations of Secs. 5 and 6.  $A_{CP}^{\text{mix}}$  must involve the phase of the  $B_d - \bar{B}_d$  box diagram, which is  $\pm(V_{ub} V_{td}^*)^2$  with the sign to be determined by a calculation of the box diagram. That is, we only need the sign, not the full analytical result of this diagram. Neglecting the penguin pollution, the decay amplitude can be written as

$$A_{f_{CP}} \equiv A(B_d \rightarrow J/\psi K[\rightarrow \pi^+ \pi^-]) = V_{cb}^* V_{cs} V_{us}^* V_{ud} A_T \quad (26)$$

where the second CKM factor  $V_{us}^* V_{ud}$  originates from the  $\bar{s} \rightarrow \bar{u}u\bar{d}$  amplitude in the  $K \rightarrow \pi^+ \pi^-$  decay. The charge conjugate mode with decay amplitude  $\bar{A}_{f_{CP}} \equiv A(\bar{B}_d \rightarrow J/\psi \bar{K}[\rightarrow \pi^+ \pi^-])$  involves the complex-conjugate CKM elements instead.

Apart from the phase of the box diagram, the desired physical *CP* phase  $\phi_{CP, B_d}^{\text{mix}}$  can only depend on the relative phase of  $A_{f_{CP}}$  and  $\bar{A}_{f_{CP}}$ , that is, the phase of  $\bar{A}_{f_{CP}}/A_{f_{CP}}$ . If we adopt the standard CKM phase convention explained before Eq. (17), we find the CKM elements

<sup>5</sup>QCD could violate *CP*, but bounds on electric dipole moments constrain the corresponding parameter  $\theta_{\text{QCD}}$  to be smaller than  $10^{-10}$ .

<sup>6</sup>In exceptional cases one can relate different decays to each other and eliminate uncalculable amplitudes [46–48].

in Eq. (26) real, except for  $V_{cs}$ , whose phase is far below  $0.01^\circ$  and negligible. Thus, the only contribution to  $\phi_{CP,B_d}^{\text{mix}}$  stems from the box diagram and (for a positive sign) one deduces

$$\phi_{CP,B_d}^{\text{mix}} = \arg((V_{tb} V_{td}^*)^2) = 2 \arg V_{td}^*, \quad \text{valid for the standard CKM phase convention.} \quad (27)$$

From Eq. (17) one realizes that this is not expected to be a small number, there is no suppression by powers of  $\lambda$  in Eq. (27). The observation that—contrary to what people were used to from Kaon physics— $B_d$  decays can exhibit large  $CP$  violation is due to Carter and Sanda [50, 51]. Thus, loosely speaking,  $A_{CP}^{\text{mix}}(B_d \rightarrow J/\psi K_{\text{short}})$  measures the phase of the  $B_d - \bar{B}_d$  mixing box diagram. But one must keep in mind that the latter is convention-dependent and unphysical, and the physical  $CP$  phase in any  $B_d(t) \rightarrow f_{CP}$  decay is the relative phase between the box diagram and the phase of  $\bar{A}_{f_{CP}}/A_{f_{CP}}$ .

In Sec. 5 we will derive

$$A_{CP}^{\text{mix}}(B_d \rightarrow J/\psi K_{\text{short}}) = -\sin \phi_{CP,B_d}^{\text{mix}}. \quad (28)$$

The overall sign of  $A_{CP}^{\text{mix}}(B_d \rightarrow J/\psi K_{\text{short}})$  is related to the  $CP$  quantum number  $\eta_{CP,J/\psi K_{\text{short}}}$  of the final state. To determine this we recall that  $K_{\text{short}}$  is a placeholder for  $\pi^+ \pi^-$  which is  $CP$  even.  $J/\psi$  is a  $J^{PC} = 1^{--}$  resonance, thus it is also  $CP$ -even. Now the quantum number of the total angular momentum of the  $J/\psi K_{\text{short}}$  state is  $j = 0$ , because  $B_d$  has zero spin. That implies that the final state has angular momentum quantum number  $l = 1$ , meaning that the wave function is proportional to  $Y_{m=0}^{l=1}(\theta, \phi)$  if the  $z$ -axis points in the flight direction of  $K_{\text{short}}$  or  $J/\psi$ . The parity transformation of  $CP$  maps  $Y_{m=0}^{l=1}(\theta, \phi)$  onto  $Y_{m=0}^{l=1}(\pi - \theta, \phi + \pi) = -Y_{m=0}^{l=1}(\theta, \phi)$ , so that we arrive at the  $CP$  quantum number  $\eta_{CP,J/\psi K_{\text{short}}} = -1$ . If we considered a  $b \rightarrow c\bar{s}$  decay into a  $CP$ -even final state, we would find  $A_{CP}^{\text{mix}} = \sin \phi_{CP,B_d}^{\text{mix}}$  instead of Eq. (28).

To describe the impact of  $CP$  asymmetries on CKM metrology one introduces *unitarity triangles* (UTs). The unitarity of  $V$  implies for  $j \neq k$ :

$$V_{1j}^* V_{1k} + V_{2j}^* V_{2k} + V_{3j}^* V_{3k} = 0 \quad \text{columns} \quad (29)$$

$$\text{and} \quad V_{j1}^* V_{k1} + V_{j2}^* V_{k2} + V_{j3}^* V_{k3} = 0 \quad \text{rows}. \quad (30)$$

The first equation expresses that any two columns of  $V$  are orthogonal to each other, the second one does this for rows. We have already used the first relation for  $j = 1$  and  $k = 3$  as  $V_{tb} V_{td}^* = -V_{cb} V_{cd}^* - V_{ub} V_{ud}^*$  above. Each of the relations in Eqs. (29) and (30) defines a triangle in the complex plane, e.g. for Eq. (29) the three corners are located at 0,  $V_{1j}^* V_{1k}$  and  $-V_{2j}^* V_{2k}$ . The three sides of this triangle are  $|V_{1j}^* V_{1k}|$ ,  $|V_{2j}^* V_{2k}|$ , and  $|V_{3j}^* V_{3k}|$ . The UTs have the important feature that the phase transformations of Eq. (16) rotate the unitarity triangles in the complex plane, but leaves their shape fixed. That is, both sides and angles of the UTs are independent of phase conventions and, indeed, we can associate physical observables with them. The angles are related to  $CP$  asymmetries.

The area of all six triangles is the same and given by  $J/2$ , where  $J$  is the *Jarlskog invariant* [52]

$$J \equiv \text{Im} \left[ V_{td}^* V_{tb} V_{ub}^* V_{ud} \right] \simeq A^2 \lambda^6 \eta. \quad (31)$$

Here last result uses the Wolfenstein approximation of Eq. (17). Four of the six *unitarity triangles* are squashed, the three sides are similar only for the choice  $(j, k) = (3, 1)$ . Moreover, within the Wolfenstein approximation the shapes of the “column” and “row” of Eqs. (29) and (30) are equal for  $(j, k) = (3, 1)$ . Seeking a definition of a completely rephasing-invariant unitarity triangle (which does not rotate under rephasings) we divide Eq. (29) (for  $(j, k) = (3, 1)$ ) by  $V_{23}^* V_{21} = V_{cb}^* V_{cd}$  to arrive at

$$\frac{V_{ub}^* V_{ud}}{V_{cb}^* V_{cd}} + \frac{V_{tb}^* V_{td}}{V_{cb}^* V_{cd}} + 1 = 0 \quad (32)$$

When people speak of “the” unitarity triangle they mean the rescaled triangle defined by Eq. (32). Since its baseline coincides with the interval  $[0, 1]$  of the real axis, the unitarity triangle is completely determined by the location of its apex  $(\bar{\rho}, \bar{\eta})$ , where

$$\bar{\rho} + i\bar{\eta} \equiv -\frac{V_{ub}^* V_{ud}}{V_{cb}^* V_{cd}}. \quad (33)$$

This is an exact expression; comparing it with the Wolfenstein approximation in Eq. (17) one finds that  $(\bar{\rho}, \bar{\eta})$  agrees with  $(\rho, \eta)$  to an accuracy of 3% [53]. The UT was used in the Wolfenstein approximation since the late 1980s [54], the notation  $\bar{\rho}, \bar{\eta}$  was introduced in Ref. [53] in which the Wolfenstein approximation was refined by expanding  $V$  to order  $\lambda^5$ . The UT is depicted in Fig. 3. The two non-trivial sides of the triangle are

$$R_u \equiv \sqrt{\bar{\rho}^2 + \bar{\eta}^2}, \quad R_t \equiv \sqrt{(1 - \bar{\rho})^2 + \bar{\eta}^2}. \quad (34)$$

$CP$ -violating quantities are associated with the triangle’s three angles

$$\alpha = \arg \left[ -\frac{V_{td} V_{tb}^*}{V_{ud} V_{ub}^*} \right], \quad \beta = \arg \left[ -\frac{V_{cd} V_{cb}^*}{V_{td} V_{tb}^*} \right], \quad \gamma = \arg \left[ -\frac{V_{ud} V_{ub}^*}{V_{cd} V_{cb}^*} \right]. \quad (35)$$

These angles were used since the late 1980s [54] in the Wolfenstein approximation and then in the improved version [53]; Eq. (35) is the exact definition, which does not employ any expansion in  $\lambda$  [55]. The Belle (-II) collaborations use the notation

$$\phi_1 \equiv \beta,$$

$$\phi_2 \equiv \alpha,$$

$$\phi_3 \equiv \gamma,$$

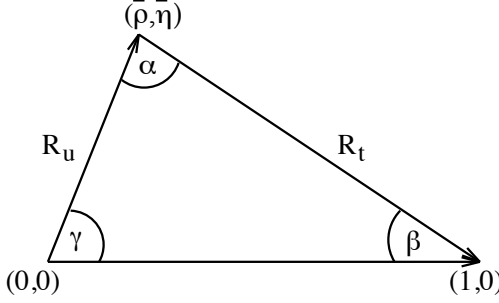


Fig. 3 The (standard) unitarity triangle. The non-trivial sides are  $R_u = \sqrt{\bar{\rho}^2 + \bar{\eta}^2}$  and  $R_t = \sqrt{(1 - \bar{\rho})^2 + \bar{\eta}^2}$ .

with the concept that in the (un-rescaled) UT the angle  $\phi_j$  is opposite to the side involving  $V_{j1}V_{j3}^*$ .

The angle  $\gamma$  coincides with the Kobayashi-Maskawa phase  $\delta_{KM}$  at the sub-permille level. With Eqs. (33–35) one obtains

$$\bar{\rho} + i\bar{\eta} = R_u e^{i\gamma}, \quad 1 - \bar{\rho} - i\bar{\eta} = R_t e^{-i\beta}. \quad (36)$$

The unitarity relation of Eq. (32) now simply reads

$$R_u e^{i\gamma} + R_t e^{-i\beta} = 1 \quad (37)$$

Taking real and imaginary parts of Eq. (37) allows us to express any two of the four quantities  $R_u, R_t, \gamma, \beta$  in terms of the remaining two ones. By multiplying Eq. (37) with either  $\exp(-i\gamma)$  or  $\exp(i\beta)$  one finds analogous relations involving  $\alpha = \pi - \beta - \gamma$ .

In the standard CKM phase convention three of the six elements entering the UT are real. Now with the improved Wolfenstein expansion of Ref. [53] one verifies

$$\arg(-V_{cd}) = A^2 \bar{\eta} \lambda^4 + O(\lambda^8) = 6 \cdot 10^{-4} = 0.03^\circ, \quad (38)$$

so that one can safely neglect this phase and take  $V_{cd}$  as a negative number. Then

$$V_{ub} = |V_{ub}|e^{-i\gamma}, \quad V_{td} = |V_{td}|e^{-i\beta}, \quad (39)$$

$$\phi_{CP, B_d}^{\text{mix}} \stackrel{\text{SM}}{\equiv} 2\beta \quad (40)$$

Eqs. (27) and (28) boil down to the famous result

$$A_{CP}^{\text{mix}}(B_d \rightarrow J/\psi K_{\text{short}}) \stackrel{\text{SM}}{\equiv} -\sin(2\beta), \quad (41)$$

which is independent of any phase conventions if  $\beta$  is defined as in Eq. (35).

We can associate with each of the four meson-antimeson mixing processes one of the six unitarity triangles, which we consider rescaled as in Eq. (32). Then  $B_d - \bar{B}_d$  probes the standard UT, while  $K - \bar{K}$  mixing discussed in Sec. 2, involving  $V_{qs}V_{qd}$  with  $q = u, c, t$ , is related to the UT expressing the orthogonality of the first two columns. The height of this rescaled “squashed” triangle is of order  $\bar{\eta} A^2 \lambda^4 \simeq 6 \cdot 10^{-4}$ , which is tiny.  $CP$  violation is thus small in  $K - \bar{K}$  mixing and the enhancement from the large top mass is instrumental to get to the —still small, but detectable— branching ratio in Eq. (13).

$CP$  violation in the  $B_d$  system was discovered through measurements of  $A_{CP}^{\text{mix}}(B_d \rightarrow J/\psi K_{\text{short}})$  by BaBar and Belle in 2001. These experiments and the B factories hosting them were designed to measure this quantity and to thereby establish  $CP$  violation beyond Kaon decays. Since the measured value complied with the expectation from the SM, this measurement was viewed as a confirmation of the KM mechanism [29], prompting the Nobel Prize for Kobayashi and Maskawa in 2008.

Today’s experimental world average is

$$A_{CP}^{\text{mix,exp}}(B_d \rightarrow J/\psi K_{\text{short}}) = -0.710 \pm 0.011 \quad \text{HFLAV 2025 [37]}, \quad (42)$$

which also involves other  $b \rightarrow c\bar{c}s$  decay modes and uses data from BaBar [56], Belle [57], Belle II [58], and LHCb [59, 60]. Eq. (42) implies

$$\beta = 22.62^\circ \pm 0.45^\circ. \quad (43)$$

To clarify this point, I first mention that in 2004 BaBar had determined sign  $\cos(2\beta)$  to be positive by scanning over the invariant mass of the  $K_{\text{short}}\pi^0$  pair in  $B_d \rightarrow J/\psi K_{\text{short}}\pi^0$  around the  $K^{*(0)}$  resonance and used interference effects of  $S$  and  $P$  waves [61]. Thus  $2\beta = \phi_{CP, B_d}^{\text{mix}}$  is determined to lie in the first quadrant with  $\sin \phi_{CP, B_d}^{\text{mix}} > 0$ ,  $\cos \phi_{CP, B_d}^{\text{mix}} > 0$ . One could still add  $\pi$  to  $\beta$ , but  $22.62^\circ + 180^\circ = 202.62^\circ$  (implying  $\bar{\eta} < 0$  and  $\bar{\rho} > 1$  from Eq. (36)) is incompatible with other measurements by far, even if these had contributions from BSM physics.

At the level of precision in Eq. (43) one must worry about the penguin pollution of order  $\text{Im}(V_{ub}^* V_{us} / (V_{cb}^* V_{cs})) \simeq \bar{\eta} \lambda^2 \sim 0.02$ , which is neglected in Eq. (43). One can estimate the size by measuring the mixing-induced  $CP$  asymmetry in the “control channel”  $B_s \rightarrow J/\psi K_{\text{short}}$  which is a  $\bar{b} \rightarrow \bar{c}cd$  decay in which both  $A_T$  and  $A_P$  come with a CKM factor of order  $\lambda^3$ , so that one can determine the here large penguin

contribution from data and relate it to the decay of interest by using the approximate U-spin symmetry of QCD [62]. This amounts to exchanging  $d$  and  $s$  quark lines, which relates  $A_{T,P}$  in  $B_d \rightarrow J/\psi K_{\text{short}}$  to  $A_{T,P}$  in  $B_s \rightarrow J/\psi K_{\text{short}}$  and would be exact if down and strange quark had the same mass. Currently this is not feasible, because  $A_{CP}^{\text{mix}}(B_d \rightarrow J/\psi K_{\text{short}})$  is measured consistent with zero with an error around 0.41 [63]. Alternatively one can calculate the penguin pollution using soft-collinear factorization, which can be applied to both  $b \rightarrow c\bar{c}d$  and  $b \rightarrow c\bar{c}s$  decay modes. The result, however, involves an unknown phase and varying this phase between 0 and  $2\pi$  only results in an upper bound on the penguin pollution, which reads  $|\delta^{\text{peng}} A_{CP}^{\text{mix}}(B_d \rightarrow J/\psi K_{\text{short}})| \leq 0.0086$  inflicting an uncertainty of  $|\delta^{\text{peng}} \beta| \leq 0.34^\circ$  on  $\beta$  in Eq. (43) [64]. For the control channel this reference finds  $|\delta^{\text{peng}} A_{CP}^{\text{mix}}(B_s \rightarrow J/\psi K_{\text{short}})| \leq 0.26$ .

$B_d - \bar{B}_d$  mixing is very sensitive to BSM physics, Ref. [34] finds a reach of  $B_d - \bar{B}_d$  mixing to virtual BSM particle effects with masses up to 350 TeV. In general, BSM physics will affect both  $\Delta M_d$  and  $\phi_{CP,B_d}^{\text{mix}}$ , and  $V_{td}$  can no more be found from these quantities. A BSM analysis of  $B_d - \bar{B}_d$  mixing requires the determination of this CKM element from other observables.

The width difference  $\Delta\Gamma_d$  stems from all decays into final states  $f$  which are common to  $B_d$  and  $\bar{B}_d$ . That is, only non-flavor-specific decays contribute to  $\Delta\Gamma_d$ . To understand this feature, note that the mass eigenstates  $|B_H\rangle$  and  $|B_L\rangle$  are linear combinations of  $|B_d\rangle$  and  $|\bar{B}_d\rangle$ ,  $|B_{L,H}\rangle = \alpha_{L,H}|B_d\rangle + \beta_{L,H}|\bar{B}_d\rangle$  with  $|\alpha_{L,H}|^2 + |\beta_{L,H}|^2 = 1$ . Introducing the decay amplitudes  $A_f = \langle f | B_d \rangle$  and  $\bar{A}_f = \langle f | \bar{B}_d \rangle$ , normalized such that  $\Gamma(B_d \rightarrow f) = |A_f|^2$ , one finds

$$\Gamma(B_{L,H} \rightarrow f) = |\langle f | B_{L,H} \rangle|^2 = (\alpha_{L,H}^* A_f^* + \beta_{L,H}^* \bar{A}_f^*)(\alpha_{L,H} A_f + \beta_{L,H} \bar{A}_f) = |\alpha_{L,H}|^2 |A_f|^2 + |\beta_{L,H}|^2 |\bar{A}_f|^2 + 2 \operatorname{Re}(\alpha_{L,H}^* \beta_{L,H} A_f^* \bar{A}_f), \quad (44)$$

so that the total widths read

$$\begin{aligned} \Gamma_{L,H} &= \sum_f \Gamma(B_{L,H} \rightarrow f) = |\alpha_{L,H}|^2 \Gamma_{\text{tot}}(B_d) + |\beta_{L,H}|^2 \Gamma_{\text{tot}}(\bar{B}_d) + 2 \operatorname{Re} \left( \alpha_{L,H}^* \beta_{L,H} \sum_f A_f^* \bar{A}_f \right) \\ &= \Gamma_{\text{tot}}(B_d) + 2 \operatorname{Re} \left( \alpha_{L,H}^* \beta_{L,H} \sum_f A_f^* \bar{A}_f \right), \end{aligned} \quad (45)$$

where I have used that the CPT theorem dictates equal total decay rates for  $B_d$  and  $\bar{B}_d$ ,  $\Gamma_{\text{tot}}(B_d) = \Gamma_{\text{tot}}(\bar{B}_d)$ . The first term in Eq. (45) is the same for  $\Gamma_L$  and  $\Gamma_H$ , thus  $\Delta\Gamma_d = \Gamma_L - \Gamma_H$  only receives contributions from the last term in Eq. (45) to which only decays into final states with  $A_f \neq 0 \neq \bar{A}_f$  contribute. Now  $\sum_f A_f^* \bar{A}_f$  corresponds to the  $B_d - \bar{B}_d$  box diagram with light quarks  $u, c$  on the internal lines. It can be read such that a  $\bar{B}_d$  meson enters the diagram from the left and a  $B_d$  enters from the right to decay into the same final state with the quark content of the internal lines. The optical theorem links inclusive quantities like  $\sum_f A_f^* \bar{A}_f$  to the so-called *absorptive part* of a loop diagram, which can be cut into two pieces such that  $f$  corresponds to the cut internal lines of this diagram. The absorptive part is calculated by taking the imaginary part of the loop integral while retaining the couplings (i.e. the CKM elements) with the full complex phases. One can view the last term in Eq. (45) as a  $\bar{B}_d \leftrightarrow f \leftrightarrow B_d$  “rescattering” transition. If we take a box diagram with internal charm and anti-up lines as an example, we can cut it through these lines and the diagrams to the left and right of the cut correspond to  $\bar{A}_f$  and  $A_f^*$  with the sum over  $f$  carried out over all  $C = 1$  final states such as  $D^+ \pi^-$ ,  $D^{*+} \pi^0 K^- K_{\text{short}}$ , ... . The crucial point is that only states which are kinematically accessible in a  $B_d$  decay can contribute to  $\Delta\Gamma_d$ , so that the box diagrams with one or two internal top quarks do *not* contribute to  $\Delta\Gamma_d$ . While  $\Delta M_d \propto m_b^2$ , one instead finds  $\Delta\Gamma_d \propto m_b^2$  and  $\Delta\Gamma_d / \Delta M_d \sim 10^{-3}$  from the calculation presented in Sec. 6.

There is yet no measurement of  $\Delta\Gamma_d$  in the  $B_d - \bar{B}_d$  system. The experimental situation is as follows:

$$\left| \frac{\Delta\Gamma_d}{\Gamma_d} \right|^{\text{exp}} = 0.001 \pm 0.010 \quad \text{HFLAV [37]} \quad (46)$$

with the average width  $\Gamma_d = 1/\tau_{B_d}$  entailing  $|\Delta\Gamma_d|^{\text{exp}} = (0.7 \pm 6.6) \cdot 10^{-3} \text{ ps}^{-1}$ . The value in Eq. (46) is dominated by measurements by ATLAS [65], CMS [66], and LHCb [67]. One measures  $\Delta\Gamma_d$  by measuring the lifetime in a  $B_d$  decay into a  $CP$  eigenstate like  $J/\psi K_{\text{short}}$  and uses the knowledge on  $\Gamma_d$ . HFLAV quotes Eq. (46) without the “ $|$ ” for the absolute value, but the cited measurements are not sensitive to the sign of  $\Delta\Gamma_d$ , i.e. whether the lighter mass eigenstate has the shorter or longer lifetime. However, they give information on whether the longer-lived or the shorter-lived eigenstates is closer to the (appropriately defined)  $CP$ -even eigenstate, as discussed in Sec. 5.

I next discuss  $B_s - \bar{B}_s$  mixing, which is very similar to  $B_d - \bar{B}_d$  mixing discussed above. The corresponding box diagram involves  $V_{ts}^2$  instead of  $V_{td}^2$ . We have seen above that  $B_d - \bar{B}_d$  physics probes the standard unitarity triangle, as we have encountered CKM elements of the first and third columns of  $V$ . Now  $B_s - \bar{B}_s$  mixing involves the CKM elements of the second and third columns and thus probes a “squashed” unitarity triangle with height of order  $\bar{\eta}\lambda^2$ , so that we expect much smaller  $CP$  asymmetries than in  $B_d - \bar{B}_d$ . It is not useful to depict results in terms of “squashed” triangles; recall that  $V$  only involves four parameters, so quoting values for  $V_{us} \simeq \lambda$  and  $V_{cb} = A\lambda^2$  and drawing the allowed range for the apex  $(\bar{\rho}, \bar{\eta})$  of the standard UT are sufficient to describe  $V$ .

We can estimate the expected value for  $\Delta M_s$  from  $\Delta M_d$  by rescaling  $\Delta M_d$  in Eq. (20) by  $|V_{ts}^2/V_{td}^2| \sim 23$ . Since  $\tau_{B_s} \simeq \tau_{B_d}$ , one realizes that  $B_s - \bar{B}_s$  oscillations are very rapid, which prohibited their detection until 2006, when the CDF collaboration at the Fermilab Tevatron collider observed these oscillations with [68, 69]

$$\Delta M_s = (17.77 \pm 0.10_{\text{stat}} \pm 0.07_{\text{syst}}) \text{ ps}^{-1} \quad \text{CDF 2006.} \quad (47)$$

This number excellently agrees with today’s world average from CDF, LHCb and CMS,

$$\Delta M_s = (17.766 \pm 0.004_{\text{stat}} \pm 0.004_{\text{syst}}) \text{ ps}^{-1}, \quad \text{HFLAV 2025 [37],} \quad (48)$$

## 14 Meson-antimeson mixing

which is also dominated by LHCb data [70, 71]. The hadronic physics in  $B_d - \bar{B}_d$  mixing and  $B_s - \bar{B}_s$  mixing would be the same in the U-spin symmetry limit of  $m_s = m_d$ , but in practice  $\Delta M_s / \Delta M_d = 35$  is larger than  $|V_{ts}^2 / V_{td}^2| \sim 23$  because of sizable (but calculable) U-spin breaking. In fact,  $\Delta M_d / \Delta M_s$  from Eqs. (20) and (48) is the most accurate way to determine  $|V_{td}/V_{ts}|$  which gives the side  $R_t$  of the UT in Fig. 3 because of  $|V_{td}/V_{ts}| = \lambda R_t (1 + \lambda^2(1/2 - \bar{\rho}) + O(\lambda^4))$ . But as a caveat,  $B - \bar{B}$  mixing is also most sensitive to new physics and whenever we want to test a BSM hypothesis in mixing observables we must not use numerical values for  $V_{td}$  or  $V_{ts}$  obtained by assuming that the SM is correct. The state-of-the-art is to perform a combined fit to CKM elements and BSM parameters to all available data and to study the likelihood ratio of the BSM best-fit point and the SM hypothesis [72–74].

In the SM one finds that to an excellent approximation  $\Delta\Gamma_s / \Delta M_s = \Delta\Gamma_d / \Delta M_d$ . Since  $\Delta M_s \gg \Delta M_d$ , one finds  $\Delta\Gamma_s$  sizable,  $\Delta\Gamma_s / \Gamma_s = \Delta\Gamma_s \tau_{B_s} \simeq 0.12$ . The current world average

$$\Delta\Gamma_s^{\text{exp}} = (0.0781 \pm 0.0035) \text{ ps}^{-1} \quad \text{HFLAV 2025 [37],} \quad (49)$$

agrees well with the SM prediction discussed in Sec. 6. The quoted number uses data from CDF, DØ, ATLAS [75], CMS [76, 77], and LHCb [78–80, 80–83]. Most of these measurements use  $B_s \rightarrow J/\psi\phi \rightarrow K^+K^-$  decays or the corresponding decay with  $\psi(2S)$ . These decays also provide information on the  $CP$  phase of mixing-induced  $CP$  violation, i.e. the analogue of  $2\beta$  in the  $B_s - \bar{B}_s$  system. Since  $\phi$  is a vector meson, there are three final states ( $J/\psi\phi$ )<sub>*l*</sub> characterized by the angular orbital momentum quantum number  $l = 0, 1$ , or  $2$ . The  $l = 0$  S-wave state is dominant and CP-even and the  $l = 2$  state is CP-even as well. The P-wave state, with  $l = 1$  and  $J/\psi$  and  $\phi$  polarizations perpendicular to each other, is CP-odd, so that one needs an angular analysis to separate the corresponding decay modes [84–88]. One observes two exponential decay distributions following  $\exp(-\Gamma_L t)$  and  $\exp(-\Gamma_H t)$ , which determines  $|\Delta\Gamma_s|$ . One further observes that the larger of  $\Gamma_L$  and  $\Gamma_H$  occurs with decays into CP-even final states, so that the mass eigenstates are, to a good approximation,  $CP$  eigenstates, with the shorter-lived state being dominantly CP-even. Interestingly, all three LHC experiments find errors for  $|\Delta\Gamma_s|$  of comparable size, namely 0.004. While the quoted measurements determine  $|\Delta\Gamma_s|$ , it is important to note that sign  $\Delta\Gamma_s$  is firmly established to be positive: LHCb had scanned the  $K^+K^-$  invariant mass in  $B_s \rightarrow J/\psi K^+K^-$  though the  $\phi$  resonance and, since the variation of strong phases around a resonance is known (from e.g. the Breit-Wigner formula), sign  $\Delta\Gamma_s$  could be determined [89] in 2012. The result complies with the SM expectation, that  $|B_{s,L}\rangle$  is the shorter-lived eigenstate (and almost exactly CP-even). Thus in this respect there is no difference between  $B_s - \bar{B}_s$  and  $K - \bar{K}$  systems.

The sizable width difference in the  $B_s - \bar{B}_s$  system opens the door to new observables. Dunietz has pointed out that one can use *untagged*  $B_s$  samples to study  $CP$  violation, essentially mimicking the situation with  $K - \bar{K}$  mixing, because the longer-lived  $B_{s,H}$  state is mostly decaying to CP-odd final states, just as  $K_{\text{long}}$ , and a  $(\bar{B}_s)$  beam enriches itself with  $B_{s,H}$  in time, because the  $B_{s,L}$  component decays faster [90]. Thus one can access  $CP$  properties from lifetime information. I will come back to this point at the end of Sec. 5.3.

The analogue of the  $\sin(2\beta)$  measurement of  $B_d - \bar{B}_d$  mixing in the  $B_s - \bar{B}_s$  system involves the time-dependent  $CP$  asymmetry in the decay  $B_s \rightarrow J/\psi\phi$ , which is driven by  $\bar{b} \rightarrow \bar{c}c\bar{s}$  like  $B_d \rightarrow J/\psi K_{\text{short}}$ . Unlike the  $\Delta\Gamma_s$  measurements described in the previous paragraph this analysis requires flavor tagging; in the papers [78–80, 80–82] cited above the  $CP$  phase  $\phi_{CP,B_s}^{\text{mix}}$  is determined together with  $\Delta\Gamma_s$ . We can take the formulae used for the phase of the  $B_d - \bar{B}_d$  box diagram in Eq. (27) with the substitution  $2\beta \rightarrow -2\beta_s$  with the definition of  $\beta_s$  through

$$\frac{V_{ts}V_{tb}^*}{V_{cs}V_{cb}^*} \equiv \left| \frac{V_{ts}V_{tb}^*}{V_{cs}V_{cb}^*} \right| e^{i\beta_s}. \quad (50)$$

Thus in the standard CKM phase convention we have

$$V_{td} \stackrel{\text{Eq. (39)}}{=} |V_{td}|e^{-i\beta}, \quad V_{ts} = |V_{ts}|e^{i\beta_s}, \quad \phi_{CP,B_s}^{\text{mix}} \stackrel{\text{SM}}{=} -2\beta_s \quad (51)$$

where  $\arg(-V_{cd}) = 0.03^\circ$  (see Eq. (38)) and  $\arg(V_{cs}) \simeq -A^2\bar{\eta}\lambda^6 = -0.002^\circ$  are neglected. Eq. (51) is the analogue of Eq. (40) in  $B_d - \bar{B}_d$  mixing. The different signs in the definitions of the phases of  $V_{td}$  and  $V_{ts}$ , first introduced in [91], were motivated by the goal to have both  $\beta$  and  $\beta_s$  positive:

$$\beta_s = \bar{\eta}\lambda^2(1 + \lambda^2(1 - \bar{\rho})) + O(\lambda^6) = 0.019 = 1.1^\circ. \quad (52)$$

In  $A_{CP}^{\text{mix}}(B_s \rightarrow (J/\psi\phi)_l)$  we must take care of the  $CP$  quantum number  $\eta_{CP,(J/\psi\phi)_l} = (-1)^l$  and furthermore include the effect from a non-negligible  $\Delta\Gamma_s$ :

$$a_{CP}(B_s(t) \rightarrow (J/\psi\phi)_l) = -\frac{A_{CP}^{\text{dir}}(B_s(t) \rightarrow (J/\psi\phi)_l) \cos(\Delta M_s t) - A_{CP}^{\text{mix}}(B_s(t) \rightarrow (J/\psi\phi)_l) \sin(\Delta M_s t)}{\cosh(\Delta\Gamma_s t/2) - (-1)^l \cos(\phi_{CP,B_s}^{\text{mix}}) \sinh(\Delta\Gamma_s t/2)} \quad (53)$$

$$A_{CP}^{\text{mix}}(B_s \rightarrow (J/\psi\phi)_l) = (-1)^l \sin \phi_{CP,B_s}^{\text{mix}} \stackrel{\text{SM}}{=} -(-1)^l \sin(2\beta_s). \quad (54)$$

This formula, which generalizes Eq. (28) to  $\Delta\Gamma_s \neq 0$ , will be derived in Sec. 5. We see that  $A_{CP}^{\text{mix}}(B_s \rightarrow (J/\psi\phi)_l)$  is expected to be small; the quantity will not significantly contribute to CKM metrology (though it could provide us with the height  $\bar{\eta}$  of the UT), but instead is a superb testing ground for BSM physics. Ref. [34] finds a reach of  $B_s - \bar{B}_s$  mixing to virtual BSM particle effects with masses up to 70 TeV.

The experimental effort [78–80, 80–82] lead to the 2025 world average

$$\phi_{CP,B_s}^{\text{mix,exp}} = -0.052 \pm 0.013 = 2.98^\circ \pm 0.74^\circ \quad \text{HFLAV 2025 [37],} \quad (55)$$

which complies with the SM expectation of  $-2\beta_s = -0.038 \pm 0.001$  [32] at  $1\sigma$ .

I further mention that sign  $\Delta\Gamma_s$  is correlated with the  $B_s - \bar{B}_s$  mixing phase as sign  $\cos\phi_{CP,B_s}^{\text{mix}} = \text{sign } \Delta\Gamma_s$  [88] in the SM and any BSM theory, in which the BSM contribution to the  $b \rightarrow c\bar{s}$  decay amplitudes constituting  $\Delta\Gamma_s$  in Eq. (45) is smaller than the SM contribution. This is plausible, because  $b \rightarrow c\bar{s}$  are large tree amplitudes and furthermore the excellent agreement of Eq. (49) with the SM prediction do not suggest BSM dominance in Eq. (45).

In Ref. [92] it was proposed to determine sign  $\Delta\Gamma_s = \text{sign } \phi_{CP,B_s}^{\text{mix}}$  with  $B_s \rightarrow D_s^\pm K^\mp$  which involves the CKM angle  $\gamma$  in the combination  $\phi_{CP,B_s}^{\text{mix}} + \gamma$  which breaks the degeneracy of the two solutions for  $\phi_{CP,B_s}^{\text{mix}}$  found from  $B_s \rightarrow J/\psi\phi$ . Conversely, once the information on sign  $\Delta\Gamma_s$  from Ref. [89] was available, one could exploit the large width difference to remove discrete ambiguities in studies of  $B_s \rightarrow D_s^\pm K^\mp$  aiming at the determination of  $\phi_{CP,B_s}^{\text{mix}} + \gamma$  [93].

In Eq. (54) and Eq. (55) the penguin pollution has been set to 0. The estimate of the size of penguin pollution using  $SU(3)_F$  symmetry is difficult, because  $\phi$  has a large  $SU(3)_F$  singlet component and one would need precise data on  $CP$  asymmetries in  $B_{d,s} \rightarrow J/\psi\omega$  decays. The dynamical calculation of Ref. [64] finds  $|\delta^{\text{peng}}\phi_{CP,B_s}^{\text{mix}}| \leq 0.97^\circ$ ,  $\leq 1.22^\circ$ , and  $\leq 0.99^\circ$  for the longitudinal, parallel, and perpendicular polarizations of  $J/\psi\phi$ , respectively, from which the  $(J/\psi)_l$  amplitudes are constructed. (Only the amplitude with perpendicular polarizations has  $l = 1$ , i.e. is CP-odd.) We see that the penguin pollution might matter in view of the experimental error in Eq. (55). For the decay mode  $B_s \rightarrow J/\psi f_0 [\rightarrow \pi^+ \pi^-]$  employed to determine  $\Delta\Gamma_s$  in Ref. [83] no estimates of the penguin pollution are available and future determinations of  $\phi_{CP,B_s}^{\text{mix}}$  from  $B_s \rightarrow J/\psi f_0$  should not be averaged with other measurements.

## 4 $D - \bar{D}$ mixing

$D - \bar{D}$  mixing is an example of a FCNC process of *up-type quarks*, since it involves  $c \rightarrow u$  transitions. Charm physics is the only way to study such processes with the needed precision because branching ratios of  $t \rightarrow c$  or  $t \rightarrow u$  decays (suffering from the large total width of the top quark) or  $u \rightarrow t$  or  $c \rightarrow t$  FCNC single-top production (i.e. without a  $\bar{b}$  quark in the final state) are not competitive yet.

The  $D - \bar{D}$  mixing amplitude, described by the  $D - \bar{D}$  box diagram in Fig. 1, involves the down-type quarks  $d$ ,  $s$ , and  $b$  on the internal lines. The CKM elements are hierarchical, with a situation similar to  $K - \bar{K}$  mixing; if we neglect the small CKM factor  $V_{ub}V_{cb}^*$  with magnitude  $|V_{ub}V_{cb}^*| \simeq R_u A^2 \lambda^5 \simeq 10^{-4}$ , we are back to the 2-flavor SM with the  $2 \times 2$  submatrix  $V_C$ . In this 2-flavor theory we find the  $D - \bar{D}$  mixing amplitude far more GIM suppressed than its  $K - \bar{K}$  mixing counterpart: Firstly, we observe that the CKM factor in both cases is  $\sin^2\theta_C \cos^2\theta_C$ . Secondly, we see that the GIM suppression factor which was  $m_c^2/M_W^2$  in  $K - \bar{K}$  mixing will (in the limit  $m_d = 0$ ) involve the much smaller  $m_s$  instead of  $m_c$  in  $D - \bar{D}$  mixing. Yet the suppression is even stronger, because  $m_c \sim 1.3$  GeV is the largest mass scale in the  $K - \bar{K}$  mixing diagram and we can set external momenta (of order  $m_s$  or the QCD scale  $\Lambda_{\text{QCD}} \sim 400$  MeV) to zero. In  $D - \bar{D}$  mixing the largest mass scale is the momentum of the external charm quark, thus it is of order  $m_c$  as well and we must keep both  $m_s$  and  $m_c$  in the calculation. The result is a GIM suppression of order  $m_s^4/(m_c^2 M_W^2)$ , which is smaller by a factor of  $m_s^4/m_c^4$  compared to  $K - \bar{K}$  mixing. Accounting for the different masses and hadronic parameters this results in a naive estimate of  $\Delta M_D \sim 2 \cdot 10^{-4} \cdot \Delta M_K = 10^{-6}$  ps<sup>-1</sup> from Eq. (11).

If we include the contributions from the internal  $b$  quarks, we encounter six combinations of  $d$ ,  $s$ ,  $b$  quarks on the internal lines of the box diagram. As usual, CKM unitarity permits to eliminate one of these, commonly this is done for  $V_{ud}V_{cd}^* = -V_{us}V_{cs}^* - V_{ub}V_{cb}^*$ . This results in three contributions to the  $D - \bar{D}$  mixing amplitude, proportional to  $(V_{us}V_{cs}^*)^2$ ,  $(V_{us}V_{cs}^* V_{ub}V_{cb}^*)$ , and  $(V_{ub}V_{cb}^*)^2$ , respectively. While the latter two CKM elements are smaller than the first one, this suppression is partially offset by the weaker GIM suppression of the loop diagrams with one or two  $b$  quarks. So while numerically sub-leading, these terms are not negligible compared to the  $(V_{us}V_{cs}^*)^2 m_s^4/(m_c^2 M_W^2)$  term.<sup>7</sup>

The experimental situation of  $\Delta M_D$  and  $\Delta\Gamma_D$  is summarized in Ref. [95]. In charm physics it is common standard to quote results in terms of

$$x_D^{\text{exp}} = \frac{\Delta M_D}{\Gamma_D}, \quad y_D^{\text{exp}} = -\frac{\Delta\Gamma_D}{2\Gamma_D}, \quad (56)$$

where the “–” sign in  $y_D$  stems from the definition in Eq. (3) which differs from the one in Ref. [95]. The first discovery of  $D - \bar{D}$  mixing,  $(x_D, y_D) \neq (0, 0)$ , from a combination of several measurements was in 2007 [37], in 2012 LHCb achieved this in a single experiment [96] and in 2021 LHCb [97] has established  $x_d \neq 0$  with a significance of more than  $5\sigma$ , see Ref. [95] for details. Apart from LHCb also BaBar, Belle, and CDF made important contributions to the discovery and quantification of  $D - \bar{D}$  mixing. The 2025 world average is

$$x_D = (0.407 \pm 0.044) \cdot 10^{-2}, \quad y_D = \left(0.645^{+0.024}_{-0.023}\right) \cdot 10^{-2} \quad \text{HFLAV 2025 [37]} \quad (57)$$

which is found from a global fit in which the CP-violating quantities are fitted together with  $x_D$  and  $y_D$ . No evidence for  $CP$  violation is found until today. With  $1/\Gamma_D = \tau_D = (0.4103 \pm 0.0010)$  ps the numbers in Eq. (57) imply

$$\Delta M_D = (0.0099 \pm 0.0011) \text{ ps}^{-1}, \quad \Delta\Gamma_D = -\left(0.01572^{+0.00058}_{-0.00056}\right) \text{ ps}^{-1} \quad (58)$$

We notice two important points here: Firstly,  $\Delta M_D$  is larger than our naive estimate by 4 orders of magnitude. For  $|\Delta\Gamma_D|$  one finds the same order-of-magnitude discrepancy between box diagram estimate and data [94]. Secondly, sign  $(\Delta M_D/\Delta\Gamma_D)$  is negative, opposite to what is observed in  $K - \bar{K}$  mixing and  $B_s - \bar{B}_s$  mixing and what the SM predicts for  $B_d - \bar{B}_d$  mixing!

<sup>7</sup>For an analysis of this feature for  $\Delta\Gamma_D$  see Ref. [94].

To understand the failure of the box diagram calculation I discuss the contribution with the large CKM factor  $(V_{us} V_{cs}^*)^2$ . The smallness of the result of the box diagram Results from four contributions which are of order 1 and combine to a result of order  $m_s^4/(m_c^2 M_W^2)$ . The box diagrams vanish in the U-spin symmetry limit  $m_d = m_s$ . The  $(V_{us} V_{cs}^*)^2$  piece of the  $D - \bar{D}$  mixing is second order in the U-spin breaking parameter  $m_s - m_d$ . Indeed, if we calculate the box diagram with  $m_s \neq 0 \neq m_d$ , we find a result proportional to

$$(m_s^2 - m_d^2)^2 = \underbrace{(m_s - m_d)^2}_{\text{U-spin breaking}} \cdot \underbrace{(m_s + m_d)^2}_{\text{artifact of perturbation theory}} \quad (59)$$

Thus indeed, the U-spin breaking is correctly reproduced, but the additional suppression by  $(m_s + m_d)^2/m_c^2$  is an artifact of the calculational method, originating from the fact that the  $W$  boson only couples to left-chiral fields and one needs an even number of chirality flips on each quark line. In Nature, left-right flips can also come from a non-perturbative object of QCD called quark condensate. So we are lead to consider alternatives to the box diagram. In Refs. [98, 99] it was pointed out that contributions in which one or both of the internal  $s$  or  $d$  lines of the box diagram are cut, so that they become external lines, (and eventually a gluon is added to get a connected diagram), the artificial suppression factor  $(m_s + m_d)^2/m_c^2$  can be avoided and the SU(3)-breaking could reside in a hadronic matrix element. To date, the proposed contributions cannot be reliable calculated. In summary, the theory community was unable to predict the results in Eq. (57) and further did not come up with convincing postdictions.

The result in Eq. (57) nevertheless teaches us about possible BSM explanations. BSM physics which contributes to the  $D - \bar{D}$  mixing amplitude through new box or even tree-level diagrams with heavy particles typically contribute much more to  $x_D$  than to  $y_D$  and it is unlikely that  $x_d \sim y_D$  originates from BSM physics in  $x_D$  and long-distance QCD dynamics in  $y_D$ . More convincingly, BSM physics comes with new complex couplings. Recall that the standard form of  $V$  with real  $V_{ud}, V_{us}$  is the result of the rephasings in Eq. (16) and these rephasing will also appear in the couplings of hypothetical BSM particles. Thus, by default, a dominant BSM contribution to  $x_D$  would give  $O(1)$  mixing-induced  $CP$  asymmetries in e.g.  $\tilde{D} \rightarrow K^\pm \pi^\mp$  decays, which are not observed. This means that BSM explanations of Eq. (57) must have a mechanism which suppresses the effect in  $x_D$  to the level of  $y_D$  and further aligns new complex phases such that  $CP$  violating observables are suppressed. The eventual discovery of BSM physics will clearly come from  $CP$  asymmetries and not from better measurements of  $x_D$  and  $y_D$ .

As discussed in the previous sections, we use  $K - \bar{K}$  mixing and  $B - \bar{B}$  mixing to study the interference effects in  $M \rightarrow f$  and  $\bar{M} \rightarrow f$  decays. Since  $D - \bar{D}$  oscillations are very slow, most of the  $\bar{D}$  sample has decayed once a sizable superposition of  $|D\rangle$  and  $|\bar{D}\rangle$  has evolved. But for such studies one can also use  $CP$ -tagged mesons, the  $CP$  eigenstates are  $|D_{CP\pm}\rangle = (|D\rangle \mp |\bar{D}\rangle)/\sqrt{2}$  and are thus maximal superpositions of  $|D\rangle$  and  $|\bar{D}\rangle$ .  $CP$ -tagged states are used at BES III to determine the strong phase in  $D \rightarrow K^\pm \pi^\mp$ . There are ways to prepare such states even at hadron colliders [100].  $D_{CP\pm} \rightarrow f$  decays are not sensitive to the  $D - \bar{D}$  box diagram, they probe  $CP$  eigenstates rather than mass eigenstates. Similarly to mixing-induced  $CP$  asymmetries,  $D_{CP\pm} \rightarrow f$  decays involve  $CP$ -violating observables which do not need a non-vanishing strong phase.

## 5 Time evolution of neutral mesons and associated $CP$ -violating quantities

In this section I will derive the formulae needed to describe meson-antimeson mixing and the  $CP$ -violating observables related to it, with emphasis on the time evolution of neutral meson states. Compared to the previous sections the presentation is more technical but is nevertheless of interest to both the theoretical and experimental community. Especially, presented aspects of the  $CP$  asymmetry in flavor-specific decays,  $a_{fs}$ , which is still to be discovered in  $B_{d,s}$  and  $D$  decays, might be helpful to devise future measurements. The formalism of the section is general and applies to the SM as well as any BSM theory. SM predictions will be presented in Sec. 6.

### 5.1 Time evolution

In order two understand the QFT formalism of the weak interaction of hadrons in general and of meson-antimeson mixing in particular, we first seek a description of fields and states which permits the application of perturbation theory to the electroweak interaction, which involves small coupling constants in which our amplitudes of interest can be expanded. In fact, for FCNC transitions the lowest non-vanishing order in the weak coupling  $g_w$  is sufficient, e.g. meson-antimeson mixing occurs first at order  $g_w^4$  (box diagrams) and corrections from diagrams with an additional electroweak boson are negligible in view of QCD uncertainties. In a first step the lagrangian of any QFT is expressed in terms of fields and states in the Heisenberg picture, meaning that the quantum fields depend on the space-time variable  $x^\mu$ , while the states (describing the particles) are time-independent. One then splits the hamiltonian density  $H$  as

$$H = H_0 + H_{\text{int}} \quad (60)$$

with  $H_{\text{int}} = -L_{\text{int}}$  containing the interaction terms with the small couplings in which we want to expand in our calculations. In the second step one applies a unitary transformation to fields and states to arrive at the interaction picture (a.k.a. Dirac picture). As a result the states  $|\psi(t)\rangle$  become time-dependent and one encounters a time evolution operator  $\mathcal{U}(t_2, t_1)$ ,

$$|\psi(t_2)\rangle = \mathcal{U}(t_2, t_1)|\psi(t_1)\rangle, \quad \text{where } \mathcal{U}(t_2, t_1) = \text{Exp} \left[ -i \int_{t_1}^{t_2} dt \int d^3 \vec{x} H_{\text{int}} \right]. \quad (61)$$

Here  $T_{\text{exp}}$  is the time-ordered exponential and  $H_{\text{int}}$  depends on  $x^\mu = (t, \vec{x})$  through the fields. In the calculation of a  $2 \times 2$  scattering process, where  $|\psi\rangle$  is a two-particle state, one encounters the S-matrix  $S = \mathcal{U}(\infty, -\infty)$  and conveniently applies covariant perturbation theory in momentum space to calculate the cross section (or other observables of interest) from the S-matrix elements in terms of the momentum four-vectors  $p_j^\mu$  of the in-going and out-going particles. For the treatment of meson-antimeson mixing and the time-dependent decay rates in Eq. (21) we need to depart from the described standard path in two aspects: Firstly, we must keep the time in the formalism, since we need  $\mathcal{U}(t_2, t_1)$  for  $t_2 \neq \infty \neq -t_1$ . This means that we cannot trade  $t$  for the energy  $E = p^0$  with the usual Fourier transform w.r.t. to time. Starting from the formalism of covariant perturbation theory we can Fourier-transform back to a world in which states are labeled as  $|\vec{p}, t\rangle$  which gives us the “old-fashioned time-dependent perturbation theory” employed in early days when QFT emerged from quantum mechanics. Secondly, in perturbation theory applied to processes of leptons and bosons (such as QED) one chooses  $H_0$  in Eq. (60) as the free hamiltonian. In perturbation theory the initial and final states of a scattering or decay process are constructed from  $H_0$ , accounting for the fact that sufficiently widely separated particles (forming so-called *asymptotic states*) behave like free particles. In our cases of interest, we encounter hadrons as asymptotic states, which are bound states of the strong interaction. Not surprisingly, since QCD is non-perturbative at large distances, we cannot apply perturbation theory in terms of the strong coupling  $\alpha_s$  from the start. Thus  $H_0$  in Eq. (60) is  $H_0 = H_{\text{QCD}}$ , which contains both the quadratic pieces of the free hamiltonian and all interaction terms with the gluon field. That is, our fields and states are still in the Heisenberg picture w.r.t. QCD. In particular, the state vectors are eigenstates of  $\widehat{H}_0 = \widehat{H}_{\text{QCD}} = \int d^3\vec{x} H_{\text{QCD}}$ . For example, in a weak two-body meson decay  $M \rightarrow h_1 h_2$  into ground-state hadrons  $h_{1,2}$  the asymptotic states for initial and final state satisfy

$$\begin{aligned}\widehat{H}_{\text{QCD}}|M(\vec{p}_M)\rangle &= E_M|M(\vec{p}_M)\rangle = \sqrt{M_M^2 + \vec{p}_M^2}|M(\vec{p}_M)\rangle, \\ \widehat{H}_{\text{QCD}}|h_1(\vec{p}_1)h_2(\vec{p}_2)\rangle &= (E_1 + E_2)|h_1(\vec{p}_1)h_2(\vec{p}_2)\rangle = \left( \sqrt{M_1^2 + \vec{p}_1^2} + \sqrt{M_2^2 + \vec{p}_2^2} \right) |h_1(\vec{p}_1)h_2(\vec{p}_2)\rangle\end{aligned}\quad (62)$$

and, in our decay,  $E_M = E_1 + E_2$ . Since the time dependence stems from  $H_1 = H_{\text{int}}$  and asymptotic states (describing  $M$  before the decay and  $h_{1,2}$  when they hit the detector (or, in a cascade decay, at the time when they decay to other particles) are obtained from  $H_0 = H_{\text{QCD}}$ , there is no time-dependence yet in Eq. (62). Ground state hadrons are those which do not decay through the strong interaction, this characterization applies to our decaying mesons  $K$ ,  $B_{d,s}$ , and  $D$ , as well as to charged or neutral  $\pi$ ,  $K$ , and  $\eta^{(\prime)}$  in the final states. A vector meson like  $K^*$  is not in this category, the strong decay  $K^* \rightarrow K\pi$  is instantaneous and the asymptotic state is  $K\pi$  in this case. In fact, there are observables in which one exploits the interference of  $K^{*0} \rightarrow K_{\text{short}}\pi^0$  and  $\bar{K}^{*0} \rightarrow K_{\text{short}}\pi^0$  in a decay chain, thus the neutral vector meson is clearly not an asymptotic state observed in a detector. The most prominent example of a quantity using the shown interference is  $A_{CP}^{\text{mix}}(B_d \rightarrow J/\psi \bar{K}^{*0} [\rightarrow K_{\text{short}}\pi^0])$ .

To derive the desired formula for the time-evolution of a weakly decaying meson, we start with the case of a charged meson  $M^+$ , for which no flavor oscillations occur. In the interaction picture, the ket  $|M^+\rangle$  of a meson produced at time  $t = 0$  evolves in time as

$$\mathcal{U}(t, 0)|M^+\rangle = |M^+(t)\rangle + \sum_f |f\rangle\langle f| \mathcal{U}(t, 0)|M^+\rangle, \quad (63)$$

with

$$|M^+(t)\rangle \equiv |M^+\rangle\langle M^+| \mathcal{U}(t, 0)|M^+\rangle \quad (64)$$

describing the situation that  $M^+$  has not decayed at the considered time  $t > 0$ . The second term in Eq. (63) involves the sum over all final states  $|f\rangle$  into which  $M^+$  can decay. In the description of time-dependent decay processes it is further common to switch from the interaction picture kets  $|\dots\rangle_I$  to the Schrödinger picture  $|\dots\rangle_S$  defined as

$$|\psi\rangle_S \equiv e^{-i\widehat{H}_0 t}|\psi\rangle_I = e^{-iE_\psi t}|\psi\rangle_I. \quad (65)$$

so that the one-particle state  $\mathcal{U}(t, 0)|M^+\rangle$  in Eq. (63) picks up an extra factor of  $\exp(-iE_{M^+}t)$  in the Schrödinger picture. We do not transform the fields, e.g.  $\mathcal{U}(t_2, t_1)$  is not changed in the  $I \rightarrow S$  transformation. By energy conservation these factors of  $\exp(-iEt)$  drop out between bras and kets, so that  $s\langle\dots\rangle_S = I\langle\dots\rangle_I$ . We can determine  $|M^+(t)\rangle$  in Eq. (63) by employing the exponential decay law to deduce

$$|M^+(t)\rangle = e^{-iM_M t} e^{-\Gamma t/2} |M^+\rangle \quad (66)$$

in the meson rest frame. The first term is the familiar time evolution factor of a stable state with energy  $E = M_M$ . We understand the second factor involving the total width  $\Gamma$  by considering the probability to find an undecayed meson at time  $t$ :

$$|\langle M^+|M^+(t)\rangle|^2 = e^{-\Gamma t}$$

Here I have normalized the states as  $\langle M^+|M^+\rangle = 1$ .

Since  $M_M - i\Gamma/2$  is independent of  $t$ , we can compute it using the familiar covariant formulation of quantum field theory and in the following calculations I comply with the standard relativistic normalization of the meson states,

$$\langle M(\vec{p}')|M(\vec{p})\rangle = 2E (2\pi)^3 \delta^{(3)}(\vec{p}' - \vec{p}). \quad (67)$$



Fig. 4 Left: generic self energy  $\Sigma$  of a charged meson. Right:  $M^0 - \bar{M}^0$  mixing amplitude  $\Sigma_{12}$ .

The optical theorem tells us that  $M_M$  and  $-\Gamma/2$  are given by the real and imaginary parts of the self-energy  $\Sigma$  (depicted in the left diagram of Fig. 4), where

$$-i(2\pi)^4 \delta^{(4)}(\vec{p}' - \vec{p}) \Sigma = \frac{\langle M^+(\vec{p}') | S | M^+(\vec{p}) \rangle}{2M_M} \quad (68)$$

This defines  $\Sigma$  in the interaction picture, in the Schrödinger picture we must add the mass  $M_M$ , i.e. the ‘‘tree-level self-energy’’, to  $\Sigma$ . The factor of  $1/(2M_M)$  in Eq. (68) originates from the normalization in Eq. (67). The truncated self-energy diagram of a boson has mass dimension 2 and by dividing by  $2M_M$  we arrive at the correct mass dimension 1 for  $\Sigma = M_M - i\Gamma/2$ . From Eq. (66) we find

$$i \frac{d}{dt} |M^+(t)\rangle = (M_M - i\frac{\Gamma}{2}) |M^+(t)\rangle. \quad (69)$$

Now this equation can be generalized to a two-state system describing neutral meson mixing. We may view  $(|K\rangle, |\bar{K}\rangle)$  as a two component object with strangeness (or U-spin quantum number  $U_3 = \pm 1$ ) as an inner degree of freedom distinguishing these components. Then

$$i \frac{d}{dt} \begin{pmatrix} |M(t)\rangle \\ |\bar{M}(t)\rangle \end{pmatrix} = \Sigma \begin{pmatrix} |M(t)\rangle \\ |\bar{M}(t)\rangle \end{pmatrix} \quad (70)$$

where now  $\Sigma$  is the  $2 \times 2$  matrix defined as

$$-i(2\pi)^4 \delta^{(4)}(p'_i - p_j) \Sigma_{ij} = \frac{\langle i, \vec{p}'_i | S^{\text{SM}} | j, \vec{p}_j \rangle}{2M_M} \quad (71)$$

in the interaction picture with  $|1, \vec{p}_1\rangle = |M(\vec{p}_1)\rangle$  and  $|2, \vec{p}_2\rangle = |\bar{M}(\vec{p}_2)\rangle$ . In the Schrödinger picture used in Eq. (70)  $\Sigma$  gets an extra additive term and is to be read as  $\Sigma_S = \Sigma_I + M \cdot 1$  with the  $2 \times 2$  unit matrix 1. Since the shift between ‘‘I’’ and ‘‘S’’ is trivial and only affects equations describing time evolutions, I omit the corresponding index.

Recalling that any matrix can be written as the sum of a hermitian and an antihermitian matrix, we write

$$\Sigma = M - i \frac{\Gamma}{2} \quad (72)$$

with the *mass matrix*  $M = M^\dagger$  and the *decay matrix*  $\Gamma = \Gamma^\dagger$ . Then

$$M_{12} = \frac{\Sigma_{12} + \Sigma_{21}^*}{2}, \quad \frac{\Gamma_{12}}{2} = i \frac{\Sigma_{12} - \Sigma_{21}^*}{2}. \quad (73)$$

Again,  $\Sigma_{12}$  and the quantities derived from it here and below are different for the four cases  $M = K, B_{d,s}$ , and  $D$  and I drop the corresponding index.

The expressions on the RHS of Eq. (73) are called *dispersive* and *absorptive* parts of  $\Sigma_{12}$ , respectively. The right diagram in Fig. 4 generically represents all contributions to  $\Sigma_{12}$ . The operational definitions of dispersive and absorptive parts, mentioned already after Eq. (45), amount to factoring out all CKM elements (or other complex couplings when BSM theories are considered) and taking the imaginary and real part of the remainder for dispersive and absorptive part, respectively. To shed light on this we discuss the  $B_d - \bar{B}_d$  box diagram in Fig. 1 and write the  $B_d - \bar{B}_d$  amplitude as  $\Sigma_{12} = (V_{tb} V_{td}^*)^2 A_{\text{rest}}$ . This quantity describes a  $|2\rangle \equiv |\bar{B}\rangle \rightarrow |1\rangle \equiv |B\rangle$  transition in which a  $b$  quark enters the diagram and a  $\bar{b}$  quark leaves it. Now  $\Sigma_{21}$  in Eq. (73) instead describes the  $|B\rangle \rightarrow |\bar{B}\rangle$  transition which involves the box diagram in which the direction of all quark lines are reversed, so that the CKM factor is complex-conjugated w.r.t.  $\Sigma_{12}$ . The remainder of the amplitude is the same, because  $\Sigma_{12}$  and  $\Sigma_{21}$  are related by  $CP$  conjugation and there are no sources of  $CP$  violation beyond the CKM factors (or, in the case of a BSM theory, the complex coupling constants factored out). Thus  $\Sigma_{21} = (V_{tb}^* V_{td})^2 A_{\text{rest}}$  and we realize that  $\Sigma_{21}^*$  appearing in the definitions of dispersive and absorptive parts in Eq. (73) are both proportional to  $(V_{tb} V_{td}^*)^2$ . Thus

$$M_{12} = (V_{tb} V_{td}^*)^2 \text{Re } A_{\text{rest}} \quad \frac{\Gamma_{12}}{2} = -(V_{tb} V_{td}^*)^2 \text{Im } A_{\text{rest}}. \quad (74)$$

From the optical theorem we know that  $\text{Im } A_{\text{rest}} \neq 0$  requires contributions from on-shell intermediate states, so that only box diagrams with internal  $u, c$  quarks contribute to  $\Gamma_{12}$  for  $B_d - \bar{B}_d$  mixing.

The diagonal elements  $M_{11}$  and  $M_{22}$  are the (equal) masses of  $M$  and  $\bar{M}$  and are generated from the quark mass terms in the lagrangian  $L$  and from the binding energy of the strong interaction. Had we stayed in the interaction picture, these diagonal elements would only contain  $\Sigma_{11} = \Sigma_{22}$ , i.e. the electroweak contributions to the meson self-energy, which are tiny electroweak corrections to the meson masses

and completely negligible. Thus the extra term  $M_M \delta_{jk}$  in the Schrödinger picture puts the full meson mass into the diagonal elements of the mass matrix.

By contrast, the off-diagonal elements  $M_{12} = M_{21}^*$  and all elements of  $\Gamma$  stem from the weak interaction and are therefore tiny in comparison with  $M_{11}$  and  $M_{22}$ . The only reason why we can experimentally access  $M_{12}$  roots in the *CPT* theorem [8–10]: Applying *CPT* to Eq. (71), which maps  $\Sigma_{11} \leftrightarrow \Sigma_{22}$ , one finds

$$M_{11} = M_{22}, \quad \Gamma_{11} = \Gamma_{22}, \quad (75)$$

so that the eigenvalues of  $\Sigma$  are exactly degenerate for  $\Sigma_{12} = \Sigma_{21} = 0$ . Even the smallest  $\Sigma_{12}$  can lift the degeneracy and can lead to large meson-antimeson mixing.

The presented derivations of Eqs. (66) and (70) were developed in [101] and use a shortcut: I have avoided to prove that Eq. (69) holds with time-independent  $M$  and  $\Gamma$  and instead used the phenomenological input that we know the time-evolution of a decaying particle. However, Eq. (69) and the equivalent equation Eq. (66) with the exponential decay law are not valid exactly, but receive tiny (and phenomenologically irrelevant) corrections [102]. The same statement is true for Eqs. (70) and (72), a proper derivation of Eq. (70) using time-dependent perturbation theory for the weak interaction employs the so-called *Wigner-Weisskopf approximation* [6, 103]. Corrections to this approximation have been addressed in Ref. [104] and are below the  $10^{-10}$  level.

Eq. (70) is sometimes referred to as a “Schrödinger equation”, while the correct phrasing is “time evolution equation in the Schrödinger picture”. A Schrödinger equation involves a hamiltonian, but  $M - i\Gamma/2$  is not (the matrix representation of) a hamiltonian, because it is not hermitian. It is also not some piece of a hamiltonian acting in a 2-dimensional subspace of the full infinite-dimensional Fock space of particle physics, because the exponential decay described by  $\Gamma$  is an effective description of the  $M \rightarrow f$  transitions in Eq. (63).

I will now present the solution of Eq. (70). We can diagonalize  $\Sigma$  as

$$Q^{-1} \Sigma Q = \begin{pmatrix} M_L - i\Gamma_L/2 & 0 \\ 0 & M_H - i\Gamma_H/2 \end{pmatrix} \quad (76)$$

with

$$Q = \begin{pmatrix} p & p \\ q & -q \end{pmatrix} \quad \text{and} \quad Q^{-1} = \frac{1}{2pq} \begin{pmatrix} q & p \\ q & -p \end{pmatrix} \quad (77)$$

and  $|p|^2 + |q|^2 = 1$ . The ansatz in Eq. (77) (with just two coefficients  $p, q$ ) works because of  $\Sigma_{11} = \Sigma_{22}$ . Thus the eigenvectors of  $\Sigma$  in Eq. (71) are the columns of  $Q$ ,  $(p, q)^T$  and  $(p, -q)^T$ , which leads to the mass eigenstates [6]

$$|M_L\rangle = p|M\rangle + q|\bar{M}\rangle, \quad |M_H\rangle = p|M\rangle - q|\bar{M}\rangle. \quad (78)$$

$|M_{L,H}(t)\rangle$  obey an exponential decay law like  $|M^+(t)\rangle$  in Eq. (66) with  $(M_M, \Gamma)$  replaced by  $(M_{L,H}, \Gamma_{L,H})$ . Transforming back to the flavour basis gives

$$\begin{pmatrix} |M(t)\rangle \\ |\bar{M}(t)\rangle \end{pmatrix} = Q \begin{pmatrix} e^{-iM_L t - \Gamma_L t/2} & 0 \\ 0 & e^{-iM_H t - \Gamma_H t/2} \end{pmatrix} Q^{-1} \begin{pmatrix} |M\rangle \\ |\bar{M}\rangle \end{pmatrix} \quad (79)$$

The average mass  $m$  and average width  $\Gamma$  have been defined in Eq. (5) and the definitions of the mass and width difference can be found in Eq. (3). The matrix appearing in Eq. (79) can be compactly written as

$$Q \begin{pmatrix} e^{-iM_L t - \Gamma_L t/2} & 0 \\ 0 & e^{-iM_H t - \Gamma_H t/2} \end{pmatrix} Q^{-1} = \begin{pmatrix} g_+(t) & \frac{q}{p} g_-(t) \\ \frac{p}{q} g_-(t) & g_+(t) \end{pmatrix} \quad (80)$$

with

$$\begin{aligned} g_+(t) &= e^{-imt} e^{-\Gamma t/2} \left[ \cosh \frac{\Delta\Gamma t}{4} \cos \frac{\Delta M t}{2} - i \sinh \frac{\Delta\Gamma t}{4} \sin \frac{\Delta M t}{2} \right], \\ g_-(t) &= e^{-imt} e^{-\Gamma t/2} \left[ -\sinh \frac{\Delta\Gamma t}{4} \cos \frac{\Delta M t}{2} + i \cosh \frac{\Delta\Gamma t}{4} \sin \frac{\Delta M t}{2} \right]. \end{aligned} \quad (81)$$

Inserting Eq. (80) into Eq. (79) gives us the desired expression for meson-antimeson oscillations:

$$\begin{aligned} |M(t)\rangle &= g_+(t)|M\rangle + \frac{q}{p} g_-(t)|\bar{M}\rangle, \\ |\bar{M}(t)\rangle &= \frac{p}{q} g_-(t)|M\rangle + g_+(t)|\bar{M}\rangle, \end{aligned} \quad (82)$$

We verify  $g_+(0) = 1$  and  $g_-(0) = 0$  and find that  $g_\pm(t)$  has no zeros for  $t > 0$  if  $\Delta\Gamma \neq 0$ . Hence the two lifetimes  $1/\Gamma_L$  and  $1/\Gamma_H$  lead to a dispersion, so that an initially produced  $M$  will never turn into a pure  $\bar{M}$  or back into a pure  $M$ .

We will frequently encounter the combinations

$$\begin{aligned} |g_{\pm}(t)|^2 &= \frac{e^{-\Gamma t}}{2} \left[ \cosh \frac{\Delta\Gamma t}{2} \pm \cos(\Delta M t) \right], \\ g_+^*(t) g_-(t) &= \frac{e^{-\Gamma t}}{2} \left[ -\sinh \frac{\Delta\Gamma t}{2} + i \sin(\Delta M t) \right]. \end{aligned} \quad (83)$$

Note that  $M - i\Gamma/2$  is not a hermitian matrix, so that we cannot expect  $Q$  linking  $(|M\rangle, |\bar{M}\rangle)$  to  $(|M_L\rangle, |M_H\rangle)$  to be unitary. As a consequence, the mass eigenstates need not be orthogonal to each other, that is

$$\langle M_L | M_H \rangle = |p|^2 - |q|^2 \quad (84)$$

need not vanish. We can use this observation to find a criterion for  $CP$  violation. If  $CP$  is conserved in meson-antimeson mixing, then  $|M_{L,H}\rangle$  are eigenstates of the  $CP$  operator with different eigenvalues  $\pm 1$ . Since the  $CP$  operator is unitary, its eigenvectors are orthogonal and in this case therefore Eq. (84) must vanish. Thus we conclude that  $|q/p| \neq 1$  implies that  $CP$  is violated in  $|\Delta F| = 2$  transitions. This phenomenon is called  *$CP$  violation in mixing* and should not be confused with the mixing-induced  $CP$  violation defined by  $A_{CP}^{\text{mix}} \neq 0$  in Eq. (25). The latter quantity is specific to the studied  $M \rightarrow f$  decay mode, while  $CP$  violation in mixing is a universal effect, which only depends on  $|q/p|$  and therefore affects *all* decays of  $M$ .

$CPT$  transforms the state  $\alpha|M(\vec{p})\rangle + \beta|\bar{M}(\vec{p})\rangle$  to  $\alpha^*|\bar{M}(\vec{p})\rangle + \beta^*|M(\vec{p})\rangle$  times an arbitrary phase factor. Thus  $|M_{L,H}\rangle$  are not  $CPT$  eigenstates for  $|p| \neq |q|$ . Since  $CPT$  is a good symmetry of the SM, this looks strange. But there is no contradiction here, because  $|M_{L,H}\rangle$  are eigenstates of  $M - i\Gamma t/2$ , which is *not* a hamiltonian.

## 5.2 $\Delta M$ , $\Delta\Gamma$ , and $CP$ violation in mixing

I will next solve the eigenvalue problem in Eq. (76) to express  $\Delta M$ ,  $\Delta\Gamma$ ,  $p$  and  $q$  in terms of  $M_{12}$  and  $\Gamma_{12}$ .

The secular equation for the two eigenvalues  $\sigma_{L,H} = M_{L,H} - i\Gamma_{L,H}/2$  of  $\Sigma$  is  $(\Sigma_{11} - \sigma_{L,H})^2 - \Sigma_{12}\Sigma_{21} = 0$ . The two solutions of this equation therefore satisfy

$$(\sigma_H - \sigma_L)^2 = 4\Sigma_{12}\Sigma_{21}$$

or

$$(\Delta M + i\frac{\Delta\Gamma}{2})^2 = 4 \left( M_{12} - i\frac{\Gamma_{12}}{2} \right) \left( M_{12}^* - i\frac{\Gamma_{12}^*}{2} \right). \quad (85)$$

Taking real and imaginary part of this equation gives

$$(\Delta M)^2 - \frac{1}{4}(\Delta\Gamma)^2 = 4|M_{12}|^2 - |\Gamma_{12}|^2, \quad (86)$$

$$\Delta M \Delta\Gamma = -4 \operatorname{Re}(M_{12}\Gamma_{12}^*), \quad (87)$$

From Eq. (76) we further infer  $[Q^{-1}\Sigma Q]_{12} = [Q^{-1}\Sigma Q]_{21} = 0$ , which determines

$$\frac{q}{p} = -\frac{\Delta M + i\Delta\Gamma/2}{2M_{12} - i\Gamma_{12}} = -\frac{2M_{12}^* - i\Gamma_{12}^*}{\Delta M + i\Delta\Gamma/2}. \quad (88)$$

(The second solution, with opposite sign, is discarded by imposing  $\Delta M > 0$ .) For the simplification of Eqs. (86–88) it is useful to identify the physical quantities of the mixing problem in Eqs. (70) and (72). Rephasing  $|M\rangle$  or  $|\bar{M}\rangle$  cannot change the physics, but it changes the phases of  $M_{12}$ ,  $\Gamma_{12}$  and  $q/p$ , none of which can therefore have any physical meaning. Thus only

$$|M_{12}|, \quad |\Gamma_{12}|, \quad \text{and} \quad \phi \equiv \arg\left(-\frac{M_{12}}{\Gamma_{12}}\right). \quad (89)$$

can be physical quantities of meson-antimeson mixing. Eq. (87) then reads

$$\Delta M \Delta\Gamma = 4|M_{12}||\Gamma_{12}|\cos\phi. \quad (90)$$

We can easily solve Eqs. (86) and (90) to express  $\Delta M$  and  $\Delta\Gamma$ , which we want to confront with the measurements in Eqs. (10), (11), (20), (46), (48), (49), and (58), in terms of the theoretical quantities  $|M_{12}|$ ,  $|\Gamma_{12}|$  and  $\phi$ .

Before doing so, we recognize that a non-vanishing phase  $\phi$  is responsible for  $|q/p| \neq 1$  identified after Eq. (84) as a criterion for  $CP$  violation: By multiplying the two expression for  $q/p$  in Eq. (88) with each other we find

$$\left(\frac{q}{p}\right)^2 = \frac{2M_{12}^* - i\Gamma_{12}^*}{2M_{12} - i\Gamma_{12}} = \frac{M_{12}^*}{M_{12}} \frac{1 + i\left|\frac{\Gamma_{12}}{2M_{12}}\right|e^{i\phi}}{1 + i\left|\frac{\Gamma_{12}}{2M_{12}}\right|e^{-i\phi}}. \quad (91)$$

and this expression shows that  $\phi \neq 0, \pi$  indeed implies  $|q/p| \neq 1$ , i.e.  $CP$  violation in mixing.

Interestingly,  $CP$  violation in mixing is found small (i.e.  $\|q/p\| - 1 \ll 1$ ) for all of the four  $K$ ,  $B_{d,s}$  and  $D$  systems, to date it is only measured non-zero in  $K-\bar{K}$  mixing, while otherwise only upper bounds have been experimentally determined. I will discuss the experimental situation below in more detail. The smallness is expected in the SM:  $K-\bar{K}$  mixing and  $D-\bar{D}$  mixing are dominated by the  $2 \times 2$  Cabibbo matrix  $V_C$  and  $CP$  violation requires contributions which are sensitive to all three fermion generations. (With the real  $V_C$  of the two-generation SM, one immediately finds  $M_{12}$  and  $\Gamma_{12}$  real in Eq. (74).) The “leakage” to the third generation from  $V_{ts}V_{td}^*$   $\neq 0$  and  $V_{ub}V_{cb}^* \neq 0$  is small, suppressing  $\sin \phi$ . In the  $B-\bar{B}$  systems the line of arguments is as follows: Since  $\Gamma_{12}$  gets no contributions from the box diagram with top quarks, which in turn dominates  $M_{12}$ , we find  $|\Gamma_{12}/M_{12}| = \mathcal{O}(m_b^2/m_t^2)$ . Even BSM physics cannot change this, because the decays contributing to  $|\Gamma_{12}|$  are experimentally studied well enough to exclude order-of-magnitude enhancements. Thus the second term in the numerator and denominator of Eq. (91) is small, irrespective of the value of  $\phi$ , and  $|q/p| \simeq 1$  for  $B_d$  and  $B_s$  mesons.

It is useful to define the quantity  $a_{fs}$  through

$$\left| \frac{q}{p} \right|^2 = 1 - a_{fs}. \quad (92)$$

From the discussion above we understand that  $a_{fs}$  quantifies  $CP$  violation in meson-antimeson mixing. For all neutral meson complexes we know that  $a_{fs}$  is very small from the experimental numbers quoted in Secs. 5.3 and 6. By expanding  $(q/p)^2$  in Eq. (91) in terms of  $\phi$  or  $\Gamma_{12}/M_{12}$  we find

$$a_{fs} = \frac{4|\Gamma_{12}| |M_{12}|}{4|M_{12}|^2 + |\Gamma_{12}|^2} \phi + \mathcal{O}(\phi^2), \quad \text{for } K-\bar{K} \text{ mixing and } D-\bar{D} \text{ mixing} \quad (93)$$

$$a_{fs} = \text{Im} \frac{\Gamma_{12}}{M_{12}} + \mathcal{O}\left(\left(\text{Im} \frac{\Gamma_{12}}{M_{12}}\right)^2\right) = \left| \frac{\Gamma_{12}}{M_{12}} \right| \sin \phi, \quad \text{for } B-\bar{B} \text{ mixing}. \quad (94)$$

With this result it is straightforward to solve Eqs. (86) and (90) for  $\Delta M$  and  $\Delta \Gamma$ . Incidentally, in both cases we have

$$\Delta M \simeq 2|M_{12}|, \quad (95)$$

$$\Delta \Gamma \simeq 2|\Gamma_{12}| \cos \phi. \quad (96)$$

which holds up to corrections of order  $\phi^2$  for Kaons and  $D$  mesons and corrections of order  $|\Gamma_{12}/M_{12}|^2$  for  $B$  mesons. In the SM we can replace  $\cos \phi$  by 1 not only in  $K-\bar{K}$  mixing but also in  $B-\bar{B}$  mixing, but there the smallness of  $\|q/p\| - 1$  is already implied by  $|\Gamma_{12}/M_{12}| \ll 1$  so that the experimental information on the smallness of  $\|q/p\| - 1$  leaves some space for non-negligible BSM contributions to  $\phi$ . Note that in  $D-\bar{D}$  mixing we have  $\cos \phi \approx -1$ , because  $\Delta \Gamma_D/\Delta M_D < 0$  is measured.

Importantly, in all neutral meson complexes one deduces from Eq. (91) that

$$\frac{q}{p} = -\frac{M_{12}^*}{|M_{12}|} [1 + \mathcal{O}(a_{fs})]. \quad (97)$$

That is, the phase of  $-q/p$  is essentially given by the phase of the box diagram in Fig. 1.  $q/p$  depends on phase conventions and is specific to the choice for the  $CP$  transformation in Eq. (23). In documents with opposite signs compared to Eq. (23) you find  $q/p$  in Eq. (97) without the “–” sign. Since  $B-\bar{B}$  mixing is dominated by the box diagram with internal tops we readily infer

$$\frac{q}{p} = -\frac{V_{tb}^* V_{tq}}{V_{tb} V_{tq}^*} = -\exp[i \arg(V_{tb}^* V_{tq})^2] \quad \text{for } B_q-\bar{B}_q \text{ mixing with } q = d, s \quad (98)$$

up to tiny corrections of order  $a_{fs}$ . Eqs. (95) and (96) further show that  $\Delta M$  is trivially related to  $|M_{12}|$  and  $\Delta \Gamma$  is essentially determined by  $|\Gamma_{12}|$ . Since  $-\Gamma_{12}/2$  is the absorptive part of  $\Sigma_{12}$ , which is the  $\bar{M} \rightarrow M$  transition amplitude, we verify that  $\Gamma_{12}$  is composed of all decays into final states  $f$  which are common to  $M$  and  $\bar{M}$  from the optical theorem:

$$\Gamma_{12} = \sum_f \langle M | f \rangle \langle f | \bar{M} \rangle = \sum_f A_f^* \bar{A}_f \quad (99)$$

We have found this feature already in the discussion of  $\Delta \Gamma$  around Eq. (45). Indeed, for  $|q/p| = 1$  one has  $|q| = |p| = 1/\sqrt{2}$  and inserting  $\alpha_H = \alpha_L = p$  and  $\beta_L = -\beta_H = q$  into Eq. (45) gives

$$\begin{aligned} \Delta \Gamma &= \Gamma_L - \Gamma_H = 4 \text{Re} \left( p^* q \sum_f A_f^* \bar{A}_f \right) \stackrel{\text{Eq. (99)}}{=} 2 \text{Re} \left( \frac{q}{p} \Gamma_{12} \right) \stackrel{\text{Eq. (97)}}{=} -2 \text{Re} \left( \frac{M_{12}^*}{|M_{12}|} \Gamma_{12} \right) \\ &= -2 \text{Re} \left( \frac{M_{12}^*}{|M_{12}|} \frac{|\Gamma_{12}|^2}{\Gamma_{12}^*} \right) \stackrel{\text{Eq. (89)}}{=} 2 \text{Re} \left( e^{-i\phi} |\Gamma_{12}| \right) = 2|\Gamma_{12}| \cos \phi \end{aligned} \quad (100)$$

in agreement with Eq. (96).

We can apply our formalism also to the width difference between  $CP$  eigenstates of the meson-antimeson systems. This is unambiguously only possible in a theory which conserves  $CP$ . But the hierarchy of the CKM matrix permits the definition of such eigenstates also in the SM: In the dominant CKM-favored tree-level decays modes we can neglect direct  $CP$  violation, because the required interfering second amplitude is CKM-suppressed. Furthermore, the amplitudes of all such CKM-favored decays can be arranged to have weak phases essentially equal to 0 or  $\pi$ ; the standard CKM phase convention, which I use in the following discussion, has this property. I exemplify the topic with  $B_s$  mesons, because it was studied for this case [88]. For example, the  $b \rightarrow c\bar{c}s$  and  $b \rightarrow c\bar{u}\bar{d}$  amplitudes have both essentially real

CKM factors. Thus we can define  $|B_s^{\text{even}}\rangle$  and  $|B_s^{\text{odd}}\rangle$  as orthogonal states with the property  $B_s^{\text{odd}} \not\rightarrow f_{\text{CP}+}$  and  $B_s^{\text{even}} \not\rightarrow f_{\text{CP}-}$  in CKM-favored decays, where  $f_{\text{CP}+}$  and  $f_{\text{CP}-}$  denote CP-even and CP-odd states, respectively. Thus e.g.  $B_s^{\text{even}}$  can decay to  $D_s^+ D_s^-$ , while  $B_s^{\text{odd}}$  cannot, as long as the CKM-suppressed penguin amplitude is neglected. In the standard CKM phase convention in which the considered decay amplitudes are real, one finds with Eq. (23):

$$|B_s^{\text{even}}\rangle = \frac{|B_s\rangle - |\bar{B}_s\rangle}{\sqrt{2}}, \quad |B_s^{\text{odd}}\rangle = \frac{|B_s\rangle + |\bar{B}_s\rangle}{\sqrt{2}}. \quad (101)$$

Note that our derivation of the mass eigenstates in Eq. (78) does not tell us anything about their relationship to the  $CP$  eigenstates in Eq. (101), i.e. whether  $|\langle D_s^+ D_s^- | B_{s,L} \rangle|^2 > |\langle D_s^+ D_s^- | B_{s,H} \rangle|^2$  or not, that is, whether  $B_{s,L}$  or  $B_{s,H}$  is closer to  $B_s^{\text{even}}$ . Now we repeat the derivation in Eq. (100) with the  $CP$  eigenstates; for this we simply replace  $p$  and  $q$  by  $+1$  and  $-1$ , respectively, in our derivation of Eq. (100) and find

$$\Delta\Gamma_{\text{CP}} \equiv \Gamma(B_s^{\text{even}}) - \Gamma(B_s^{\text{odd}}) = \sum_f \left( |\langle f | B_s^{\text{even}} \rangle|^2 - |\langle f | B_s^{\text{odd}} \rangle|^2 \right) = -2 \text{Re } \Gamma_{12}, \quad (102)$$

valid for the standard CKM phase convention.  $\Gamma_{12}$  in the  $B_s - \bar{B}_s$  mixing system is dominated by  $b \rightarrow c\bar{c}s$  decays, so that  $\Gamma_{12}$  has the essentially real CKM factor  $(V_{cb} V_{cs}^*)^2$  and one can omit the “Re” in Eq. (102). In Ref. [88] it is explained how one can measure  $\Gamma(B_s^{\text{even/odd}})$ . We realize that  $\Delta\Gamma_{\text{CP}}$  is a mixing observable which probes  $\Gamma_{12}$  but is not sensitive to  $M_{12}$ . The SM prediction discussed in Sec. 6 predicts  $\Gamma_{12} < 0$  and BSM physics cannot be so large that this sign is flipped. Thus, independently of any BSM physics in  $M_{12}$ , theory predicts  $\Delta\Gamma_{\text{CP}} > 0$ , so that the  $CP$ -even eigenstate is shorter-lived. The measurement of sign  $\Delta\Gamma_s > 0$  (predicted in the SM as well) was needed to identify  $B_{s,L}$  with the shorter-lived eigenstate and  $\Delta\Gamma_{\text{CP}} > 0$  means that it is also mostly CP-even. In the limit  $\cos\phi = 1$   $CP$  is a good symmetry and the mass and  $CP$  eigenstates coincide.  $\Delta\Gamma_{\text{CP}} > 0$  has been established experimentally as a byproduct of the analyses determining  $\phi_{CP,B_s}^{\text{mix}}$  in Eq. (55) together with  $1/\Gamma_{L,H}$ , which find that the  $\langle \bar{B}_s \rangle$  decays into the CP-even final states  $(J/\psi\phi)_{l=0,2}$  with a lifetime  $1/\Gamma_L$ . The measurement of  $\Delta\Gamma_{\text{CP}}$  in the  $B_s$  system, described in Ref. [88], was originally proposed to determine  $\cos\phi$  through a comparison of  $\Delta\Gamma_{\text{CP}}$  in Eq. (102) and  $\Delta\Gamma$  in Eq. (96). This is of little interest today, because we know that  $\cos\phi$  is close to 1 from bounds on  $|\sin\phi|$  discussed below.

Interestingly, in  $D - \bar{D}$  mixing it is also experimentally firmly established that the shorter-lived eigenstate is dominantly  $CP$ -even [37], which seems to be a common feature of all four meson-antimeson systems. So while we cannot calculate  $\Gamma_{12}$  reliably for  $D - \bar{D}$  mixing, experiment tells us that  $\Gamma_{12} < 0$  from Eq. (102). In the  $B_d - \bar{B}_d$  case  $\Delta\Gamma_{\text{CP}} > 0$  is a SM prediction and not yet verified experimentally.  $B_d - \bar{B}_d$  mixing is special, because the  $CP$  eigenstates defined through  $B_d^{\text{odd}} \not\rightarrow D^+ D^-$  are not close to the mass eigenstates, because  $M_{12}$  has the phase  $2\beta$  in the standard phase convention, so that in the SM one has  $|\langle B_d^{\text{even}} | B_{s,\text{short}} \rangle|^2 = (1 + \cos(2\beta))/2$  and  $|\langle B_d^{\text{even}} | B_{s,\text{long}} \rangle|^2 = (1 - \cos(2\beta))/2$  [88, 105]. This factor is taken into account when  $|\Delta\Gamma_d|$  is constrained from lifetime measurements in  $\bar{B}_d \rightarrow J/\psi K_{\text{short}}$  in Eq. (46).

Next I discuss  $CP$  violation in mixing, which we have identified in Eq. (84) as a consequence of  $|q/p| \neq 1$ . The standard way to define the corresponding  $CP$  asymmetry employs the flavor-specific decays  $M \rightarrow f_{\text{fs}}$  and  $\bar{M} \rightarrow \bar{f}_{\text{fs}}$  with  $\bar{M} \not\rightarrow f_{\text{fs}}$  and  $\bar{M} \not\rightarrow \bar{f}_{\text{fs}}$ . With our result in Eq. (82) for the states  $|M(t)\rangle$  and  $|\bar{M}(t)\rangle$  and Eq. (83) we can calculate the time-dependent decay rates defined in Eq. (21) for the decays of interest:

$$\Gamma(M(t) \rightarrow f_{\text{fs}}) = |\langle f_{\text{fs}} | M(t) \rangle|^2 = |g_+(t)|^2 |A_{f_{\text{fs}}}|^2 = |A_{f_{\text{fs}}}|^2 \frac{e^{-\Gamma t}}{2} \left[ \cosh \frac{\Delta\Gamma t}{2} + \cos(\Delta M t) \right] \quad (103)$$

$$\begin{aligned} \Gamma(M(t) \rightarrow \bar{f}_{\text{fs}}) = |\langle \bar{f}_{\text{fs}} | M(t) \rangle|^2 &= \left| \frac{q}{p} \right|^2 |g_-(t)|^2 |\bar{A}_{\bar{f}_{\text{fs}}}|^2 = \left| \frac{q}{p} \right|^2 |\bar{A}_{\bar{f}_{\text{fs}}}|^2 \frac{e^{-\Gamma t}}{2} \left[ \cosh \frac{\Delta\Gamma t}{2} - \cos(\Delta M t) \right] \\ &= (1 - a_{\text{fs}}) \frac{e^{-\Gamma t}}{2} \left[ \cosh \frac{\Delta\Gamma t}{2} - \cos(\Delta M t) \right] \end{aligned} \quad (104)$$

$$\begin{aligned} \Gamma(\bar{M}(t) \rightarrow f_{\text{fs}}) = |\langle f_{\text{fs}} | \bar{M}(t) \rangle|^2 &= \left| \frac{p}{q} \right|^2 |g_-(t)|^2 |A_{f_{\text{fs}}}|^2 = \left| \frac{p}{q} \right|^2 |A_{f_{\text{fs}}}|^2 \frac{e^{-\Gamma t}}{2} \left[ \cosh \frac{\Delta\Gamma t}{2} - \cos(\Delta M t) \right] \\ &= (1 + a_{\text{fs}}) \frac{e^{-\Gamma t}}{2} \left[ \cosh \frac{\Delta\Gamma t}{2} - \cos(\Delta M t) \right] \end{aligned} \quad (105)$$

$$\Gamma(\bar{M}(t) \rightarrow \bar{f}_{\text{fs}}) = |\langle \bar{f}_{\text{fs}} | \bar{M}(t) \rangle|^2 = |g_+(t)|^2 |\bar{A}_{\bar{f}_{\text{fs}}}|^2 = |\bar{A}_{\bar{f}_{\text{fs}}}|^2 \frac{e^{-\Gamma t}}{2} \left[ \cosh \frac{\Delta\Gamma t}{2} + \cos(\Delta M t) \right] \quad (106)$$

I have neglected  $O(a_{\text{fs}}^2)$  corrections in Eq. (105) and will do so from now on. From these four equations one can extract  $a_{\text{fs}}$ ,  $|\bar{A}_{\bar{f}_{\text{fs}}}|^2 / |A_{f_{\text{fs}}}|^2$ , and the overall normalization. The second quantity determines the direct  $CP$  asymmetry

$$A_{CP}^{\text{dir}}(M \rightarrow \bar{f}_{\text{fs}}) = \frac{|A_{f_{\text{fs}}}|^2 - |\bar{A}_{\bar{f}_{\text{fs}}}|^2}{|A_{f_{\text{fs}}}|^2 + |\bar{A}_{\bar{f}_{\text{fs}}}|^2}, \quad (107)$$

which is different for every decay mode, while  $a_{\text{fs}}$  is universal and can be determined by combining many different decay channels. Since four observables depend on three quantities, there is redundant information in Eqs. (103–106), which can be used to eliminate experimental uncertainties. One may worry about the charge symmetry of the detector and add a parameter  $\epsilon_c$  for some unaccounted charge asymmetry to the formulae. Likewise one can do so with a parameter  $\epsilon_p$  for the production asymmetry between  $M$  and  $\bar{M}$ . As shown in Ref. [106] one cannot disentangle  $A_{CP}^{\text{dir}}(M \rightarrow \bar{f}_{\text{fs}})$  from  $\epsilon_c$ , as these quantities always appear in the same combination. However, it is possible to identify  $a_{\text{fs}}$  and  $\epsilon_p$  uniquely from the four measurements associated with Eqs. (103–106). Thus insufficient knowledge of neither  $\epsilon_c$  nor  $\epsilon_p$  is a

show-stopper for a measurement of  $a_{fs}$ . The time-dependent  $CP$  asymmetry associated with Eqs. (103–106) reads

$$a_{CP}(M(t) \rightarrow \bar{f}_{fs}) \equiv \frac{\Gamma(\bar{M}(t) \rightarrow f_{fs}) - \Gamma(M(t) \rightarrow \bar{f}_{fs})}{\Gamma(\bar{M}(t) \rightarrow f_{fs}) + \Gamma(M(t) \rightarrow \bar{f}_{fs})}. \quad (108)$$

One usually uses semileptonic decays to measure  $a_{fs}$ , i.e. one uses  $f_{fs} = X\ell^+\nu$  with e.g.  $X = D^-, D^{*-}$ , or the fully inclusive final state. Then  $a_{CP}(M(t) \rightarrow \bar{\ell}^+\nu)$  is called *semileptonic CP asymmetry*. Inserting Eqs. (104) and (105) into Eq. (108) gives

$$a_{CP}(M(t) \rightarrow \bar{f}_{fs}) = a_{fs} + A_{CP}^{\text{dir}}(M \rightarrow f_{fs}). \quad (109)$$

we note that the time-dependence cancels between numerator and denominator in Eq. (108). Moreover, the measurement of  $a_{fs}$  requires no flavor tagging [107]. Defining the *untagged decay rate* as

$$\Gamma[f, t] = \Gamma(M(t) \rightarrow f) + \Gamma(\bar{M}(t) \rightarrow f), \quad (110)$$

one finds from Eqs. (103–106) [88, 106]:

$$a_{fs,\text{unt}}(t) = \frac{\Gamma[f_{fs}, t] - \Gamma[\bar{f}_{fs}, t]}{\Gamma[f_{fs}, t] + \Gamma[\bar{f}_{fs}, t]} = A_{CP}^{\text{dir}}(M \rightarrow f_{fs}) + \frac{a_{fs}}{2} - \frac{a_{fs}}{2} \frac{\cos(\Delta M t)}{\cosh(\Delta \Gamma t/2)}. \quad (111)$$

Thus one does not have to pay the price of the lower statistics of a tagged sample. Unlike the tagged asymmetry in Eq. (109) the untagged version in Eq. (111) depends on  $t$ , which is a welcome feature to separate  $A_{CP}^{\text{dir}}$  from  $a_{fs}$  and signal from background. Note that at  $t = 0$  there is no sensitivity to  $a_{fs}$  as  $M$  needs time to mix into  $\bar{M}(t)$ . Adding charge and production asymmetries,  $\epsilon_c$  will only change the first term, while  $\epsilon_p$  only appears in the time-dependent second term [106]. One needs another observable to extract  $a_{fs}$  then, for example the “right-sign asymmetry”  $a_{\text{right}} \equiv (\Gamma(M(t) \rightarrow f_{fs}) - \Gamma(\bar{M}(t) \rightarrow \bar{f}_{fs})) / (\Gamma(M(t) \rightarrow f_{fs}) + \Gamma(\bar{M}(t) \rightarrow \bar{f}_{fs}))$  which equals  $A_{CP}^{\text{dir}}(M \rightarrow f_{fs})$  in the absence of  $\epsilon_c$  [106].

One can probe direct  $CP$  violation in  $M^\pm \rightarrow f_{fs}^\pm$  decays and, if one finds a null result, one may gain confidence that  $A_{CP}^{\text{dir}}(M \rightarrow f_{fs})$  also vanishes in the neutral mode of interest and that one further has  $\epsilon_c$  under control. If in addition there is no  $\epsilon_p$ <sup>8</sup>, one could use time-integrated measurements:

$$A_{fs,\text{unt}} \equiv \frac{\int_0^\infty dt [\Gamma[f_{fs}, t] - \Gamma[\bar{f}_{fs}, t]]}{\int_0^\infty dt [\Gamma[f_{fs}, t] + \Gamma[\bar{f}_{fs}, t]]} = \frac{a_{fs}}{2} \frac{x_M^2 - y_M^2}{x_M^2 - 1}, \quad (112)$$

with  $x_M \equiv \Delta M/\Gamma$  and  $y_M \equiv -\Delta \Gamma/\Gamma$  which we have already encountered for the case  $M = D$  in Eq. (56). For the semileptonic decays one often studies *dilepton asymmetries* at  $B$  factories by comparing the number  $N_{++}$  of decays  $(M(t), \bar{M}(t)) \rightarrow (f, f)$  with the number  $N_{--}$  of decays to  $(\bar{f}, \bar{f})$  for  $f = X\ell^+\nu_\ell$ . Then one finds  $a_{fs} = (N_{++} - N_{--}) / (N_{++} + N_{--})$  in time-integrated measurements. Also in  $K - \bar{K}$  mixing one studies time-independent  $CP$ -violating quantities;  $a_{fs}^K$  can be measured in semileptonic  $K_{\text{long}}$  decays. I will discuss  $a_{fs}^K$  and  $a_{fs}^D$  together with mixing-induced  $CP$  violation in Sec. 5.3.

The experimental situation for  $CP$  violation in  $B - \bar{B}$  mixing is as follows:

$$a_{fs}^{d,\text{exp}} = -0.0021 \pm 0.0017. \quad \text{HFLAV [37]} \quad (113)$$

$$a_{fs}^{s,\text{exp}} = -0.0006 \pm 0.0028, \quad \text{LHCb [108]} \quad (114)$$

The number for  $a_{fs}^{d,\text{exp}}$  is an average of BaBar, Belle, and LHCb measurements presented in Refs. [109–112] and earlier, less precise values from CLEO, OPAL, ALEPH, and DØ. All measurements have used semileptonic decays. Since we have precise data on  $\Delta \Gamma_s$  in Eq. (49), we can combine Eqs. (94–96) to place a bound on  $\phi_s$ , the  $CP$  phase in  $B_s - \bar{B}_s$  mixing:

$$a_{fs}^s = \left| \frac{\Gamma_{12}^s}{M_{12}^s} \right| \sin \phi_s = \frac{\Delta \Gamma_s}{\Delta M_s} \tan \phi_s = (4.40 \pm 0.20) \cdot 10^{-3} \tan \phi_s \quad (115)$$

so that Eq. (114) implies

$$\phi_s = -0.14^{+0.60}_{-0.52} = (-7.8^{+34}_{-30})^\circ, \quad (116)$$

showing that the  $CP$  phase in  $B_s - \bar{B}_s$  mixing is not very well constrained. In Sec. 6 we will see that the SM prediction for  $\phi_s$  is unmeasurably small, so that  $a_{fs}^s$  is a BSM topic. The measurement in Eq. (55) does not leave much space for BSM contributions to  $\arg M_{12}^s$  and BSM contributions to  $\arg \Gamma_{12}^s$  are somewhat exotic and can barely exceed a few percent, so that we need a reduction of the error in  $a_{fs}^s$  by at least a factor 10 compared to Eq. (114).

$a_{fs}^d$  can more easily be enhanced by BSM physics, because  $\Gamma_{12}^d$  is suppressed by two powers of  $\lambda$ . Furthermore,  $|M_{12}^d|$  in the denominator is 35 times smaller than  $|M_{12}^s|$  in  $a_{fs}^s$ , which lifts  $|a_{fs}^d|$  into a region which is better accessible by experiment.  $a_{fs}^d$  will be discussed in Sec. 6.

One can use many more decays beyond semileptonic ones, examples for flavor-specific decays to measure  $a_{fs}^d$  are  $B_d \rightarrow J/\psi K^+ \pi^-$ ,  $B_d \rightarrow D_s^+ D^-$ ,  $B_d \rightarrow D^- K^+$ , and multi-body decays with strangeness  $S = \pm 1$ . When studying those decays it is mandatory to include the

<sup>8</sup>There is no production asymmetry in  $B$  factories, but  $\epsilon_p \neq 0$  could occur from different acceptances of  $B_d$  and  $\bar{B}_d$  related to the asymmetric beam energies

$A_{CP}^{\text{dir}}$  term in time evolution formulae like Eq. (111). For  $a_{fs}^s$  the decays  $B_s \rightarrow D_s^- \pi^+$  and  $B_s \rightarrow D_s^- X$  with  $X = \pi^+ \pi^+ \pi^-$ ,  $\pi^+ K^+ K^-$ , or any other  $X$  with zero strangeness come to mind.

In summary, to fully determine the time evolution of any meson-antimeson system governed by Eqs. (70) and (72) one must calculate and measure the three quantities  $\Delta M$ ,  $\Delta\Gamma$ , and  $a_{fs}$ , the latter of which determines the fundamental  $CP$  phase  $\phi = \arg(-M_{12}/\Gamma_{12})$  which describes  $CP$  violation in mixing through  $|q/p| \neq 1$ . The relations between the phenomenological quantities  $\Delta M$ ,  $\Delta\Gamma$ ,  $a_{fs}$  and the theoretical quantities  $|M_{12}|$ ,  $|\Gamma_{12}|$ ,  $\phi$  are given in Eqs. (93) and (94) as well as Eqs. (95) and (96). The mentioned quantities are universal in the sense that they appear in the time-dependent decay rate of any  $M(t) \rightarrow f$  decay and do not depend on  $f$ . The smallness of  $a_{fs}$  is understood within the SM in  $K - \bar{K}$ ,  $D - \bar{D}$ , and  $B_s - \bar{B}_s$  mixing from the structure of the CKM matrix which aligns the phases of  $M_{12}$  and  $\pm\Gamma_{12}$  to a large degree and suppresses  $\sin\phi$ , and in  $B - \bar{B}$  mixing from the smallness of  $|\Gamma_{12}/M_{12}|$ , which holds also in BSM theories.  $\phi$  can be best measured in flavour-specific decays and the corresponding  $CP$  asymmetry  $a_{fs} \equiv 1 - |q/p|^2$  can be measured without flavor tagging.

### 5.3 Mixing-induced $CP$ asymmetries, $CP$ violation in $K - \bar{K}$ mixing, and time-dependence of exclusive decays

We have seen in Sec. 3 that mixing-induced  $CP$  asymmetries can provide a clean access to fundamental  $CP$ -violating quantities in the gold-plated decay modes, which essentially only involve a single  $CP$ -violating phase, i.e. the penguin pollution is suppressed or even absent. In the following we first study a mixing-induced  $CP$  asymmetry in Kaon physics. Subsequently, to derive expressions like Eqs. (41) and (54) for the mixing-induced  $CP$  asymmetries, we will study  $\Gamma(M(t)) \rightarrow f$  for a given final state  $f$ . I have already derived the corresponding expression for the case  $f = f_{fs}$  in Eqs. (103–106). In the beginning I take  $f$  arbitrary and will later specify to the case  $f = f_{CP}$  used in Eqs. (41) and (54).

Next I elaborate further on the decay amplitudes  $A_f = A(M \rightarrow f)$  and  $\bar{A}_f = A(\bar{M} \rightarrow f)$  introduced in Eq. (26) for  $f = f_{CP}$  and before Eq. (44) for any  $f$ . Their precise definition is

$$(2\pi)^4 \delta^{(4)}(p_M - p_f) A_f = N_f i \langle f | S | M \rangle, \quad (2\pi)^4 \delta^{(4)}(p_M - p_f) \bar{A}_f = N_f i \langle f | S | \bar{M} \rangle. \quad (117)$$

with the S-matrix

$$S \equiv \text{Texp} \left[ -i \int d^4x H_{\text{int}} \right] \quad (118)$$

involving  $H_{\text{int}} = -L_{\text{int}}$  which is the hamiltonian of the electroweak interaction of the SM (possibly amended by BSM terms), in the interaction picture. The decay rate is calculated from  $|A_f|^2$ ,  $|\bar{A}_f|^2$  and multiplies these expressions with inverse powers of  $\pi$  and other numerical factors. All these factors are absorbed into the normalization factor  $N_f$  such that  $\Gamma(M \rightarrow f) = |A_f|^2$ , cf. the calculation in Eqs. (44) and (45).  $N_f$  is the same for  $A_f$ ,  $\bar{A}_f$ ,  $A_{\bar{f}}$ , and  $\bar{A}_{\bar{f}}$ . In two-body decays the amplitudes are just numbers, because the kinematics is fixed. In multi-body decays the amplitudes depend on the kinematical variables specifying the studied point in the Dalitz plot. The variation of  $CP$  asymmetries over the Dalitz plot is extensively used in the experimental analyses, e.g. to find regions with a large strong phase difference between the tree and penguin amplitudes adding to  $A_f$  to maximize  $|A_{CP}^{\text{dir}}|$ . In decays into polarized final states (like  $J/\psi\phi$ ) or differential decay rates the amplitudes are further labeled with the polarization of the final state or, equivalently, with the angular momentum quantum number.

If we switch off QCD and replace the external hadrons by quark states, we can simply calculate  $A_f$  and  $\bar{A}_f$  in perturbation theory. In the case of tree-level decays, Eq. (170) is expanded to second order in  $H_{\text{int}}$  (i.e. to second order in  $g_w$ ) and we find Feynman diagrams with one virtual  $W$  boson connecting the quark line with the decaying  $b$ ,  $c$ , or  $s$  quark with a quark or lepton line.

The key quantity to describe mixing-induced  $CP$  violation is the combination

$$\lambda_f = \frac{q}{p} \frac{\bar{A}_f}{A_f}. \quad (119)$$

$\lambda_f$  encodes the essential feature of the interference of the  $M \rightarrow f$  and  $\bar{M} \rightarrow f$  decays:  $\arg \lambda_f$  is the relative phase between  $\bar{A}_f/A_f$  (stemming from the decay) and  $-M_{12}$  (from  $q/p$  in Eq. (97)).

In a first application, I discuss the decays of neutral Kaons into two charged or neutral pions. Kaons are simpler than  $D$  or  $B_{d,s}$ , because the observables are expressed in terms of the mass eigenstates, so that no explicit time appears in the formulae.

A neutral  $K$  or  $\bar{K}$  meson state is a superposition of  $K_H = K_{\text{long}}$  and  $K_L = K_{\text{short}}$ . At short times the decays of the  $K_{\text{short}}$  component of our Kaon beam will vastly dominate over the  $K_{\text{long}}$  decays and one can access the decay rates  $\Gamma(K_{\text{short}} \rightarrow \pi\pi)$  for  $\pi\pi = \pi^+ \pi^-$ ,  $\pi^0 \pi^0$ . At large times, say, after 20 times the  $K_{\text{short}}$  lifetime, our beam is practically a pure  $K_{\text{long}}$  beam and we can study the  $CP$ -violating  $\Gamma(K_{\text{long}} \rightarrow \pi\pi)$  decays. For this discussion I switch to the eigenbasis of strong isospin  $I$ :

$$\begin{aligned} |\pi^0 \pi^0\rangle &= \sqrt{\frac{1}{3}} |\pi\pi\rangle_{I=0} - \sqrt{\frac{2}{3}} |\pi\pi\rangle_{I=2}, \\ |\pi^+ \pi^-\rangle &= \sqrt{\frac{2}{3}} |\pi\pi\rangle_{I=0} + \sqrt{\frac{1}{3}} |\pi\pi\rangle_{I=2}, \end{aligned} \quad (120)$$

The strong interaction respects strong-isospin symmetry to an accuracy of typically 2%, so that we can neglect any rescattering between the  $I = 0$  and  $I = 2$  states. Any *direct*  $CP$  violation requires two interfering amplitudes which differ in their weak and strong phases. Since we can neglect all final states beyond  $\pi^+ \pi^-$  and  $\pi^0 \pi^0$ , we encounter a two-state problem in which  $|\pi\pi\rangle_{I=0}$  can only scatter elastically into itself and the same statements holds for  $|\pi\pi\rangle_{I=2}$ . Consequently, neither strong-isospin eigenstate can interfere with another state and no direct  $CP$

violation contributes to the famous  $CP$ -violating quantity

$$\epsilon_K \equiv \frac{\langle (\pi\pi)_{I=0} | K_{\text{long}} \rangle}{\langle (\pi\pi)_{I=0} | K_{\text{short}} \rangle}. \quad (121)$$

Abbreviating  $A_0 \equiv A_{(\pi\pi)_{I=0}}$ ,  $\bar{A}_0 \equiv \bar{A}_{(\pi\pi)_{I=0}}$  and (see Eq. (119))  $\lambda_0 \equiv \lambda_{(\pi\pi)_{I=0}}$  I insert Eq. (78) into Eq. (121) to find

$$\epsilon_K = \frac{1 - \lambda_0}{1 + \lambda_0}. \quad (122)$$

The experimental value [1]

$$\epsilon_K^{\text{exp}} = e^{i\phi_\epsilon} (2.228 \pm 0.011) \times 10^{-3} \quad \text{with} \quad \phi_\epsilon = (43.5 \pm 0.5)^\circ = (0.97 \pm 0.01) \frac{\pi}{4}. \quad (123)$$

therefore allows us to determine  $\lambda_0$ , which in our example is apparently close to 1. The number in Eq. (123) is calculated Eq. (120) from the measured quantities  $A(K_{\text{long}} \rightarrow \pi^+ \pi^-)/A(K_{\text{short}} \rightarrow \pi^+ \pi^-)$  and  $A(K_{\text{long}} \rightarrow \pi^0 \pi^0)/A(K_{\text{short}} \rightarrow \pi^0 \pi^0)$  by expressing  $|\pi^+ \pi^- \rangle$  and  $|\pi^0 \pi^0 \rangle$  in terms of  $|\pi\pi\rangle_I$  with Eq. (120). In our case with  $|A_0| = |\bar{A}_0|$  (absence of direct  $CP$  violation in a  $K \rightarrow f_{\text{CP}}$  decay) we have  $|\lambda_0| = |q/p|$ . With Eq. (122) we find

$$\epsilon_K \simeq \frac{1}{2} [1 - \lambda_0] \simeq \frac{1}{2} \left( 1 - \left| \frac{q}{p} \right| - i \text{Im } \lambda_0 \right) \quad (124)$$

up to corrections of order  $\epsilon_K^2$ . Remarkably, from the real and imaginary part of  $\epsilon_K$  we infer two  $CP$ -violating quantities:

$$a_{\text{fs}}^K = 4 \text{Re } \epsilon_K = 2 \left( 1 - \left| \frac{q}{p} \right| \right) \quad (125)$$

and the deviation of  $\text{Im } \lambda_0$  from 0. We have already encountered the first quantity, thus  $\text{Re } \epsilon_K$  quantifies  $CP$  violation in mixing. The second quantity,  $\text{Im } \lambda_0$ , is sensitive to the studied final state and measures mixing-induced  $CP$  violation in the decay  $K \rightarrow (\pi\pi)_{I=0}$ .

In the further discussion I exploit two more features of Kaon physics: Firstly,  $\Delta\Gamma_K = \Gamma_{\text{short}}$  up to corrections of  $\Gamma_{\text{long}}/\Gamma_{\text{short}} = 0.002$ . Secondly,  $\Gamma_{\text{short}}$  is almost completely dominated by  $K_{\text{short}} \rightarrow (\pi\pi)_{I=0}$ . The second largest contribution is  $K_{\text{short}} \rightarrow (\pi\pi)_{I=2}$ , whose decay rate is smaller by a factor of 500. Thus

$$\Gamma_{12} = \sum_f \langle K | f \rangle \langle f | \bar{K} \rangle \simeq A_0^* \bar{A}_0 = |A_0|^2 \frac{\bar{A}_0}{A_0} \quad (126)$$

implying  $\bar{A}_0/A_0 = \Gamma_{12}/|\Gamma_{12}|$  and, using Eq. (88),

$$\lambda_0 \simeq -\frac{2M_{12}^{K*} - i\Gamma_{12}^{K*}}{\Delta M_K + i\Delta\Gamma_K/2} \frac{\Gamma_{12}^K}{|\Gamma_{12}^K|} = \frac{2|M_{12}^K| e^{-i\phi_K} + i|\Gamma_{12}^K|}{\Delta M_K + i\Delta\Gamma_K/2}, \quad \text{where } \phi_K = \arg \left( -\frac{M_{12}^K}{\Gamma_{12}^K} \right). \quad (127)$$

With Eqs. (95) and (96) we can trade  $M_{12}^K$  for  $\Delta M_K$  and  $\Gamma_{12}^K$  for  $\Delta\Gamma_K$ :

$$\lambda_0 \simeq 1 - i\phi_K \frac{\Delta M_K}{\Delta M_K + i\Delta\Gamma_K/2}, \quad \text{Im } \lambda_0 \simeq -\phi_K \frac{4\Delta M_K^2}{4\Delta M_K^2 + \Delta\Gamma_K^2}. \quad (128)$$

Here and I the following I neglect higher-order terms in  $\phi_K$ . In Eq. (93) we can also use Eqs. (95) and (96) to find

$$a_{\text{fs}}^K = \frac{4\Delta\Gamma_K \Delta M_K}{4\Delta M_K^2 + \Delta\Gamma_K^2} \phi_K \quad (129)$$

We can now relate  $\epsilon_K$  in Eq. (124) to the desired  $CP$  phase  $\phi_K$  and start with the phase:

$$\tan \phi_\epsilon = \frac{\text{Im } \epsilon_K}{\text{Re } \epsilon_K} = \frac{-2 \text{Im } \lambda_0}{a_{\text{fs}}^K} = \frac{2\Delta M_K}{\Delta\Gamma_K} = 0.947 \pm 0.002, \quad (130)$$

where I have used the experimental numbers in Eqs. (10) and (11) in the last step. We realize that  $\phi_\epsilon$  gives redundant information, it is determined by  $\Delta M_K$  and  $\Delta\Gamma_K$  and insensitive to the  $CP$  phase of interest. The result in Eq. (130), amounting to  $\phi_\epsilon = 43.45^\circ \pm 0.051^\circ$ , is in reasonable agreement with the experimental value in Eq. (123). One may use Eq. (130) to derive

$$\sin(\phi_\epsilon) = \frac{2\Delta M_K}{\sqrt{4\Delta M_K^2 + \Delta\Gamma_K^2}}, \quad (131)$$

and to express  $|q/p|$  and  $\text{Im } \lambda_0$  in Eq. (124) in terms of  $\phi_\epsilon$  to find the compact formula

$$\epsilon_K \simeq \frac{1}{2} \sin(\phi_\epsilon) e^{i\phi_\epsilon} \phi_K + O(\phi_K^2). \quad (132)$$

In the real part of this expression only  $O(\phi_K^2)$  terms have been neglected, while the imaginary part is also affected by approximating  $\Delta\Gamma_K$  by  $\Gamma(K_{\text{short}} \rightarrow (\pi\pi)_{I=0})$ , which might explain the  $\sim 2\sigma$  tension in  $\tan \phi_\epsilon$  between Eqs. (123) and (130).

Next we determine  $a_{\text{fs}}^K$  from a flavour-specific decay: With Eqs. (78) and (92) one easily finds

$$A_L \equiv \frac{\Gamma(K_{\text{long}} \rightarrow \ell^+ \nu \pi^-) - \Gamma(K_{\text{long}} \rightarrow \ell^- \bar{\nu} \pi^+)}{\Gamma(K_{\text{long}} \rightarrow \ell^+ \nu \pi^-) + \Gamma(K_{\text{long}} \rightarrow \ell^- \bar{\nu} \pi^+)} = \frac{1 - |q/p|^2}{1 + |q/p|^2} \simeq \frac{a_{\text{fs}}^K}{2} = \frac{1}{2} \sin(2\phi_\epsilon) \phi_K + O(\phi_K^2), \quad (133)$$

where I have used Eq. (131);  $A_L$  should be used with  $\phi_\epsilon = 43.45^\circ \pm 0.051^\circ$  or  $\sin \phi_\epsilon = 0.68776 \pm 0.00063$  found from  $\Delta\Gamma_K$  and  $\Delta M_K$  in Eqs. (10) and (11); and in the prefactor  $\sin \phi_\epsilon$  in Eq. (132) this should be done as well.

The data [1] are

$$A_L^{\text{exp}} = (3.32 \pm 0.06) \times 10^{-3} \quad (134)$$

and give

$$\phi_K^{\text{exp}} = (6.64 \pm 0.12) \times 10^{-3}. \quad (135)$$

This number is in good agreement with

$$\phi_K^{\text{exp}} = (6.48 \pm 0.03) \times 10^{-3}. \quad (136)$$

found from the experimental value for  $|\epsilon_K|$  in Eq. (132) with Eq. (132). The accuracy of the various approximation used in the derivations of the formulae above is discussed in [91].

Next I will generalize Eqs. (103–106) to the case of any decay  $M(t) \rightarrow f$ , thus  $f$  is not necessary flavor-specific or  $CP$  eigenstate. We seek

$$\Gamma(M(t) \rightarrow f) = |\langle f|M(t) \rangle|^2, \quad \Gamma(\bar{M}(t) \rightarrow f) = |\langle f|\bar{M}(t) \rangle|^2 \quad (137)$$

and inserting Eq. (82) leads to an expression involving  $A_f$  and  $\bar{A}_f$  as well as  $|g_\pm|^2$  and  $g_+(t) g_-(t)$  quoted in Eq. (83). The amplitudes appear in the normalization of  $\Gamma(M(t) \rightarrow f)$  and  $\Gamma(\bar{M}(t) \rightarrow f)$  and otherwise combine with  $q/p$  to  $\lambda_f$ :

$$\begin{aligned} \Gamma(M(t) \rightarrow f) &= N_f |A_f|^2 e^{-\Gamma t} \left\{ \frac{1 + |\lambda_f|^2}{2} \cosh \frac{\Delta\Gamma t}{2} + \frac{1 - |\lambda_f|^2}{2} \cos(\Delta M t) \right. \\ &\quad \left. - \text{Re } \lambda_f \sinh \frac{\Delta\Gamma t}{2} - \text{Im } \lambda_f \sin(\Delta M t) \right\}, \end{aligned} \quad (138)$$

$$\begin{aligned} \Gamma(\bar{M}(t) \rightarrow f) &= N_f |A_f|^2 \frac{1}{1 - a_{\text{fs}}} e^{-\Gamma t} \left\{ \frac{1 + |\lambda_f|^2}{2} \cosh \frac{\Delta\Gamma t}{2} - \frac{1 - |\lambda_f|^2}{2} \cos(\Delta M t) \right. \\ &\quad \left. - \text{Re } \lambda_f \sinh \frac{\Delta\Gamma t}{2} + \text{Im } \lambda_f \sin(\Delta M t) \right\}. \end{aligned} \quad (139)$$

We recall Eq. (18) for the definition of the  $CP$ -transformed state. In the  $M(t) \rightarrow \bar{f}$  decay rates it is advantageous to keep  $\bar{A}_{\bar{f}}$  while trading  $A_{\bar{f}}$  for  $\lambda_{\bar{f}}$ :

$$\begin{aligned} \Gamma(M(t) \rightarrow \bar{f}) &= N_f |\bar{A}_{\bar{f}}|^2 e^{-\Gamma t} (1 - a_{\text{fs}}) \left\{ \frac{1 + |\lambda_{\bar{f}}|^{-2}}{2} \cosh \frac{\Delta\Gamma t}{2} - \frac{1 - |\lambda_{\bar{f}}|^{-2}}{2} \cos(\Delta M t) \right. \\ &\quad \left. - \text{Re } \frac{1}{\lambda_{\bar{f}}} \sinh \frac{\Delta\Gamma t}{2} + \text{Im } \frac{1}{\lambda_{\bar{f}}} \sin(\Delta M t) \right\}, \end{aligned} \quad (140)$$

$$\begin{aligned} \Gamma(\bar{M}(t) \rightarrow \bar{f}) &= N_f |\bar{A}_{\bar{f}}|^2 e^{-\Gamma t} \left\{ \frac{1 + |\lambda_{\bar{f}}|^{-2}}{2} \cosh \frac{\Delta\Gamma t}{2} + \frac{1 - |\lambda_{\bar{f}}|^{-2}}{2} \cos(\Delta M t) \right. \\ &\quad \left. - \text{Re } \frac{1}{\lambda_{\bar{f}}} \sinh \frac{\Delta\Gamma t}{2} - \text{Im } \frac{1}{\lambda_{\bar{f}}} \sin(\Delta M t) \right\}. \end{aligned} \quad (141)$$

Eqs. (138–139) and Eqs. (140–141) are our master formulae to calculate any time-dependent decay rate of interest.

For  $f = f_{\text{fs}}$  we have  $\lambda_f = 1/\lambda_{\bar{f}} = 0$  and reproduce Eqs. (103–106). Defining the *mixing asymmetry*,

$$\mathcal{A}_0(t) = \frac{\Gamma(M(t) \rightarrow f) - \Gamma(M(t) \rightarrow \bar{f})}{\Gamma(M(t) \rightarrow f) + \Gamma(M(t) \rightarrow \bar{f})}, \quad (142)$$

we find to order  $a_{\text{fs}}$ :

$$\mathcal{A}_0(t) = \frac{\cos(\Delta M t)}{\cosh(\Delta\Gamma t/2)} + \frac{a_{\text{fs}}}{2} \left[ 1 - \frac{\cos^2(\Delta M t)}{\cosh^2(\Delta\Gamma t/2)} \right]. \quad (143)$$

Note that  $\mathcal{A}_0(t)$  is not a  $CP$  asymmetry. Instead  $\Gamma(M(t) \rightarrow f) \propto |\langle M|M(t) \rangle|^2$  quantifies the probability that an “unmixed”  $M$  decays to  $f$  at time  $t$ , while  $\Gamma(M(t) \rightarrow \bar{f}) \propto |\langle \bar{M}|M(t) \rangle|^2$  does so for the corresponding probability for the process  $M \rightarrow \bar{M} \rightarrow f$ . The asymmetry  $\mathcal{A}_0(t)$  can be employed to measure  $\Delta M$ . To determine the expression describing the ARGUS discovery of  $B_d - \bar{B}_d$  mixing one must integrate

Eqs. (139) and (141) over  $t$  to find the probabilities  $\int_0^\infty dt |\langle B_d | B_d(t) \rangle|^2$ ,  $\int_0^\infty dt |\langle \bar{B}_d | B_d(t) \rangle|^2$ , and their  $\bar{B}_d(t)$  counterparts, to which the numbers  $N_{+-}$ ,  $N_{++}$ , and  $N_{--}$  of opposite-sign and like-sign dilepton events are related. The integrated quantities determine  $x_d \equiv x_{B_d} = \Delta M_d \tau_{B_d}$  (and further depend on the tiny  $y_d \equiv -\Delta \Gamma_d \tau_{B_d}/2$ ), as we have seen in Eq. (19).

Next we apply our master formulae to decays into  $CP$  eigenstates,  $M \rightarrow f_{CP}$ , thus  $|\tilde{f}_{CP}\rangle = \eta_{CP,f} |f_{CP}\rangle$  with  $CP$  quantum number  $\eta_{CP,f} = \pm 1$ . I will set  $a_{fs}$  to zero, because we are interested in large  $CP$  asymmetries like in Eq. (41), compared to which  $a_{fs}$  is negligible. Thus, I use  $|q/p| = 1$  in the following. The time-dependent  $CP$  asymmetry reads

$$a_{f_{CP}}(t) = \frac{\Gamma(\bar{M}(t) \rightarrow f_{CP}) - \Gamma(M(t) \rightarrow f_{CP})}{\Gamma(\bar{M}(t) \rightarrow f_{CP}) + \Gamma(M(t) \rightarrow f_{CP})}. \quad (144)$$

Using Eq. (138) and Eq. (139) one finds

$$a_{f_{CP}}(t) = -\frac{A_{CP}^{\text{dir}} \cos(\Delta M t) + A_{CP}^{\text{mix}} \sin(\Delta M t)}{\cosh(\Delta \Gamma t/2) + A_{\Delta \Gamma} \sinh(\Delta \Gamma t/2)} + O(a_{fs}), \quad (145)$$

with (for  $f = f_{CP}$ )

$$A_{CP}^{\text{dir}} = \frac{1 - |\lambda_f|^2}{1 + |\lambda_f|^2}, \quad A_{CP}^{\text{mix}} = -\frac{2 \text{Im } \lambda_f}{1 + |\lambda_f|^2}, \quad A_{\Delta \Gamma} = -\frac{2 \text{Re } \lambda_f}{1 + |\lambda_f|^2}. \quad (146)$$

where I have used the notation of [88, 113]. The interpretation of  $A_{CP}^{\text{dir}}$  as the direct  $CP$  asymmetry is possible, because I have set  $|q/p| = 1$ , so that  $|\lambda_{f_{CP}}| = |\bar{A}_{f_{CP}}/A_{f_{CP}}|$ . Note that  $|A_{CP}^{\text{dir}}|^2 + |A_{CP}^{\text{mix}}|^2 + |A_{\Delta \Gamma}|^2 = 1$ . Experimentally one can study the time-dependence of  $a_f(t)$  and read off the coefficients of  $\cos(\Delta M t)$  and  $\sin(\Delta M t)$ , so that one can determine  $|\lambda_f|$  and  $\text{Im } \lambda_f$ .

In a gold-plated  $M \rightarrow f_{CP}$  decay we have  $|\lambda_{f_{CP}}| = 1$  and thus  $A_{CP}^{\text{dir}} = 0$  in Eqs. (145), (25), (53), and (146). Furthermore,

$$A_{CP}^{\text{mix}} = -\text{Im } \lambda_{f_{CP}}. \quad (147)$$

Moreover, the phase of

$$\frac{\bar{A}_{f_{CP}}}{A_{f_{CP}}} = -\frac{V_{q_1 b} V_{q_2 q_3}^* A_T}{V_{q_1 b}^* V_{q_2 q_3} A_T} = -\frac{V_{q_1 b} V_{q_2 q_3}^*}{V_{q_1 b}^* V_{q_2 q_3}} \quad (148)$$

is trivially read off from the phase of the CKM elements, which are here exemplified for a  $b \rightarrow q_1 \bar{q}_2 q_3$  decay.  $A_T$  is the “tree” amplitude introduced after Eq. (25). In  $B$  physics, where we also know the phase of  $q/p$  from Eq. (98), we can therefore directly relate the measured  $\text{Im } \lambda_{f_{CP}}$  to phases of CKM elements, if  $M \rightarrow f_{CP}$  is gold-plated.

In  $B_d \rightarrow J/\psi K^- [\rightarrow \pi^+ \pi^-]$  one finds (with  $\eta_{J/\psi K^- [\rightarrow \pi^+ \pi^-]} = -1$ )

$$\lambda_{J/\psi K_{\text{short}}} = \underbrace{-\frac{V_{tb}^* V_{td}}{V_{tb}^* V_{td}}}_{\text{from } -\frac{q}{p}} \underbrace{\frac{V_{cb} V_{cs}^* V_{us} V_{ud}^*}{V_{cb}^* V_{cs} V_{us}^* V_{ud}}}_{\text{from } -\frac{\bar{A}_{B_d \rightarrow J/\psi K}}{A_{B_d \rightarrow J/\psi K}} \frac{\bar{A}_{K \rightarrow \pi\pi}}{A_{K \rightarrow \pi\pi}}} \quad (149)$$

$$\simeq -e^{-i2\beta} \quad (150)$$

Thus

$$A_{CP}^{\text{mix}}(B_d \rightarrow J/\psi K_{\text{short}}) = -\text{Im } \lambda_{J/\psi K_{\text{short}}} = -\sin(2\beta) \quad (151)$$

We had motivated this result earlier from considerations of the box diagram and using the standard CKM phase convention for  $V$ , for which the second factor in Eq. (149) is real. In Eq. (40) the result of Eq. (149) was quoted as  $\phi_{CP, B_d}^{\text{mix}} = 2\beta$ . The same derivation for  $A_{CP}^{\text{mix}}(B_s \rightarrow (J/\psi \phi)_l)$  reads

$$\lambda_{(J/\psi \phi)_l} = (-1)^l \frac{V_{tb}^* V_{ts} V_{cb} V_{cs}^*}{V_{tb}^* V_{ts} V_{cb}^* V_{cs}} = (-1)^l e^{i2\beta_s} \quad (152)$$

$$A_{CP}^{\text{mix}}(B_s \rightarrow (J/\psi \phi)_l) = -\text{Im } \lambda_{(J/\psi \phi)_l} = -(-1)^l \sin(2\beta_s) \quad (153)$$

$$A_{\Delta \Gamma} = -\text{Re } \lambda_{(J/\psi \phi)_l} = -(-1)^l \cos(2\beta_s) \quad (154)$$

which was quoted as  $\phi_{CP, B_s}^{\text{mix}} = -2\beta_s$  in Eq. (51). We further recognize  $A_{\Delta \Gamma}$  in Eq. (53).

One can also identify gold-plated modes in  $B_{d,s}$  decays to  $CP$  non-eigenstates [114]. For example,  $B_s \rightarrow D_s^- K^+$  is a  $\bar{b} \rightarrow \bar{c} u \bar{s}$  decay interfering with  $\bar{B}_s \rightarrow D_s^- K^+$ , which is a  $b \rightarrow u \bar{c} s$  mode [92, 93, 115, 116]. (The valence quark  $s$ ,  $\bar{s}$  makes the final state a  $u \bar{c} s \bar{s}$  state, with the  $s$  and  $\bar{s}$  ending up in  $D_s^-$  and  $K^+$ , permitting the mentioned interference.) The mentioned decay mode is gold-plated, because there is no penguin contribution. Since  $f = D_s^- K^+$  is not a  $CP$  eigenstate, we cannot expect  $|\bar{A}_f/A_f| = 1$  and  $(|\bar{A}_f|^2 - |A_f|^2)/(|\bar{A}_f|^2 + |A_f|^2)$  is not a  $CP$  asymmetry. In studies of decays to  $CP$  non-eigenstates one fits the four expressions in Eqs. (138–141) to the four decay modes, in the exemplified decay these are  $B_s(t) \rightarrow D_s^- K^+$ ,  $\bar{B}_s(t) \rightarrow D_s^- K^+$ ,  $B_s(t) \rightarrow D_s^+ K^-$ , and  $\bar{B}_s(t) \rightarrow D_s^+ K^-$ . The ratio  $\bar{A}_f/A_f$  not only involves the  $CP$  phase of interest, but also a strong phase  $\delta$ . While  $\delta$  cancels from  $\lambda_{f_{CP}}$  in decays to  $CP$  eigenstates, this is not the case for

$CP$  non-eigenstates, where  $\bar{A}_f$  and  $A_f$  are completely unrelated. Studying the four decay rates one can extract four quantities, which are  $\arg \lambda_{D_s^+ K^+} = -\gamma - \phi_{CP, B_s}^{\text{mix}} + \delta$ ,  $\arg \lambda_{D_s^+ K^-} = -\gamma - \phi_{CP, B_s}^{\text{mix}} - \delta$ ,  $|\lambda_{D_s^+ K^+}| = 1/|\lambda_{D_s^+ K^-}|$ , and the overall normalization [92, 93, 115, 116]. The LHCb analysis of  $(\bar{B}_s(t) \rightarrow D_s^\mp K^\pm)$  has found [109]

$$\gamma + \phi_{CP, B_s}^{\text{mix}} = (79^{+12}_{-11})^\circ \quad (155)$$

With  $\phi_{CP, B_s}^{\text{mix}}$  from Eq. (55) this complies with the result found for  $\gamma$  from other measurements, but the large error in Eq. (155) currently limits the information on  $\phi_{CP, B_s}^{\text{mix}}$  or  $\gamma$  from this measurement. Unlike in  $B_d \rightarrow J/\psi K_s$  and  $B_s \rightarrow J/\psi \phi$ , there is no penguin pollution at all in decays like  $B_s(t) \rightarrow D_s^\mp K^\pm$ , in which mixing-induced  $CP$  violation stems from the interference of  $b \rightarrow c\bar{s}$  and  $\bar{b} \rightarrow c\bar{s}$  (or in the corresponding decays with  $s \rightarrow d$ ) amplitudes.

To avoid penguin pollution, one can also exploit the interference of  $b \rightarrow c\bar{s}$  and  $b \rightarrow u\bar{s}$  amplitudes in decays to  $\bar{D}$ , in which the  $D$  meson is identified in a  $CP$  eigenstate like  $\pi^+\pi^-$  [47], which also works for direct  $CP$  asymmetries [48]. The penguin pollution in  $B_d \rightarrow J/\psi K_s$  and  $B_s \rightarrow J/\psi \phi$  is discussed above after Eqs. (43) and (55). In the future one could precisely determine  $\phi_{CP, B_{d,s}}^{\text{mix}}$  (together with  $\gamma$ ) from  $B_d \rightarrow \bar{D}K_{\text{short}}$  and  $B_s \rightarrow \bar{D}\phi$ , where no penguin pollution is present. Another issue concerns the neutral Kaon: In future more precise measurements one may further wonder whether the  $CP$  violation in  $K-\bar{K}$  mixing will lead to a bias in the extraction of  $2\beta$  from  $B_d \rightarrow J/\psi K[\rightarrow \pi^+\pi^-]$ . If the  $K$  meson does not decay instantaneously, it undergoes  $K-\bar{K}$  oscillations, which introduces some sensitivity to  $\epsilon_K$ . This effect, however, is calculable and one can correct for it [117, 118].

Flavor tagging at a hadron collider costs statistics, but one can exploit the lifetime difference  $\Delta\Gamma_s$  to determine the cosines of  $CP$ -violating phases of mixing-induced  $CP$  asymmetries from *untagged decays*, as pointed out by Dunietz [90]. We can add Eqs. (138) and (139) to find the untagged decay rate, which was defined in Eq. (110). For clarity, I express the result in terms of  $\Gamma_{L,H} = \Gamma_s \pm \Delta\Gamma_s/2$ :

$$\begin{aligned} \Gamma[f, t] &= A e^{-\Gamma_L t} + B e^{-\Gamma_H t} \\ \text{with } A = A(f) &= \frac{|A_f|^2}{2} (1 + |\lambda_f|^2) (1 - A_{\Delta\Gamma}) = \frac{|A_f|^2}{2} |1 + \lambda_f|^2 \\ B = B(f) &= \frac{|A_f|^2}{2} (1 + |\lambda_f|^2) (1 + A_{\Delta\Gamma}) = \frac{|A_f|^2}{2} |1 - \lambda_f|^2 \end{aligned} \quad (156)$$

where I have used Eq. (146). With the precisely measured  $\Gamma_{L,H}$  we can fit the measured time evolution of a chosen  $(\bar{B}_s \rightarrow f)$  decay to Eq. (156) to extract  $A(f)$  and  $B(f)$ . The ratio  $A(f)/B(f)$ , from which  $|A_f|^2$  drops out, provides information on  $\lambda_f$  without determining it completely. If one fits the time evolution to a single exponential  $\exp(-i\Gamma_{\text{eff}}t)$ , one can calculate  $A(f)/B(f)$  from  $\Gamma_{\text{eff}}$  [88, 119], one therefore often calls this approach *effective lifetime method*. It is, however, safer to fit the time evolution to the two-exponential formula than to use  $\Gamma_{\text{eff}}$ , which needs a good control of detection efficiencies.

In gold-plated  $B_s \rightarrow f_{CP}$  decays, we can use  $|\lambda_{f_{CP}}| = 1$  to infer  $A_{\Delta\Gamma} = -\text{Re } \lambda_{f_{CP}}$  from Eq. (146), so that

$$\begin{aligned} A = A(f_{CP}) &= |A_{f_{CP}}|^2 (1 + \text{Re } \lambda_{f_{CP}}) = |A_{f_{CP}}|^2 (1 + \cos \phi_{CP, B_s \rightarrow f_{CP}}^{\text{mix}}), \\ B = B(f_{CP}) &= |A_{f_{CP}}|^2 (1 - \text{Re } \lambda_{f_{CP}}) = |A_{f_{CP}}|^2 (1 - \cos \phi_{CP, B_s \rightarrow f_{CP}}^{\text{mix}}). \end{aligned} \quad (157)$$

Here  $\phi_{CP, B_s \rightarrow f_{CP}}^{\text{mix}}$  is the phase of  $\lambda_{f_{CP}}$ , which quantifies the mixing-induced  $CP$  violation in the studied decay. We have encountered the special case  $\phi_{CP, B_s}^{\text{mix}} \equiv \phi_{CP, B_s \rightarrow (J/\psi\phi)}^{\text{mix}}|_{l=0,2}$  in our discussion of  $B_s - \bar{B}_s$  mixing and quoted  $A_{\Delta\Gamma}$  for this case in Eq. (154). Thus for the gold-plated decays into  $CP$  eigenstates we can determine  $\cos \phi_{CP, B_s \rightarrow f_{CP}}^{\text{mix}}$  from the ratio  $A(f_{CP})/B(f_{CP})$ . The method works as well for gold-plated decays into  $CP$  non-eigenstates, in which case one needs the time evolution for both  $(\bar{B}_s \rightarrow f)$  and  $(\bar{B}_s \rightarrow \bar{f})$ .

Prominent applications of the lifetime method have addressed  $B_s$  decays to  $\rho_0 K_{\text{short}}$ ,  $D_s^{(*)\pm} K^{*\mp}$  [90],  $D_s^{(*)+} D_s^{*-}$ ,  $J/\psi \phi$ ,  $\rho^0 \phi$ ,  $B_s \rightarrow K^* \bar{K}^*$  [120], and the rare decay  $B_s \rightarrow \mu^+ \mu^-$ , which is an important new-physics analyzer [121]. Another application is the measurement of  $\Delta\Gamma_{CP}$  through lifetime studies of  $D_s^{(*)+} D_s^{(*)-}$  [88].

The ongoing search for  $CP$  violation in  $D - \bar{D}$  mixing is discussed in detail in [95]. The slow  $D - \bar{D}$  oscillations make this difficult, one can safely expand the time evolution formulae in Eqs. (138–141) to the second order in  $t$ ; the physical interpretation of the coefficients of the linear and quadratic terms were derived in Ref. [122]. The prime effort in the search for  $CP$  violation in  $D - \bar{D}$  mixing is devoted to the interference of Cabibbo-favored (CF) and doubly Cabibbo-suppressed (DCS) decay amplitudes, where a meson produced as  $D$  decays through a  $c \rightarrow d\bar{s}$  amplitude, which is proportional to  $\lambda^2$ . In time the  $D$  evolves into a superposition of  $D$  and a tiny admixture of  $\bar{D}$ , which decays with the CF  $\bar{c} \rightarrow d\bar{s}$  amplitude. Interference is possible because of the valence  $\bar{u}$  quark in  $D$ , so that the final state has the same quark content  $d\bar{u}\bar{s}\bar{u}$  as the final state of the  $\bar{D}$  decay. The standard analysis studying  $D \rightarrow K_{\text{short}} \pi^+ \pi^-$  gives both  $a_{fs}$  and  $\text{Im } \lambda_{K_{\text{short}} \pi^+ \pi^-}$ . From Ref. [95] one finds the 2025 world averages

$$a_{fs} = 2 \left( 1 - \left| \frac{q}{p} \right| \right) = 0.008 \pm 0.104, \quad \text{arg } \lambda_{K_{\text{short}} \pi^+ \pi^-} = -0.056^{+0.047}_{-0.051}. \quad (158)$$

In summary, mixing-induced  $CP$  violation in gold-plated modes, which are dominated by a single combination of CKM elements, can give access to fundamental  $CP$  phases, without the problem of penguin pollution. Prime examples are the measurements of  $2\beta$  and  $2\beta_s$  from  $B_{d,s}$  decays to charmonium. There are gold-plated modes with no penguin pollution at all like the decay  $(\bar{B}_s(t) \rightarrow D_s^\mp K^\pm)$  involving  $CP$  non-eigenstates. In  $K - \bar{K}$  mixing  $\text{Im } \epsilon_K$  quantifies mixing-induced  $CP$  violation in  $K \rightarrow \pi\pi$ , while  $\text{Re } \epsilon_K$  quantifies  $CP$  violation in mixing.

In  $D - \bar{D}$  mixing the most promising avenue to mixing-induced  $CP$  violation and  $CP$  violation in mixing utilizes the interference of DCS  $c \rightarrow d\bar{s}$  and the CF  $\bar{c} \rightarrow d\bar{u}\bar{s}$  decays.

## 6 Meson-antimeson mixing in the Standard Model and beyond

The confirmation of the KM mechanism of  $CP$  violation, which lead to the 2008 Nobel Prize for Kobayashi and Maskawa, required the proof that the  $CP$  phase  $\delta_{KM} \simeq \gamma$  extracted from the measured  $\epsilon_K$  correctly predicts  $\phi_{CP,B_s}^{\text{mix}} = 2\beta$  as measured by the asymmetric  $B$  factories BaBar and Belle built for this purpose. Both  $\epsilon_K$  and  $\phi_{CP,B_s}^{\text{mix}}$  involve other parameters beyond the  $CP$  phases; one needs two quantities to construct the UT in Fig. 3. Thus the prediction of  $\phi_{CP,B_s}^{\text{mix}}$  from  $\epsilon_K$  also needed measurements and SM predictions of other,  $CP$ -conserving quantities; altogether they constrain the allowed region for the apex of the UT in the  $\bar{\rho}-\bar{\eta}$  plane. From Fig. 3 one realizes that the measurement of  $A_{CP}^{\text{mix}}(B_d \rightarrow J/\psi K_{\text{short}}) = -\sin(2\beta)$  defines an inclined line in the  $\bar{\rho}-\bar{\eta}$  plane which intersects the point  $(1, 0)$ . The litmus test for the KM mechanism was the confirmation that this line indeed intersects the previously determined allowed region. The  $CP$ -conserving input for the described UT analysis were the ratio of the semileptonic  $b \rightarrow u$  and  $b \rightarrow c$  branching ratios determining one side of the UT trough  $|V_{ub}/V_{cb}| \simeq \lambda R_u$  and  $\Delta M_d$  determining the other side  $R_t$  through  $\Delta M_d \propto |V_{td}|^2 \propto |R_t|^2 |V_{cb}|^2$ . This procedure would not have been possible without the theory effort to calculate these quantities, which include with  $\epsilon_K$  and  $\Delta M_d$  two different meson-antimeson mixing systems. At the beginning of the 1990s it was unclear, whether prediction beyond semi-quantitative estimates were possible at all.

As will be discussed in this section, predictions of flavor-changing processes involve a perturbative piece, obtained by loop calculations in perturbative QCD, and a non-perturbative calculation of hadronic matrix elements. The gold standard for the latter are computations with *lattice QCD*, in which the QCD path integral is discretized on a space-time lattice and calculated with Monte-Carlo techniques. In the early 1990s lattice QCD studies were still in an exploratory stage and, for example, did not include dynamical quarks (i.e. instead employed the “quenched approximation”) even at the time Belle and BaBar went into operation. The field of *precision flavor physics*, with the scope on FCNC processes in  $K$  and  $B$  physics, was founded in the late 1980s by Buras who initiated a program addressing the calculation of radiative corrections to essentially all FCNC processes. The aim —and result— of this endeavour were robust predictions with theoretically well-founded uncertainties, which, moreover, could be systematically reduced with additional calculational effort to match the size of shrinking error bars of modern experiments. I mention a few milestones in this paragraph (for overviews see Refs. [123, 124]). To establish the field, conceptual problems had to be solved to define a rigorous theoretical framework for the calculations. This progress included the proofs of proper factorization of infrared singularities and of the renormalization-scheme independence [125] of the predicted observables, the development of the correct treatment of bilocal matrix elements [126–128], and the understanding of the renormalization of evanescent operators [125, 129].

Both  $\Delta M_{d,s}$  in  $B - \bar{B}$  mixing and the largest contribution to  $\epsilon_K$  calculated from the  $K - \bar{K}$  mixing amplitude involve box diagrams with top quarks, the QCD corrections are proportional to  $\alpha_s(m_t) \sim 0.1$  and perturbation theory was found to work well [130]. For  $K - \bar{K}$  mixing, however, also contributions with light  $u, c$  quarks in the box diagrams are relevant for  $\epsilon_K$  and are even dominant for  $\Delta M_K$ . Since the leading-order prediction for  $\Delta M_K$  fell short of the experimental value by more than a factor of 2, there was doubt that perturbation theory works for  $K - \bar{K}$  mixing and uncontrolled additive hadronic long-distance effects were invoked to explain the experimental value of  $\Delta M_K$ . The issue was alleviated by QCD corrections and Ref. [127] established short-distance dominance of  $\Delta M_K$  in agreement with the expected suppression of additive long-distance effects by a factor of  $\Lambda_{\text{QCD}}^2/m_c^2$ . By 1995 all QCD contributions to  $|\Delta B| = 2$  transitions with heavy or light internal quarks had been calculated at the two-loop level [127, 128, 130, 131] and a complete QCD-corrected prediction of  $\epsilon_K$  in terms of  $(\bar{\rho}, \bar{\eta})$  became possible [131]. The corrections to  $\Delta M_K$  were disturbingly large and called for a calculation of one higher order in  $\alpha_s$ , requiring a three-loop calculation [132]. With the corresponding result of Ref. [133]  $\epsilon_K$  has become a high-precision observable [134].

The path to precision required a parallel effort on hadronic matrix elements. One result of the definition of the perturbative framework was the observation that a certain arbitrary element, the dependence on the renormalization scheme, must cancel between perturbative pieces and hadronic matrix elements. This criterion eliminated hadronic models and, more generally, any approach without control over the renormalization scheme, from the theorists’ toolbox and strengthened the case for lattice-QCD computations. There were also early analytical methods compatible with precision perturbative calculations, most prominently QCD sum rules [135, 136]. In Kaon physics the large- $N_c$  framework (a systematic expansion in terms of the inverse number of colors) gave the correct value for the hadronic matrix element of  $K - \bar{K}$  mixing [137].

In the remainder of this section I will first discuss the Yukawa interaction in the SM, which is the origin of flavor mixing. Then, in Sec. 6.2, I will explain the concept of an effective hamiltonian, exemplified for  $|\Delta B| = 2$  transitions and applied to  $\Delta M_{d,s}$ . Here also precise SM predictions for these quantities and the associated phenomenology will be presented. In Sec. 6.3 the effective  $|\Delta B| = 1$  will be introduced and applied to mixing-induced  $CP$  asymmetries and  $\Gamma_{12}^{d,s}$ , with numerical predictions for  $\Delta\Gamma_{d,s}$  and  $a_{fs}^{d,s}$ . Sec. 6.4 covers  $K - \bar{K}$  mixing with predictions for  $\epsilon_K$  and  $\Delta M_K$  and presents the overall picture on the UT from all quantities discussed in this section.

### 6.1 Yukawa interaction as the origin of flavor violation

The  $W$  boson is the gauge boson related to the quantum numbers  $(I, I_3)$  of the *weak isospin*. The SM implements maximal parity violation by placing right-handed quark field into singlets of the weak gauge group SU(2), while left-handed quark fields reside in doublets

$$\mathcal{Q}_1 = \begin{pmatrix} u'_L \\ d'_L \end{pmatrix}, \quad \mathcal{Q}_2 = \begin{pmatrix} c'_L \\ s'_L \end{pmatrix}, \quad \mathcal{Q}_3 = \begin{pmatrix} t'_L \\ b'_L \end{pmatrix}. \quad (159)$$

SU(2) doublets have weak isospin quantum number  $I = 1/2$  with  $I_3 = \pm 1/2$  for the up-type and down-type component, respectively. The prime at the quark fields indicates that these fields are *weak eigenstates* (a.k.a. as *gauge* or *interaction eigenstates*). SU(2) gauge symmetry dictates that the weak interaction is built from the doublets  $Q_j$  which leaves no room for the CKM matrix  $V$  at this stage. Thus we conclude that  $V$  must stem from a transformation of the weak eigenstates in Eq. (159) to the physical quark fields  $d_L, \dots, t_L$  in Eq. (8) and that  $(u_L, d_L)$ ,  $(c_L, s_L)$ , and  $(t_L, b_L)$  are *not* SU(2) doublets.

To understand the relation between weak and physical quark eigenstate fields we must study the mechanism to generate fermion masses in the SM. Mass terms in the lagrangian involve quark fields of both chiralities, for example  $m_t \bar{t}_R t_L + m_b \bar{t}_L t_R$  for the top quark. Such a term cannot be simply added to the lagrangian, because it violates SU(2) symmetry. But it is possible to give masses to fermions by employing gauge-invariant terms with the Higgs doublet field  $H = (G^+, v + (h^0 + iG^0)/\sqrt{2})^T$  by introducing the *Yukawa interaction*. The corresponding lagrangian for quarks reads

$$L_Y^q = - \sum_{j,k=1,2,3} [Y_{jk}^d \bar{Q}_j H d'_{k,R} + Y_{jk}^u \bar{Q}_j \tilde{H} u'_{k,R}] + \text{H.c.}, \quad (160)$$

where  $\tilde{H} = v + \frac{h^0 - iG^0}{\sqrt{2}}, -G^-)^T$  is the charge-conjugate Higgs doublet. The Yukawa interaction involves two complex  $3 \times 3$  matrices  $Y^d$  and  $Y^u$  with row and column indices  $j$  and  $k$  referring to the three fermion generations. We can readily identify the terms in Eq. (160) which are proportional to the Higgs vacuum expectation value  $v = 174$  GeV:

$$L_Y^q \supset L_m^q = - \sum_{j,k=1,2,3} \left[ (d'_L, s'_L, b'_L) M^d \begin{pmatrix} d'_R \\ s'_R \\ b'_R \end{pmatrix} + (u'_L, c'_L, t'_L) M^u \begin{pmatrix} u'_R \\ c'_R \\ t'_R \end{pmatrix} \right] \quad (161)$$

with the *quark mass matrices*

$$M^d = Y^d v \quad \text{and} \quad M^u = Y^u v. \quad (162)$$

With four unitary rotations we can diagonalize the two mass matrices. To this end we rotate the quark fields as

$$\begin{pmatrix} d'_{L,R} \\ s'_{L,R} \\ b'_{L,R} \end{pmatrix} = S_{L,R}^d \begin{pmatrix} d_{L,R} \\ s_{L,R} \\ b_{L,R} \end{pmatrix}, \quad \begin{pmatrix} u'_{L,R} \\ c'_{L,R} \\ t'_{L,R} \end{pmatrix} = S_{L,R}^u \begin{pmatrix} u_{L,R} \\ c_{L,R} \\ t_{L,R} \end{pmatrix} \quad (163)$$

and choose the four unitary matrices  $S_{L,R}^{d,u}$  such that the mass matrices in the new basis of physical quark fields are diagonal,

$$\widehat{M}^u \equiv \begin{pmatrix} m_u & 0 & 0 \\ m_c & 0 & 0 \\ 0 & 0 & m_t \end{pmatrix} = S_L^{u\dagger} M^u S_R^u \quad \widehat{M}^d \equiv \begin{pmatrix} m_d & 0 & 0 \\ m_s & 0 & 0 \\ 0 & 0 & m_b \end{pmatrix} = S_L^{d\dagger} M^d S_R^d. \quad (164)$$

One cannot choose non-unitary matrices for this purpose, because this would destroy the kinetic term of the lagrangian. The physical quark field eigenstates are also called *mass eigenstates*. Next we observe that all unitary rotations drop out in the flavour conserving couplings of the gauge bosons, because they appear as  $S_L^{d\dagger} S_L^d = \dots S_R^{u\dagger} S_R^u = 1$  in the vertices. This is the origin of the important feature of the SM that there are no *flavor-changing neutral currents* at tree-level, meaning that Z boson, photon, and gluon all couple flavor-diagonal! The  $W$  vertex, however, involves

$$L_W = \frac{g_W}{\sqrt{2}} [\bar{u}'_{JL} \gamma^\mu d'_{KL} + \bar{d}'_{KL} \gamma^\mu u'_{JL} W_\mu^-] = \frac{g_W}{\sqrt{2}} \sum_{j,k=1,2,3} \left[ (S_L^{u\dagger} S_L^d)_{jk} \bar{u}_{JL} \gamma^\mu d_{KL} W_\mu^+ + (S_L^{d\dagger} S_L^u)_{kj} \bar{d}_{KL} \gamma^\mu u_{JL} W_\mu^- \right],$$

which coincides with Eq. (8) for  $V = S_L^{u\dagger} S_L^d$ . Thus the CKM matrix is indeed unitary and stems from the mismatch of rotations of left-handed up-type and down-type quark fields from the weak basis to the physical basis. The unitarity of  $V$  is automatic in the SM, it is not possible to “test CKM unitarity” by comparing SM predictions against a theory with SM particles but non-unitary  $V$ . Such a theory is inconsistent and renders FCNC loops divergent which impedes any experimentally testable prediction.

When the Yukawa interaction in Eq. (160) is expressed in terms of the physical quark fields,  $Y^d$  and  $Y^u$  are diagonal and the SM Higgs boson field  $h^0$  couples also flavor-diagonally. Contrary to the case of the neutral gauge bosons, the absence of flavour-changing Higgs couplings is not a consequence of any symmetry, but originates from the *minimality of the Higgs sector*. This is an ad-hoc choice in the construction of the SM, there is no reason why Nature does not provide several Higgs doublets. Already in a two-Higgs-doublet model (2HDM) the four Yukawa matrices cannot all be brought to diagonal form and one expects flavour-changing couplings of the three neutral Higgs bosons of the 2HDM. Thus one finds contributions to, say,  $K - \bar{K}$  mixing at tree-level, mediated by a new Higgs boson  $H^0$  with  $s\bar{s}H^0$  coupling. Meson-antimeson mixing is instrumental to constrain the parameter spaces of multi-Higgs-doublet models. This also holds true for multi-Higgs boson models, in which the FCNC couplings are switched off by invoking new symmetries, because a charged Higgs boson can contribute to meson-antimeson mixing amplitudes at loop-level like the  $W$  boson.

The electroweak and strong interactions of the SM are constrained by a powerful principle, gauge symmetry, which dictates that the boson-fermion and boson-boson couplings of a given interaction involve the same coupling constant. With the two parameters of the Higgs potential, the three gauge couplings and  $\theta_{\text{QCD}}$  quantifying strong  $CP$  violation, this makes six parameters in total. By contrast, the quark Yukawa sector with the matrices  $Y^d$  and  $Y^u$  involves 10 physical parameters, which determine six quark masses and the four parameters of  $V$ . In the lepton sector there are 10 or 12 parameters, depending on whether neutrinos are Majorana or Dirac fermions. There

a several hierarchies in the elements of  $Y^{d,u}$ , resulting in  $m_u < m_d \ll m_s \ll m_c \sim m_b \ll m_t$  and the pattern in  $V$  described by the Wolfenstein parametrization in Eq. (17). An explanation of these features is the subject of *flavor model building*, which aims at reducing the number of parameters from symmetry considerations (see e.g. Ref. [138]) and finding dynamical explanations of their values [139].

Another ad-hoc feature of the Yukawa sector is the number of fermion generations. Why did Nature provide us with three fermion families (and the  $CP$  violation which came with it)? Could there be more? The information from meson-antimeson mixing helped us to constrain the parameter space of a hypothetical fourth fermion generation by severely constraining the mixing of the fourth family with the other generations [140–142], paving the way for the exclusion of a fourth fermion generation by more than  $5\sigma$  [143].

In summary, flavor violation encoded in  $V$  appears in the weak interaction of  $W$  bosons, but originates from the Yukawa interaction of the Higgs field. The diagonalization of  $Y^d$  and  $Y^u$  rotates the quark fields from eigenstates of the weak interaction to mass eigenstates.  $V$  is a remnant of these unitary rotations. Thus flavor physics probes the Yukawa sector of the SM, which is poorly understood and involves 10 free parameters in the quark sector. The loop suppression of FCNC processes like meson-antimeson mixing amplitudes results from the minimality of the SM Higgs sector and is a priori absent in models with more than one Higgs doublet, which involve neutral Higgs bosons with FCNC couplings.

## 6.2 Effective $|\Delta B| = 2$ hamiltonian and Standard-Model prediction for $\Delta M_{d,s}$

In the following I derive the formalism needed to calculate the mass difference for the  $B_d - \bar{B}_d$  and  $B_s - \bar{B}_s$  mixing system. The central element is an *effective hamiltonian* describing the  $\Delta B = 2$  transition mediated by the box diagrams proportional to  $(V_{tb} V_{tq}^*)^2$ . We can cover the cases  $q = d$  and  $q = s$  simultaneously, because the corresponding effective hamiltonians only differ by the exchange  $d \leftrightarrow s$ .

So far we have applied perturbation theory to the electroweak interaction only, while the strong interaction is fully contained in  $H_0$  in Eq. (60). In order to apply perturbative methods to QCD as well, we must first separate *short-distance* and *long-distance* interactions from each other. Short-distance QCD is associated with high energy and mass scales, far above the scale  $\Lambda_{\text{QCD}} \sim 400$  MeV determining the size of typical strong binding energies. Due to the asymptotic freedom of QCD one can apply perturbation theory to the short-distance piece of the studied process by calculating Feynman diagrams with quarks and gluons. Long-distance QCD is non-perturbative and confines the external quarks of our box diagrams in Fig. 1 into mesons. The theoretical tool for the desired separation is the *Operator Product Expansion (OPE)*, which expresses a hadronic amplitude as a sum of terms which factorize into a short-distance *Wilson coefficient* and a *hadronic matrix element* containing the long-distance QCD effects. The Wilson coefficients are calculable in perturbation theory and the contributions are categorized by the order of  $\alpha_s = g^2/(4\pi)$  to which they are calculated, where  $g$  is the QCD coupling constant. These coefficients depend on the heavy masses in the problem, the dependence of the meson-antimeson mixing amplitudes on  $M_W$  and  $m_t$  is fully contained in the Wilson coefficients. The hadronic matrix elements instead contain the dynamics associated with Compton wavelengths of order  $\Lambda_{\text{QCD}}$ , which cannot resolve the  $W$  propagation. For instance, the box diagram of  $B - \bar{B}$  mixing with two heavy top quarks reduces to a point-like four-quark interaction for the long-distance piece of the transition amplitude; pictorially we can shrink the heavy box diagram to a point for the long-distance piece of the  $B - \bar{B}$  mixing amplitude.

The result of the OPE is an *effective field theory* with a simpler interaction, in our case described by four-quark vertices whose effective coupling constants are the Wilson coefficients. Technically, one distinguishes light and heavy degrees of freedom, the quantum fields describing the former are kept as dynamical degrees of freedom, while the fields corresponding to the heavy particles are removed from the theory, their effect is fully contained in the Wilson coefficients. In the following  $m_{\text{heavy}}$  represents  $M_W$  or  $m_t$  while  $m_{\text{light}}$  stands for  $m_b$ ,  $m_c$ , or  $\Lambda_{\text{QCD}}$ , while smaller quark masses are set to zero. The corresponding effective hamiltonian  $H^{\text{eff}}$  is designed to reproduce the S-matrix elements of the Standard Model up to corrections of order  $(m_{\text{light}}/m_{\text{heavy}})^n$  where  $n$  is a positive integer:

$$\langle f | \mathbf{T} e^{-i \int d^4x H_{\text{int}}^{\text{SM}}(x)} | i \rangle = \langle f | \mathbf{T} e^{-i \int d^4x H^{\text{eff}}(x)} | i \rangle \left[ 1 + \mathcal{O}\left(\frac{m_{\text{light}}}{m_{\text{heavy}}}\right)^n \right] \quad (165)$$

I explain the method with an effective hamiltonian which reproduces the amplitude for  $B - \bar{B}$  mixing up to corrections of order  $m_b^2/M_W^2$ . That is, I employ Eq. (165) for the case  $i = \bar{B}$  and  $f = B$  (where  $B = B_d$  or  $B_s$ ),  $m_{\text{light}} = m_b$  and  $m_{\text{heavy}} = M_W \sim m_t$ . In the effective theory  $H_0$  and  $H_1$  in Eq. (60) are replaced by

$$H_0 = H^{\text{QCD}(f=5)}, \quad H_1 = H^{\text{eff}} = H^{\text{QED}(f=5)} + H^{|\Delta B|=2}. \quad (166)$$

Here the first term is the usual QED hamiltonians with 5 “active flavours”, meaning that there is no top quark included and  $H^{|\Delta B|=2}$  describes the weak interaction mediated by the  $\Delta B = 2$  box diagrams proportional to  $(V_{tb} V_{tq}^*)^2$  and their  $\Delta B = -2$  counterparts with outgoing  $b$  quark lines and CKM factor  $(V_{tb}^* V_{tq})^2$ . Also in  $H^{\text{QCD}(f=5)}$  there is no top quark field.

Adapted to the process under study,  $H^{|\Delta B|=2}$  only encodes the physics related to  $B - \bar{B}$  mixing, but does not describe other weak processes such as meson decays. The  $\Delta B = 2$  transition of the box diagram in Fig. 1 is mediated by an effective four-quark coupling, the four-quark operator

$$Q = \bar{q}_L \gamma^\nu b_L \bar{q}_L \gamma^\nu b_L \quad \text{with } q = d \text{ or } s, \quad (167)$$

shown in Fig. 5. We have

$$H^{|\Delta B|=2} = \frac{G_F^2}{4\pi^2} (V_{tb} V_{tq}^*)^2 C^{|\Delta B|=2}(m_t, M_W, \mu) Q(\mu) + \text{H.c.}, \quad (168)$$

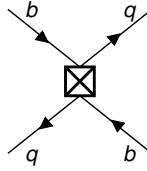


Fig. 5 The four-quark operator  $Q$  for  $B_q - \bar{B}_q$  mixing with  $q = d$  or  $s$ .

where the lengthy prefactor of  $Q$  is just the effective coupling constant multiplying the four-quark interaction of Fig. 5. The Fermi constant  $G_F$ , which is proportional to  $1/M_W^2$ , enters quadratically and thus contains four powers of  $1/m_{\text{heavy}}$ .

The CKM elements of the box diagram are factored out to get a real Wilson coefficient  $C^{|\Delta B|=2}(m_t, M_W, \mu)$  and has mass dimension two.  $\mu$  is the renormalization scale, familiar from any QCD calculation. Just as any other interaction term, also  $Q$  must be renormalized. The renormalized operator  $Q$  depends on  $\mu$  through the renormalization constant  $Z_Q(\mu)$  via  $Q = Z_Q Q^{\text{bare}}$  and (in a mass-independent scheme like  $\overline{\text{MS}}$ ) the latter dependence is only implicit through  $g(\mu)$ , where  $g$  is the QCD coupling constant.<sup>9</sup> The coefficient  $C^{|\Delta B|=2}$  is calculated from the definition of  $H^{\text{eff}}$  in Eq. (165): We compute the  $\Delta B = 2$  process both in the Standard Model and with the interactions of  $H^{\text{eff}}$  and adjust  $C^{|\Delta B|=2}$  such that the two results are the same, up to corrections of order  $m_b^2/M_W^2$ . Obviously we cannot do this with mesons as external states  $i$  and  $f$ . But a crucial property of  $H^{\text{eff}}$  is the independence of the Wilson coefficient on the external states. We can calculate it for an arbitrary momentum configuration for the external quarks as long as the external momenta are of the order of  $m_{\text{light}}$ . That is, we do not need to know the complicated momentum configuration of quarks bound in a hadron. In this step, we switch from the Heisenberg picture to the interaction picture for  $H^{\text{QCD}(\ell=5)}$ , because we perform the calculation in an entirely perturbative world with external quark rather than hadron states. The strong coupling is determined at a renormalization scale of the order of  $m_{\text{heavy}}$ , where  $g$  is small enough to expand amplitudes in  $\alpha_s$ . Furthermore, we write  $C^{|\Delta B|=2}$  as an expansion in  $\alpha_s$ :

$$C^{|\Delta B|=2} = C^{|\Delta B|=2,(0)} + \frac{\alpha_s(\mu)}{4\pi} C^{|\Delta B|=2,(1)} + \dots \quad (169)$$

Since we aim at an expansion of the  $B - \bar{B}$  mixing amplitude in terms of  $m_{\text{light}}/m_{\text{heavy}}$ , we can expand the box diagram of Fig. 1 in terms of the momenta of the external quarks, which are at most of order  $m_b$ . Thus to leading order in  $m_b/M_W$  (“leading power”) we can simply set the external momenta to zero. Now the “effective theory side” of Eq. (165) involves the tree-level diagram corresponding to

$$\begin{aligned} \langle f | \mathbf{T} e^{-i \int d^4x H^{\text{eff}}(x)} | i \rangle^{(0)} &\simeq -i \int d^4x \langle f | H^{\text{eff}}(x) | i \rangle^{(0)} = -i \int d^4x \langle f | H^{|\Delta B|=2}(x) | i \rangle^{(0)} \\ &= -i(2\pi)^4 \delta^{(4)}(p_f - p_i) \frac{G_F^2}{4\pi^2} (V_{tb} V_{tq}^*)^2 C^{|\Delta B|=2,(0)} \langle f | Q | i \rangle^{(0)} \end{aligned}$$

where  $|i\rangle = |p_b, s_b; p_{\bar{q}}, s_{\bar{q}}\rangle$  and  $|f\rangle = |p_q, s_q; p_{\bar{b}}, s_{\bar{b}}\rangle$  are the external states characterized by the momenta and spins of the quarks. The superscript “(0)” indicates the lowest order of QCD everywhere. Since  $\langle f | Q | i \rangle$  reproduces the spinor structure (“Dirac algebra”) of the box diagram, the coefficient  $C^{|\Delta B|=2,(0)}$  inferred from this *matching calculation* is solely determined in terms of the loop integral and therefore only depends on  $M_W$  and  $m_t$ .

The matching calculation becomes more interesting at the *next-to-leading order (NLO)* of QCD. Now  $H^{\text{QCD}}$  enters the matching calculation and we must dress both the box diagram and the effective diagram in Fig. 5 with gluons in all possible ways. Denoting the SM amplitude by

$$\mathcal{M} = \mathcal{M}^{(0)} + \frac{\alpha_s}{4\pi} \mathcal{M}^{(1)} + \dots, \quad (170)$$

our NLO matching calculation amounts to the determination of  $C^{|\Delta B|=2,(1)}$  from

$$-\mathcal{M}^{(0)} - \frac{\alpha_s}{4\pi} \mathcal{M}^{(1)} = \frac{G_F^2}{4\pi^2} (V_{tb} V_{tq}^*)^2 \left[ C^{|\Delta B|=2,(0)} + \frac{\alpha_s}{4\pi} C^{|\Delta B|=2,(1)} \right] \left[ \langle Q \rangle^{(0)} + \frac{\alpha_s}{4\pi} \langle Q \rangle^{(1)} \right] \left[ 1 + O\left(\frac{m_b^2}{M_W^2}\right) \right] + O(\alpha_s^2) \quad (171)$$

On the RHS the external states are omitted for simplicity of notation and I have expanded  $\langle Q \rangle \equiv \langle f | Q | i \rangle$  in  $\alpha_s$  as well. The QCD corrections to the box diagram in  $\mathcal{M}^{(1)}$  not only depend on the light scales, i.e. external momenta and light quark masses, they also suffer from infrared (IR) divergences. These divergences signal the breakdown of QCD perturbation theory at low energies. However, the gluonic corrections to Fig. 5, which are comprised in  $\langle Q \rangle^{(1)}$ , exactly reproduce the infrared structure of the SM diagrams, with the same IR divergences and the same dependence on the light mass scales. Collecting the  $O(\alpha_s)$  terms from Eq. (171),

$$-\mathcal{M}^{(1)} = \frac{G_F^2}{4\pi^2} (V_{tb} V_{tq}^*)^2 \left[ C^{|\Delta B|=2,(0)} \langle Q \rangle^{(1)} + C^{|\Delta B|=2,(1)} \langle Q \rangle^{(0)} \right], \quad (172)$$

<sup>9</sup>The analogy with the renormalization of the QCD coupling constant is more obvious if one interprets the product  $CZ_Q Q^{\text{bare}}$  in a different way: By grouping  $Z_Q$  with  $C$  rather than  $Q$  one recognizes  $C$  as a renormalized coupling constant. The notion of a “renormalized” operator instead of a “renormalized Wilson coefficient” has historical reasons.

one finds identical IR structures on the LHS and in the first term in the square brackets, while  $C^{|\Delta B|=2,(1)}$  only contains heavy masses and no IR divergences. We conclude that the IR structure of the SM amplitude properly factorizes with an ‘‘infrared-safe’’  $C^{|\Delta B|=2}$ . The reason for the successful IR factorization is the fact that for a soft gluon connecting two external quark lines the box diagram and the four-quark operator look the same, so that the region of the loop integral with small loop momentum gives the same result for  $-\mathcal{M}^{(1)}$  and  $C^{|\Delta B|=2,(0)}\langle Q \rangle^{(1)}$ . There is only a mismatch stemming from the hard loop momenta, which are not IR sensitive and feed into the other term in Eq. (172), namely  $C^{|\Delta B|=2,(1)}\langle Q \rangle^{(0)}$ .

Our quark-level calculation is meaningful for  $C^{|\Delta B|=2}$ , but not for  $\langle Q \rangle$ . In order to make a theoretical prediction for the  $B - \bar{B}$  mixing amplitude, we must compute  $\langle B|Q|\bar{B}\rangle$  with nonperturbative methods such as lattice QCD.

Next I derive the result for the leading-order (LO) Wilson coefficient  $C^{|\Delta B|=2,(0)}$ . In a first step let us decompose  $\mathcal{M}^{(0)}$  as

$$\mathcal{M}^{(0)} = \sum_{j,k=u,c,t} V_{jb} V_{jq}^* V_{kb} V_{kq}^* \mathcal{M}_{jk}^{(0)} \langle Q \rangle^{(0)}, \quad q = d \text{ or } s, \quad (173)$$

where  $\mathcal{M}_{jk}^{(0)}\langle Q \rangle^{(0)}$  is the result of the box diagram containing internal quark flavours  $(j, k)$  with the CKM elements factored out. We then write

$$\mathcal{M}_{jk}^{(0)} = -\frac{G_F^2}{4\pi^2} M_W^2 \tilde{S}(x_j, x_k) \quad (174)$$

with  $x_j = m_j^2/M_W^2$ . The function  $\tilde{S}(x_j, x_k)$  is symmetric,  $\tilde{S}(x_j, x_k) = \tilde{S}(x_k, x_j)$ . Using CKM unitarity to eliminate  $V_{ub}V_{uq}^* = -V_{tb}V_{tq}^* - V_{cb}V_{cq}^*$  one finds Eq. (173):

$$-\mathcal{M}^{(0)} = \frac{G_F^2}{4\pi^2} M_W^2 \left[ (V_{tb}V_{tq}^*)^2 S(x_t) + 2V_{tb}V_{tq}^* V_{cb}V_{cq}^* S(x_c, x_t) + (V_{cb}V_{cq}^*)^2 S(x_c) \right] \langle Q \rangle^{(0)}. \quad (175)$$

$S$  and  $\tilde{S}$  are related as

$$\begin{aligned} S(x_j, x_k) &= \tilde{S}(x_j, x_k) - \tilde{S}(x_j, 0) - \tilde{S}(0, x_k) + \tilde{S}(0, 0), & \text{for } j, k = c, t, \\ S(x) &\equiv S(x, x), \end{aligned} \quad (176)$$

for zero up-quark mass. In Eq. (175) the last two terms are tiny, because  $x_c \sim 10^{-4}$  and

$$S(x_c) = \mathcal{O}(x_c), \quad S(x_c, x_t) = \mathcal{O}(x_c \ln x_c). \quad (177)$$

where we recognize the GIM suppression discussed after Eq. (13), as four  $\mathcal{O}(1)$  loop functions combine to something much smaller. There is no GIM suppression in top loops, because  $x_t \sim 4$ . The dominant contribution to Eq. (173) involves

$$S(x_t) = x_t \left[ \frac{1}{4} + \frac{9}{4} \frac{1}{1-x_t} - \frac{3}{2} \frac{1}{(1-x_t)^2} \right] - \frac{3}{2} \left[ \frac{x_t}{1-x_t} \right]^3 \ln x_t \approx 2.3. \quad (178)$$

The tiny charm contribution does not contribute to  $C^{|\Delta B|=2,(0)}$  at all; to accommodate for it we must refine our operator product expansion to include higher powers of  $(m_{\text{light}}/m_{\text{heavy}})$  in Eq. (165). We can read off  $C^{|\Delta B|=2,(0)}$  from Eqs. (171) and (175):

$$C^{|\Delta B|=2,(0)}(m_t, M_W, \mu) = M_W^2 S(x_t). \quad (179)$$

The functions  $S(x)$  and  $S(x_c, x_t)$  are called *Inami-Lim* functions [144].

The factorization in Eqs. (165) and (171) also solves another problem: No largely separated scales appear in  $C^{|\Delta B|=2}(m_t, M_W, \mu)$  provided that we take  $\mu = \mathcal{O}(M_W, m_t)$ , so that no large logarithms can spoil the convergence of the perturbative series.  $\mu$  enters our matching calculation at NLO as  $\ln(\mu/M_W)$  in  $C^{|\Delta B|=2,(1)}$  and through  $\alpha_s(\mu)$ . While no explicit  $\mu$ -dependence is present in our LO result in Eq. (179), there is an implicit  $\mu$ -dependence through  $m_t(\mu)$ , which is a running quark mass (typically defined in the  $\overline{\text{MS}}$  scheme). The mentioned  $\ln(\mu/M_W)$  term in  $C^{|\Delta B|=2,(1)}$  has two sources: Firstly, there is already a  $\ln(\mu/M_W)$  term in  $\mathcal{M}^{(1)}$ , familiar to us from matrix elements with  $\overline{\text{MS}}$ -renormalized UV divergences. Secondly,  $\mathcal{M}^{(1)}$  contains the large logarithm  $\ln(m_b/M_W)$  which is split between matrix elements and Wilson coefficients as

$$\ln \frac{m_b}{M_W} = \ln \frac{m_b}{\mu} + \ln \frac{\mu}{M_W}. \quad (180)$$

This feature is clear from Eq. (172), because  $\langle Q \rangle^{(1)}$  can only contain  $\ln(m_b/\mu)$ , as it is independent of  $M_W$ , and conversely  $C^{|\Delta B|=2}$  is independent of light scales like  $m_b$ .

The scale  $\mu_{tW} = \mathcal{O}(M_W, m_t)$  at which we invoke Eq. (171) to find  $C^{|\Delta B|=2}$  is called the *matching scale* (or *factorization scale*) and  $C^{|\Delta B|=2}(m_t, M_W, \mu_{tW})$  has a good perturbative behaviour. Similarly, no large logarithms occur in  $\langle Q(\mu_b) \rangle$ , if we choose a scale  $\mu_b \sim m_b$  in the matrix element. Since  $H^{|\Delta B|=2}$  does not depend on the unphysical scale  $\mu$ , we can choose any value for  $\mu$ , but this value must be the same in  $C(\mu)$  and  $\langle Q(\mu) \rangle$ . That forces us to either relate  $C(\mu_{tW})$  to  $C(\mu_b)$  or to express  $\langle Q(\mu_b) \rangle$  in terms of  $\langle Q(\mu_{tW}) \rangle$  in such a way that large logarithms

$$\alpha_s^n \ln^n \frac{\mu_{tW}}{\mu_b} \quad (181)$$

are summed to all orders  $n = 0, 1, 2 \dots$  in perturbation theory. This can be achieved by solving the *renormalization group (RG) equation* for either  $C(\mu)$  or  $\langle Q(\mu) \rangle$ . All steps of this procedure are analogous to the calculation of the running quark mass, which can be found in any textbook on QCD. RG-improvement promotes our LO result to a *leading-log* quantity:

$$C^{|\Delta B|=2,(0)}(m_t, M_W, \mu_b) = u^{(0)}(\mu_b, \mu_{tW}) C^{|\Delta B|=2,(0)}(m_t, M_W, \mu_{tW}) \quad (182)$$

$$\langle Q(\mu_{tW}) \rangle = u^{(0)}(\mu_b, \mu_{tW}) \langle Q(\mu_b) \rangle \quad (183)$$

$$u^{(0)}(\mu_b, \mu_{tW}) = \left( \frac{\alpha_s(\mu_{tW})}{\alpha_s(\mu_b)} \right)^{\frac{\gamma_+^{(0)}}{2\beta_0^{(0)}}} \quad \text{with } \gamma_+^{(0)} = 4. \quad (184)$$

In flavor physics expressions like “leading-order (LO)” and “next-to-leading order (NLO)” are meant to include the RG resummation, because fixed-order calculations are not common. I.e. “(N)LO” really means “(next-to-)leading log”.

The evolution factor  $u^{(0)}(\mu_b, \mu_{tW})$  depends on the *anomalous dimension* of  $Q$ , which equals  $(\alpha_s/(4\pi))\gamma_+^{(0)}$  to leading-log accuracy.  $\beta_0^{(f)} = 11 - 2f/3$  is the first term of the QCD  $\beta$  function. One usually writes

$$C^{|\Delta B|=2}(m_t, M_W, \mu_b) = \eta_B b_B(\mu_b) C^{|\Delta B|=2,(0)}(m_t, M_W, \mu_{tW}) \quad (185)$$

where all dependence on  $\mu_b$  is absorbed into  $b_B(\mu_b)$  and all heavy scales reside in  $\eta_B$ . This factorization is possible to all orders in  $\alpha_s$ . It is trivially verified in the LO approximation of Eq. (184), where one simply has  $u^{(0)}(\mu_b, \mu_{tW}) = \eta_B b_B(\mu_b)$ . The anomalous dimension  $\gamma_+^{(0)}$  is calculated from the UV-divergent pieces of the one-loop diagrams found by dressing  $Q$  in Fig. 5 with a gluon. In Eq. (185)  $m_t$  is understood as  $m_t(m_t)$  (and not as  $m_t(\mu_{tW})$ ). In this way  $\eta_B$  is independent of  $\mu_{tW}$  to the calculated order; the residual  $\mu_{tW}$  dependence is already tiny in the NLO result. The NLO result for  $C^{|\Delta B|=2}$  comprises all terms of order  $\alpha_s^{n+1} \ln^n(\mu_{tW}/\mu_b)$  and includes two ingredients: first, the two-loop diagrams in which the box is dressed with an additional gluon in all possible ways [130] and second, the NLO evolution factor  $u^{(1)}(\mu_b, \mu_{tW})$  refining  $u^{(0)}$  in Eq. (184) by corrections of order  $\alpha_s$  found by calculating the two-loop contribution  $\gamma_+^{(1)}$  to the anomalous dimension of  $Q$  [125].

$\eta_B$  mildly depends on  $x_t = m_t^2/M_W^2$  and in practice one can treat it as a constant number [130]:

$$\eta_B = 0.55, \quad b_B(\mu_b = m_b) = 4.2 \text{ GeV} = 1.5. \quad (186)$$

The dependences of  $b_B$  on  $\mu_b$  and the chosen renormalization scheme cancel in the product  $b_B(\mu_b)\langle Q(\mu_b) \rangle$ . The quoted number is for the  $\overline{\text{MS}}\text{-NDR}$  scheme, where “NDR” refers to the treatment of the Dirac matrix  $\gamma_5$ . Details on this topic can be found in [125]. We see that the impact of short-distance QCD corrections is moderate, since  $\eta_B b_B(\mu_b) = 0.84$ . The NLO calculation of Ref. [130] has found only small two-loop corrections and the remaining uncertainty affects  $\eta_B$  is around 2%. Combining Eqs. (168), (179) and (185) we arrive at our final result for the  $|\Delta B| = 2$  hamiltonian:

$$H^{|\Delta B|=2} = \frac{G_F^2}{4\pi^2} M_W^2 (V_{tb} V_{tq}^*)^2 \eta_B S(x_t) b_B(\mu_b) \langle Q(\mu_b) \rangle + \text{H.c.} \quad (187)$$

Turning to the non-perturbative piece of the  $B - \bar{B}$  mixing amplitude, we first introduce the conventional parameterization of the hadronic matrix element,

$$\langle B_q | Q(\mu_b) | \bar{B}_q \rangle \equiv \frac{2}{3} M_{B_q}^2 f_{B_q}^2 B_{B_q}(\mu_b) \equiv \frac{2}{3} M_{B_q}^2 f_{B_q}^2 \frac{\widehat{B}_{B_q}}{b_B(\mu_b)} \quad (188)$$

with the  $B_q$  meson decay constant  $f_{B_q}$  and the *bag factor*, which is sometimes chosen as  $B_{B_q}(\mu_b)$  and in other occasions as  $\widehat{B}_{B_q} = B_{B_q}(\mu_b)b_B(\mu_b)$ . The second parameterization incorporates the feature that the dependence on renormalization scheme and scale must cancel between  $b_B(\mu_b)$  and  $B_{B_q}(\mu_b)$ , so that one can quote numbers for the scheme and scale independent quantity  $\widehat{B}_{B_q}$  without referring to details of the renormalization. The parameterization in Eq. (188) is chosen in such a way that  $B_{B_q}(\mu_b) = \widehat{B}_{B_q}/b_B(\mu_b)$  is close to one for  $\mu_b \sim m_b$ . With the help of our effective field theory we have reduced the problem of long-distance QCD in  $B - \bar{B}$  mixing to the calculation of a single number. Lattice gauge theory computations cover the ranges [145, 146]

$$f_{B_d} \sqrt{\widehat{B}_{B_d}} = (210 \pm 11) \text{ MeV}, \quad f_{B_s} \sqrt{\widehat{B}_{B_s}} = (254 \pm 12) \text{ MeV}, \quad \xi = \frac{f_{B_s} \sqrt{\widehat{B}_{B_s}}}{f_{B_d} \sqrt{\widehat{B}_{B_d}}} = 1.216 \pm 0.016. \quad (189)$$

The quoted hadronic uncertainties are the dominant source of uncertainty for the extraction of  $|V_{tb} V_{tq}|$  from the measured  $\Delta M_{B_q}$ .

Putting Eqs. (187) and (188) together we find the desired element of the  $B - \bar{B}$  mass matrix:

$$M_{12}^q = \frac{\langle B_q | H^{|\Delta B|=2} | \bar{B}_q \rangle}{2M_{B_q}} = \frac{G_F^2}{12\pi^2} \eta_B M_{B_q} \widehat{B}_{B_q} f_{B_q}^2 M_W^2 S\left(\frac{m_t^2}{M_W^2}\right) (V_{tb} V_{tq}^*)^2. \quad (190)$$

We can now use  $\Delta M_d = 2|M_{12}^d|$  to determine  $|V_{td}|$ :

$$\Delta M_d = (0.51 \pm 0.02) \text{ ps}^{-1} \left( \frac{|V_{td}|}{0.0086} \right)^2 \left( \frac{f_{B_d} \sqrt{\widehat{B}_{B_d}}}{210 \text{ MeV}} \right)^2. \quad (191)$$

For  $\Delta M_s = 2|M_{12}^s|$  one finds

$$\Delta M_s = (16.3 \pm 0.6) \text{ ps}^{-1} \left( \frac{|V_{ts}|}{0.04} \right)^2 \left( \frac{f_{B_d} \sqrt{\bar{B}_{B_d}}}{254 \text{ MeV}} \right)^2. \quad (192)$$

$\Delta M_s$  involves  $|V_{ts}|$  which is fixed by CKM unitarity to  $|V_{ts}| = 0.98|V_{cb}|$ . Thus if one uses  $|V_{cb}|$  as input,  $\Delta M_s$  is a direct test of the SM without sensitivity to  $(\bar{\rho}, \bar{\eta})$ . Eq. (192) reproduces the experimental value in Eq. (48) for  $|V_{cb}| = 0.0426^{+0.0022}_{-0.0019}$ .

As mentioned after Eq. (48), we can determine the side  $R_t$  from the ratio  $\Delta M_d/\Delta M_s$  which is proportional to  $|V_{td}/V_{ts}| = 1.02 \lambda R_t$ , where the factor 1.02 subsumes the higher-order terms in  $\lambda$  mentioned in the text after Eq. (48). With  $\xi$  from Eq. (189) and  $M_{B_s}/M_{B_d} = 1.017$  we find the “pocket calculator formula”:

$$R_t = \frac{1}{1.02 \lambda} \sqrt{\frac{\Delta M_d}{\Delta M_s}} \sqrt{\frac{M_s}{M_d}} \xi = 0.905 \frac{0.225}{\lambda} \sqrt{\frac{\Delta M_d}{0.507 \text{ ps}^{-1}}} \sqrt{\frac{17.77 \text{ ps}^{-1}}{\Delta M_s}} \frac{\xi}{1.216}. \quad (193)$$

In summary,  $M_{12}^q$  can be calculated with the help of an OPE with a particularly simple result, involving only a single Wilson coefficient  $C^{|\Delta B|=2}$  and a single hadronic  $\Delta B = 2$  matrix element  $\langle B_q | Q | \bar{B}_q \rangle$ . The former is calculated to NLO in QCD perturbation theory; the missing three-loop contribution inflicts an error of 4% on this coefficient. The hadronic matrix elements in Eq. (189) are determined from lattice QCD with a current accuracy of slightly less than 11%.  $\Delta M_q \simeq 2|M_{12}^q| \propto |V_{tb} V_{tq}^*|^2$  determines  $|V_{tq}|$  with a current precision of 11%, with the theoretical uncertainty dominated by the lattice calculations of the hadronic parameters in Eq. (189). Since CKM unitarity fixes  $|V_{ts}| = 0.98|V_{cb}|$ , measurements of  $\Delta M_s$  directly probe the SM, but this test currently suffers from the controversy on the value of  $|V_{cb}|$ . The ratio  $\Delta M_d/\Delta M_s \propto |V_{td}/V_{ts}|^2 \propto R_t^2$  provides a precise determination of the side  $R_t$  of the UT, because the perturbative coefficient and the implicit dependence on  $|V_{cb}|$  drops out and the uncertainty of the hadronic parameter  $\xi$  in Eq. (189) is below 1.5%. Easy-to-use formulae for phenomenological analyses are given in Eqs. (191–193).

### 6.3 Effective $|\Delta B| = 1$ hamiltonian and Standard-Model predictions for $\Delta\Gamma_{ds}$ and $a_{fs}^{ds}$

$B$  decays are processes in which the beauty quantum number changes by one unit. The tree-level contribution to such decays involves the exchange of one  $W$  boson and the corresponding effective four-quark operator is obtained by contracting the  $W$  line to a point. Thus the  $|\Delta B| = 1$  hamiltonian found in this way is modeled after the Fermi theory of beta decay.  $H^{|\Delta B|=1}$  comprises many operators, because there are many non-leptonic decay channels; one further categorizes the different terms by the other flavor quantum numbers. For example,  $b \rightarrow c\bar{u}\bar{d}$  decays are described by  $H^{b \rightarrow c\bar{u}\bar{d}} = H^{|\Delta B=\Delta C=\Delta D=1} + \text{H.c.}$  and when mentioning  $H^{|\Delta B|=1}$  one usually only refers to the piece which applies to the studied decay. Another reason for the proliferation of operators compared to the Fermi theory is QCD: When we include diagrams with gluons we find new contributions in which color indices are contracted in a different way compared to the original operator found from the tree diagram with  $W$  exchange. For the description of  $b \rightarrow s$  decays one needs

$$H^{|\Delta B|=1} = \frac{4G_F}{\sqrt{2}} \left[ -\lambda_t^s \left( \sum_{i=1}^6 C_i Q_i + C_8 Q_8 \right) - \lambda_u^s \sum_{i=1}^2 C_i (Q_i - Q_i^u) + V_{us}^* V_{cb} \sum_{i=1}^2 C_i Q_i^{cu} + V_{cs}^* V_{ub} \sum_{i=1}^2 C_i Q_i^{uc} \right] + \text{H.c.}, \quad (194)$$

with

$$\lambda_a^s = V_{as}^* V_{ab}, \quad (195)$$

where  $a = u, c, t$  and  $\lambda_t^s = -\lambda_c^s - \lambda_u^s$ .  $G_F$  stands for the Fermi constant. The operators are [147]

$$Q_1 = Q_1^c = \bar{s}_L^\alpha \gamma_\mu c_L^\beta \bar{c}_L^\beta \gamma^\mu b_L^\alpha, \quad Q_2 = Q_2^c = \bar{s}_L^\alpha \gamma_\mu c_L^\alpha \bar{c}_L^\beta \gamma^\mu b_L^\beta, \quad (196)$$

$$Q_1^u = \bar{s}_L^\alpha \gamma_\mu u_L^\beta \bar{u}_L^\beta \gamma^\mu b_L^\alpha, \quad Q_2^u = \bar{s}_L^\alpha \gamma_\mu u_L^\alpha \bar{u}_L^\beta \gamma^\mu b_L^\beta, \quad (197)$$

$$Q_1^{cu} = \bar{s}_L^\alpha \gamma_\mu u_L^\beta \bar{c}_L^\beta \gamma^\mu b_L^\alpha, \quad Q_2^{cu} = \bar{s}_L^\alpha \gamma_\mu u_L^\alpha \bar{c}_L^\beta \gamma^\mu b_L^\beta, \quad (198)$$

$$Q_1^{uc} = \bar{s}_L^\alpha \gamma_\mu c_L^\beta \bar{u}_L^\beta \gamma^\mu b_L^\alpha, \quad Q_2^{uc} = \bar{s}_L^\alpha \gamma_\mu c_L^\alpha \bar{u}_L^\beta \gamma^\mu b_L^\beta. \quad (199)$$

$$Q_3 = \bar{s}_L^\alpha \gamma_\mu b_L^\alpha \sum_q \bar{q}_L^\beta \gamma^\mu q_L^\beta, \quad Q_4 = \bar{s}_L^\alpha \gamma_\mu b_L^\beta \sum_q \bar{q}_L^\beta \gamma^\mu q_L^\alpha, \quad (200)$$

$$Q_5 = \bar{s}_L^\alpha \gamma_\mu b_L^\alpha \sum_q \bar{q}_R^\beta \gamma^\mu q_R^\beta, \quad Q_6 = \bar{s}_L^\alpha \gamma_\mu b_L^\beta \sum_q \bar{q}_R^\beta \gamma^\mu q_L^\alpha, \quad (201)$$

$$Q_8 = \frac{g_s}{16\pi^2} m_b \bar{s}_L \sigma^{\mu\nu} T^a b_R G_{\mu\nu}^a \quad (202)$$

with color indices  $\alpha$  and  $\beta$ . The operators are depicted in Fig. 6. Those in Eqs. (196–199) are called *current-current* operators and are generated by tree diagrams. For the current-current operators  $Q_{1,2}$  and  $Q_{1,2}^u$  we can draw the penguin diagrams of Fig. 6, which require a counterterm proportional to a linear combination of the four-quark *penguin operators*  $Q_{3-6}$ . This feature is called *operator mixing*. Other diagrams giving rise to operator mixing are those found by dressing the diagrams in the first row of Fig. 6 with a gluon. Thus e.g. also  $Q_1^{cu}$  and  $Q_2^{cu}$  mix with each other. Furthermore, diagrams like the one in Fig. 2 match onto penguin operators, so that their Wilson coefficients depend on  $m_t/M_W$ . The corresponding hamiltonian for  $b \rightarrow d$  transitions is found from Eq. (194) by changing the CKM factors

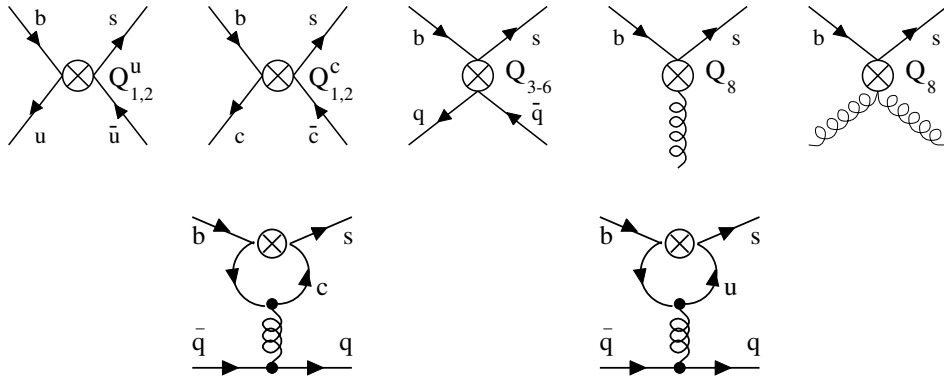


**Fig. 6** Upper row: Operators in  $H^{\Delta B=1}$  of Eqs. (194–202). The operators of  $H^{\Delta B=-1} = H^{\Delta B=1\dagger}$  are found by reversing the direction of the quark lines. Lower row: Penguin diagrams describing the mixing of  $Q_2^{(u)}$  in Eqs. (196) and (197) into the penguin operators  $Q_{3-6}$  in Eqs. (200) and (201)

to  $\lambda_a^d = V_{ad}^* V_{ab}$  and replacing the  $s$  field by  $d$  in the definitions of the operators. The Wilson coefficients are the same.

Operator mixing implies that the renormalization group equations for the Wilson coefficients  $C_{1-6}$  are coupled, so that the low-energy values  $C_j(\mu_b)$  also depend on the initial conditions  $C_k(\mu_{tW})$  of other coefficients. At two-loop level and beyond, the four-quark operators also mix into the *chromomagnetic penguin operator*. The RG evolution factor  $u^{(0)}(\mu_b, \mu_{tW})$  of Eq. (184) is replaced by matrices in the case of  $H^{\Delta B=1}$ , the term proportional to  $\lambda_t^x$  involves a  $7 \times 7$  RG evolution matrix and the terms with the other three CKM factors instead involve (the same)  $2 \times 2$  matrix. This  $2 \times 2$  matrix is diagonal if one switches from the operator basis  $(Q_1^x, Q_2^x)$  (with  $x = u, c, cu, uc$ ) to  $(Q_+^x, Q_-^x)$  where  $Q_\pm^x = (Q_2^x \pm Q_1^x)/2$ . The first diagonal element, i.e. the anomalous dimension of  $Q_+^x$ , is the same as for  $Q$  in Eq. (167), which explains the notation in Eq. (184), and  $\gamma_-^{(0)} = -8$ . Details on  $H^{\Delta B=1}$  and the RG evolution of its coefficients can be found in Refs. [124, 125, 148–151], which report the two-loop results for the NLO anomalous dimension matrix and the NLO initial conditions for the Wilson coefficients,  $C_k(\mu_{tW})$ . The calculation of the latter involve the one-loop QCD corrections to the SM  $b$  decay amplitude and the corresponding corrections to the four quark operators. The NNLO result for  $H^{\Delta B=1}$ , which required a three-loop calculation, has been presented in Ref. [152].

As a first application, I discuss the mixing-induced  $CP$  asymmetries, for which we do not need to know the values of the Wilson coefficients. The amplitudes  $A_f$  and  $\bar{A}_f$  of Eq. (117) read, with  $H_{\text{int}}$  of Eq. (118) replaced by  $H^{\Delta B=1} = H^{\Delta B=1} + H^{\Delta B=-1}$ ,

$$A_f = \langle f | H^{\Delta B=1} | B \rangle, \quad \bar{A}_f = \langle f | H^{\Delta B=-1} | \bar{B} \rangle \quad (203)$$

where I have expanded the S-matrix to the lowest order in  $G_F$ .

Taking the  $CP$  phase  $\phi_{CP, B_s}^{\text{mix}}$  (equal to  $-2\beta_s$  in the SM) as an example, we identify the terms with  $Q_{1,2}$  in Eq. (194) as responsible for the dominant tree amplitude. Neglecting penguin contributions we set  $\lambda_u^s = 0$  and replace  $\lambda_c^s$  by  $-\lambda_c^s$ . Then

$$A_{(J/\psi\phi)_l} = \frac{4G_F}{\sqrt{2}} \lambda_c^{s*} \sum_j C_j \langle (J/\psi\phi)_l | Q_j^\dagger | B_s \rangle, \quad \bar{A}_{(J/\psi\phi)_l} = \frac{4G_F}{\sqrt{2}} \lambda_c^s \sum_j C_j \langle (J/\psi\phi)_l | Q_j | \bar{B}_s \rangle. \quad (204)$$

Applying the  $CP$  transform of Eq. (15) to the quark currents in  $Q_j$  on finds  $CPQ_j(CP)^\dagger = Q_j^\dagger$ . Then we insert  $(CP)^\dagger CP = 1$  into our matrix element and use Eq. (23) and  $\eta_{CP, (J/\psi\phi)_l} = (-1)^l$  to find

$$\bar{A}_{(J/\psi\phi)_l} = \frac{4G_F}{\sqrt{2}} \lambda_c^s \sum_j C_j \langle (J/\psi\phi)_l | (CP)^\dagger CP Q_j (CP)^\dagger CP | \bar{B}_s \rangle = -\frac{4G_F}{\sqrt{2}} (-1)^l \lambda_c^s \sum_j C_j \langle (J/\psi\phi)_l | Q_j^\dagger | B_s \rangle = -(-1)^l \frac{\lambda_c^s}{\lambda_c^{s*}} A_{(J/\psi\phi)_l} \quad (205)$$

which fills in the missing details of the derivation of  $\bar{A}_{(J/\psi\phi)_l}/A_{(J/\psi\phi)_l}$  in Eq. (152).

Next I discuss the calculation of  $\Gamma_{12}^{d,s}$ . There is no contribution of  $H^{\Delta B=2}$  to  $\Gamma_{12}^{d,s}$ , because  $\langle B_q | H^{\Delta B=2} | \bar{B}_q \rangle$  has no absorptive part. The relevant contributions instead come from two transitions mediated by  $H^{\Delta B=1}$ . We expanding the S-matrix to second order:

$$S = T \exp \left[ -i \int d^4 x \left( H^{\Delta B=2}(x) + H^{\Delta B=1}(x) \right) \right] = -i \int d^4 x H^{\Delta B=2}(x) - \frac{1}{2} \int d^4 x d^4 y T \left[ H^{\Delta B=1}(x) H^{\Delta B=1}(y) \right] + \dots \quad (206)$$

where the dots represent terms which do not contribute to  $|\Delta B| = 2$  transitions. The  $\Delta B = 2$  matrix element in the effective theory then reads

$$\Sigma_{12} = M_{12} - \frac{i}{2} \Gamma_{12} = \langle B | H^{\Delta B=2}(0) | \bar{B} \rangle - \frac{i}{2} \langle B | \int d^4 x T \left[ H^{\Delta B=1}(x) H^{\Delta B=1}(0) \right] | \bar{B} \rangle. \quad (207)$$

The LO contributions to  $\Gamma_{12}$ , which stem from the second term in Eq. (207), are shown in Fig. 7 for the case of  $B_s - \bar{B}_s$  mixing. The contribution from the second, bilocal term Eq. (207) to  $B - \bar{B}$  mixing is much smaller than the one from  $H^{\Delta B=2}$ , which is enhanced due to the heavy top mass entering Eq. (178) while  $\Gamma_{12}$  scales like  $m_t^2$ . Therefore we can neglect the bilocal contribution in  $M_{12}$  and only need to consider it for  $\Gamma_{12}$ . From this observation we also verify that  $|\Gamma_{12}/M_{12}| = O(m_b^2/m_t^2)$ , which we used in the discussion after Eq. (91).

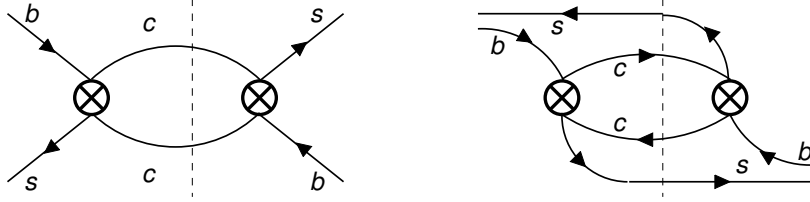


**Fig. 7** Second-order contribution of  $H^{|\Delta B|=1}$  to  $B_s - \bar{B}_s$  mixing. The diagrams with two charm quarks, found by contracting the  $W$  lines in the corresponding box diagrams to a point, constitute the dominant contribution to  $\Gamma_{12}^s$  and involve two insertions of  $Q_2$  of Eq. (196).

Eqs. (94–96) relate  $\Gamma_{12}^q$  and  $M_{12}^q$  to  $\Delta\Gamma_q$  and  $a_{fs}^q$  for  $q = d$  or  $s$ :

$$\frac{\Delta\Gamma_q}{\Delta M_q} \simeq -\text{Re} \frac{\Gamma_{12}^q}{M_{12}^q}, \quad a_{fs}^q \simeq \text{Im} \frac{\Gamma_{12}^q}{M_{12}^q}. \quad (208)$$

The calculation of the ratio  $\Gamma_{12}^q/M_{12}^q$  has two advantages over the calculation of  $\Gamma_{12}^q$ : The dependence on  $V_{cb} = A\lambda^2$ , which normalizes the CKM parameter  $V_{tq}$ , drops out from the ratio. Furthermore, the dominant contribution to  $\Gamma_{12}^q$  is proportional to the hadronic matrix element in Eq. (188) which also enters  $M_{12}^q$  and therefore cancels to a large extent from the ratio.

$\Gamma_{12}^q$  involves two novel features compared to  $M_{12}^q$ : Firstly, it is calculated in a power series in  $\Lambda_{\text{QCD}}/m_b$  which results from an OPE with  $m_b$  as the hard scale called *Heavy Quark Expansion (HQE)* [153, 154]. Technically, one expands the loop diagrams of Fig. 7 in the inverse of the external  $b$ -quark momentum and matches the different terms onto matrix elements of local  $\Delta B = 2$  operators. These operators are pictorially found by contracting the hard loop momentum in bilocal diagrams like those in Fig. 7 to a point, leading to the effective interaction of Fig. 5. Higher powers of  $1/m_b$  in the coefficients come with higher dimensions of the corresponding operators, thus the  $1/m_b$  corrections to the leading-power result involve dimension-7 operators, whose matrix elements have an extra power of  $\Lambda_{\text{QCD}}$  compared to Eq. (188) (entering e.g. as a power of  $M_B - m_b$ ). Thus the prediction of  $\Gamma_{12}^q$  is a double expansion in the two parameters  $\Lambda_{\text{QCD}}/m_b$  and  $\alpha_s(m_b)$ . Secondly, the leading-power contribution involves two operators, apart from  $Q$  in Eq. (77) this is [155]

$$\tilde{Q}_S = \bar{q}_L^\alpha b_R^\beta \bar{q}_L^\beta b_R^\alpha \quad (209)$$

with matrix element

$$\langle B_q | \tilde{Q}_S(\mu_2) | \bar{B}_q \rangle = \frac{1}{3} M_{B_q}^2 f_{B_q}^2 \tilde{B}'_{S,B_q}(\mu_2) \quad (210)$$

With  $B'_{S,B_s}(m_b) = 1.31 \pm 0.09$  and  $B'_{S,B_d}(m_b) = 1.20 \pm 0.09$  [146] we find this matrix element smaller than  $\langle B_q | Q | \bar{B}_q \rangle$  in Eq. (188) and the uncertainty in  $\Gamma_{12}^q/M_{12}^q$  from these matrix element is not an issue in the predictions of the quantities in Eq. (208).

For the discussion of  $a_{fs}^q$  it helps to decompose  $\Gamma_{12}^q$  as [156]

$$\Gamma_{12}^q = -(\lambda_c^q)^2 \Gamma_{12}^{cc} - 2\lambda_c^q \lambda_u^q \Gamma_{12}^{uc} - (\lambda_u^q)^2 \Gamma_{12}^{uu} \quad (211)$$

$$= -(\lambda_t^q)^2 \left[ \Gamma_{12}^{cc} + 2 \frac{\lambda_u^q}{\lambda_t^q} \left( \Gamma_{12}^{cc} - \Gamma_{12}^{uc} \right) + \left( \frac{\lambda_u^q}{\lambda_t^q} \right)^2 \left( \Gamma_{12}^{uu} + \Gamma_{12}^{cc} - 2\Gamma_{12}^{uc} \right) \right]. \quad (212)$$

Here the superscript labels the quark flavors on the two internal lines,  $-(\lambda_c^q)^2 \Gamma_{12}^{cc}$  is shown in Fig. 7. To prepare for the normalization to  $M_{12}^q \propto \lambda_t^q$  I have traded  $\lambda_c^q = -\lambda_t^q - \lambda_u^q$  for  $\lambda_t^q$  in the second line of Eq. (212). We observe that the terms proportional to  $\lambda_u^q/\lambda_t^q$  and  $(\lambda_u^q/\lambda_t^q)^2$  are GIM-suppressed, since they vanish for  $m_c = m_u$ .

To discuss  $\Delta\Gamma_q/\Delta M_q$  and  $a_{fs}^q$  it is useful to define real parameters  $a$ ,  $b$  and  $c$  through [157]

$$\begin{aligned} \frac{\Gamma_{12}^d}{M_{12}^d} &= \frac{\lambda_t^d}{M_{12}} \left[ -\Gamma_{12}^{cc} + 2 \left( \Gamma_{12}^{uc} - \Gamma_{12}^{cc} \right) \frac{\lambda_u^d}{\lambda_t^d} + \left( 2\Gamma_{12}^{uc} - \Gamma_{12}^{cc} - \Gamma_{12}^{uu} \right) \frac{\lambda_u^d}{\lambda_t^d} \right] \\ &\equiv 10^{-4} \left[ c + a \frac{\lambda_u^d}{\lambda_t^d} + b \frac{\lambda_u^{d2}}{\lambda_t^{d2}} \right]. \end{aligned} \quad (213)$$

$a$ ,  $b$ , and  $c$  depend on the particle masses and, in particular, are functions of

$$z = \frac{m_c^2}{m_b^2} \quad (214)$$

By calculating  $\Gamma_{12}^{ab}$  one finds that  $a$  is linear in  $z$ ,  $b$  is proportional to  $(\lambda_u^q/\lambda_t^q)^2$  and negligible, because it is proportional to  $z^3$  at LO and  $\alpha_s z^2$  at NLO. Furthermore we verify from Eq. (35) that both  $|\lambda_u^s/\lambda_t^s| \propto \lambda^2$  and  $\text{Re}(\lambda_u^d/\lambda_t^d) \propto \cos \alpha$  are small; in the latter case this stems from the fact that  $\alpha$  happens to be close to  $90^\circ$ . Thus  $\Delta\Gamma_q/\Delta M_q = -\text{Re}(\Gamma_{12}^q/M_{12}^q)$  is dominated by  $c$  for both  $q = d$  and  $q = s$ .

For  $a_{\text{fs}}^q$ , however, one observes

$$a_{\text{fs}}^q = \left[ a \text{Im} \frac{\lambda_u^d}{\lambda_t^d} + b \text{Im} \frac{(\lambda_u^d)^2}{(\lambda_t^d)^2} \right] \cdot 10^{-4} \propto z \quad (215)$$

from Eq. (213), so that  $a_{\text{fs}}^d$  is suppressed w.r.t.  $\Delta\Gamma_d/\Delta M_d$  by a factor of  $z$ . Furthermore, in  $a_{\text{fs}}^s$  there is an additional CKM suppression from  $\text{Im}(\lambda_u^s/\lambda_t^s) \propto \lambda^2 \simeq 0.05$ .

With

$$\frac{\lambda_u^d}{\lambda_t^d} = \frac{1 - \bar{\rho} - i\bar{\eta}}{(1 - \bar{\rho})^2 + \bar{\eta}^2} - 1. \quad (216)$$

we can express  $\text{Im}(\lambda_u^d/\lambda_t^d)$  in terms of UT parameters. Neglecting the small term with  $b$  one finds

$$a_{\text{fs}}^d = \text{Im} \frac{\lambda_u^q}{\lambda_t^q} a \cdot 10^{-4} = -\frac{\bar{\eta}}{(1 - \bar{\rho})^2 + \bar{\eta}^2} a \cdot 10^{-4} = -\frac{\sin\beta}{R_t} a \cdot 10^{-4} \quad (217)$$

from Eq. (215). From the third expression one realizes that a future improved measurement of  $a_{\text{fs}}^d$  in Eq. (113) will define a circle in the  $\bar{\rho}$ - $\bar{\eta}$  plane which gives complementary information to the circle found from  $\Delta M_d$ , the line from  $A_{CP}^{\text{mix}}(B_d \rightarrow J/\psi K_{\text{short}}) = -\sin(2\beta)$ , and other standard observables used in UT phenomenology, see Fig. 8. From Eq. (217) one easily finds the equation for the desired new circle:

$$(\bar{\eta} - R_{\text{fs}})^2 + (1 - \bar{\rho})^2 = R_{\text{fs}}^2 \quad \text{with} \quad R_{\text{fs}} = -\frac{a}{2a_{\text{fs}}^{\text{exp}}}, \quad (218)$$

where  $a_{\text{fs}}^{\text{exp}}$  denotes the experimental value of  $a_{\text{fs}}^d$ . Thus the circle is centered on the vertical line with  $\bar{\rho} = 1$  and intersects the point  $(\bar{\rho}, \bar{\eta}) = (1, 0)$ ; its radius  $R_{\text{fs}}$  is slightly larger than 1 if the SM describes  $a_{\text{fs}}^d$  correctly.

The last expression in Eq. (217) involves the two quantities inferred from measurements of  $A_{CP}^{\text{mix}}(B_d \rightarrow J/\psi K_{\text{short}})$  and  $\Delta M_d$ . Thus measuring all of  $A_{CP}^{\text{mix}}(B_d \rightarrow J/\psi K_{\text{short}})$ ,  $\Delta M_d$ , and  $a_{\text{fs}}^d$  over-constrains  $\beta$  and  $R_t$  and thus constitutes a probe of BSM physics in  $B_d - \bar{B}_d$  mixing *alone*, without the need of input from other quantities. Pictorially, BSM physics in  $B_d - \bar{B}_d$  mixing will reveal itself in this way if the intersection of the circles from  $\Delta M_d$  and  $a_{\text{fs}}^d$  will not be spiked by the line inferred from  $A_{CP}^{\text{mix}}(B_d \rightarrow J/\psi K_{\text{short}})$ .

The OPE matches the result of the diagrams in Fig. 7 (and the corresponding ones with one or two up quarks) onto local  $\Delta B = 2$  operators to yield an expression of the form

$$\Gamma_{12}^{ab} = \frac{G_F^2 m_b^2}{24\pi M_{B_q}} \left[ H^{ab}(z) \langle B_q | Q | \bar{B}_q \rangle + \tilde{H}_S^{ab}(z) \langle B_q | \tilde{Q}_S | \bar{B}_q \rangle \right] + \mathcal{O}\left(\frac{\Lambda_{\text{QCD}}}{m_b}\right), \quad (219)$$

with new Wilson coefficients  $H^{ab}(z)$  and  $\tilde{H}_S^{ab}(z)$ . The diagrams of Fig. 7 determine them to LO, for the NLO and NNLO results one had to calculate diagrams with one and two extra gluons, respectively, as well as the corresponding diagrams for the  $\Delta B = 2$  operators.

$\Gamma_{12}^q$  has been calculated to LO in Refs. [154, 158–163] with focus on the predictions of  $\Delta\Gamma_s$  and  $a_{\text{fs}}^d$ . The NLO prediction of the contribution with the large Wilson coefficients  $C_1$ ,  $C_2$ , and  $C_8$  to  $\Delta\Gamma_s$  was presented in Refs. [155, 156, 164], the NLO results for  $a_{\text{fs}}^{d,s}$  and  $\Delta\Gamma_d$  were derived in Refs. [155, 157, 164]. The NLO contribution with the small (of order 0.05) four-quark penguin coefficients  $C_3 \dots C_6$  was obtained in Ref. [165, 166]. The NNLO calculation of the three-loop diagrams has been tackled in terms of an expansion in  $z$ . The contribution calculated first only involved three-loop diagrams with fermion loops [167–169]. Ref. [166] contains the NNLO results with one  $C_8$  and one four-quark coefficient, which only involve two-loop diagrams. The numerically most important piece of the NNLO prediction stems from three-loop diagrams with two current-current operator coefficients  $C_{1,2}$ , found in an expansion to order  $z$  in Ref. [170] and to order  $z^{50}$  in Ref. [171], except for the charm mass effects in the tiny gluon self-energy diagrams, which are only known to order  $z^6$ . The result of Ref. [170] is satisfactory for  $\Delta\Gamma_q$ , but not for  $a_{\text{fs}}^q \propto z$ , for which the calculation in Ref. [171] was needed. Ref. [166] also contains a first step towards NNNLO, with the calculation of two-loop diagrams proportional to  $C_8^2$ .

The cited calculations are all for the leading-power term, i.e. they address QCD corrections to  $H^{ab}(z)$  and  $\tilde{H}_S^{ab}(z)$  in Eq. (219). The NNLO predictions are [171]

$$\begin{aligned} \frac{\Delta\Gamma_s}{\Delta M_s} &= (4.37_{-0.44}^{0.23} \text{scale} \pm 0.12_{\text{matrixel.}} \pm 0.79_{1/m_b} \pm 0.05_{\text{input}}) \times 10^{-3} \text{ (MS)} \\ \frac{\Delta\Gamma_s}{\Delta M_s} &= (4.27_{-0.37}^{0.36} \text{scale} \pm 0.12_{\text{matrixel.}} \pm 0.79_{1/m_b} \pm 0.05_{\text{input}}) \times 10^{-3} \text{ (PS)} \end{aligned} \quad (220)$$

The two results correspond to the modified minimal subtraction ( $\overline{\text{MS}}$ ) and potential-subtracted (PS) renormalization schemes. The dependence on renormalization scheme and scale diminishes order-by-order of  $\alpha_s$ ; it is commonly used as an estimate of the uncertainty related to the omission of unknown higher orders of  $\alpha_s$ . The indicated scale dependence of the NNLO result in Eq. (220) is slightly below 9%, which is larger, but close to the experimental error in Eq. (49). The second uncertainty stems from the ratio of the hadronic matrix elements, i.e. from  $B'_{S,B_s}/B_{B_s}$ . The dominant source of uncertainty are the poorly known matrix elements of the dimension-7 operators entering the  $\Lambda_{\text{QCD}}/m_b$  corrections. Moreover, the coefficients of the dimension-7 operators are only known to LO [172], and an NLO calculation is necessary for a meaningful lattice-continuum matching of the matrix elements. The last uncertainty in Eq. (220) stems from the physical parameters, mostly from CKM elements. One should keep in mind that their values and uncertainties are found under the assumption that there is no new physics in the quantities entering the global fit of  $\bar{\rho}$  and  $\bar{\eta}$  from data. Thus future measurements in tension with the presented

SM predictions may not necessarily be related to new physics in the quoted quantities but instead in the quantities from which  $\bar{\rho}$  and  $\bar{\eta}$  are determined.

Currently, we are far away from a measurement of  $\Delta\Gamma_d$  with a precision comparable to  $\Delta\Gamma_s$  in Eq. (49). The SM predictions for  $\Delta\Gamma_d/\Delta M_d$  and  $\Delta\Gamma_s/\Delta M_s$  are almost equal and, for the time being, one can use

$$\frac{\Delta\Gamma_d}{\Delta M_d} = 0.963 \frac{\Delta\Gamma_s}{\Delta M_s} \quad (221)$$

for the results in both renormalization schemes. Once better measurements than those summarized in Eq. (46) will be available, one should use the precise formulae of Ref. [171].

One can use the experimental values in Eqs. (20) and (48) to predict [171]

$$\Delta\Gamma_d = \frac{\Delta\Gamma_d}{\Delta M_d} \Delta M_d^{\text{exp}} = (0.00211 \pm 0.00045) \text{ ps}^{-1}, \quad \Delta\Gamma_s = \frac{\Delta\Gamma_s}{\Delta M_s} \Delta M_s^{\text{exp}} = (0.077 \pm 0.016) \text{ ps}^{-1} \quad (222)$$

from Eq. (220), with the numbers being the averages of the  $\overline{\text{MS}}$  and PS schemes. The benefit of a future measurement of  $\Delta\Gamma_d$  will be a precise test of BSM physics in  $\Gamma_{12}^{d,s}$  through the ratio  $\Delta\Gamma_d/\Delta\Gamma_s$ , because most of the uncertainties in Eq. (220) drop out from this ratio.

The NNLO predictions for the coefficients in Eq. (213) are [171]

$$a = 12.2 \pm 0.6, \quad b = 0.23 \pm 0.06 \quad (223)$$

and a breakdown of the different sources of uncertainties can be found in Ref. [171].  $c$  in Eq. (213) essentially equals  $10^4 \cdot \text{Re}(\Gamma_{12}^d/M_{12}^d) = -10^4 \cdot \Delta\Gamma_d/\Delta M_d$ , which amounts to

$$c = -42 \pm 9. \quad (224)$$

Using the values from a recent global fit [173],

$$\frac{\lambda_u^d}{\lambda_t^d} = (0.0105 \pm 0.0107) - (0.4259 \pm 0.0091)i, \quad \frac{\lambda_u^s}{\lambda_t^s} = -(0.00877 \pm 0.00043) + (0.01858 \pm 0.00038)i, \quad (225)$$

one finds [171]

$$a_{\text{fs}}^d = -(5.21 \pm 0.32) \times 10^{-4}, \quad a_{\text{fs}}^s = (2.28 \pm 0.14) \times 10^{-5}.$$

Note that the parameters  $a, b, c$  for  $B_s - \bar{B}_s$  mixing are slightly different from those in  $B_d - \bar{B}_d$  mixing, similar to the situation in Eq. (221). The smallness of  $a_{\text{fs}}^s$  compared to  $a_{\text{fs}}^d$  stems from the small imaginary part of the CKM factor in Eq. (225),  $\text{Im}(\lambda_u^s/\lambda_t^s) \approx \bar{\eta}\lambda^2$ .

In Ref. [174] it was pointed out that  $a_{\text{fs}}^d$  is very sensitive to new physics in  $M_{12}^d$ , as a small BSM  $CP$  phase spoils the approximate phase alignment of  $\Gamma_{12}^d$  and  $M_{12}^d$ , so that  $a_{\text{fs}}^d$  picks up a term with the large coefficient  $c$  in Eq. (224) which is not suppressed by  $z$ . This analysis was later extended to BSM physics in  $\Gamma_{12}^d$  [175, 176]. If one parameterizes BSM physics as

$$\frac{\Gamma_{12}^q}{M_{12}^q} = \frac{\Gamma_{12,\text{SM}}^q}{M_{12,\text{SM}}^q} d_{\text{NP}}^q e^{i\phi_{\text{NP}}^q}, \quad (226)$$

with  $d_{\text{NP}}^q > 0$  and a BSM  $CP$  phase  $\phi_{\text{NP}}^q$ , one finds [157, 174, 175]

$$a_{\text{fs}}^q = a_{\text{fs,SM}}^q d_{\text{NP}}^q \cos \phi_{\text{NP}}^q - \frac{\Delta\Gamma_{q,\text{SM}}}{\Delta M_{q,\text{SM}}} d_{\text{NP}}^q \sin \phi_{\text{NP}}^q. \quad (227)$$

Thus new physics enhances  $a_{\text{fs}}^q$  with a lever arm of  $(\Delta\Gamma_{q,\text{SM}}/\Delta M_{q,\text{SM}})/a_{\text{fs,SM}}^q$  multiplying  $\sin \phi_{\text{NP}}^q$ . This enhancement factor equals 8 for  $q = d$  and 190 for  $q = s$  when using the central values in Eqs. (220) and (226). While the effect of BSM physics is spectacular for  $a_{\text{fs}}^s$ , the experimental value in Eq. (55) permits only BSM contributions of a few degrees in  $M_{12}^s$ .  $\Gamma_{12}^s$  cannot receive sizable BSM contributions either. Still, for  $\phi_{\text{NP}}^s = -5^\circ$  and  $d_{\text{NP}}^s = 1$  we find  $a_{\text{fs}}^s$  enhanced by more than a factor of 15 to  $a_{\text{fs}}^s = 4 \cdot 10^{-4}$ . The room for BSM physics in  $a_{\text{fs}}^d$  is larger, because a precise SM prediction for  $M_{12}^d$  suffers from the unclear situation with  $V_{cb}$  and  $V_{ub}$  and the doubly Cabibbo-suppressed  $\Gamma_{12}^d$  can receive BSM contributions as well, so that  $|a_{\text{fs}}^d|$  above  $10^{-3}$  cannot be excluded now.

In summary, the decay matrix element  $\Gamma_{12}^{d,s}$  determines  $\Delta\Gamma_{d,s}$  and  $a_{\text{fs}}^{d,s}$ . While  $\Gamma_{12}^{d,s}$  originates from a  $\Delta B = 2$  transition, there is no contribution from the  $|\Delta B| = 2$  hamiltonian to this quantity, which instead involves two  $|\Delta B| = 1$  interactions as shown in Fig. 7. The corresponding  $|\Delta B| = 1$  hamiltonian in Eq. (194) describes decays of  $b$ -flavored hadrons;  $\Gamma_{12}^q$  receives contributions from all decays to final states which are common to  $B_q$  and  $\bar{B}_q$ , as shown in Eq. (99).  $\Delta\Gamma_s$  is precisely measured and a calculation of QCD corrections to  $\Gamma_{12}^q$  at NNLO was necessary to bring the perturbative uncertainty to a level which is similar to the experimental error. A future measurement of  $a_{\text{fs}}^{d,s}$  will define the circle of Eq. (218) in the  $\bar{\rho}-\bar{\eta}$  plane, which gives new information on  $(\bar{\rho}, \bar{\eta})$ , complementary to other constraints. In particular, in combination with  $\Delta M_d$  and  $A_{CP}^{\text{mix}}(B_d \rightarrow J/\psi K_{\text{short}})$  a measurement of the  $CP$  asymmetry  $a_{\text{fs}}^d$  will over-constrain the UT and provide a SM test of BSM physics in  $B_d - \bar{B}_d$  mixing without the need of external input from other observables entering the global UT fit.  $\Delta\Gamma_d$  and  $a_{\text{fs}}^s$  play roles as BSM physics tests; in the case of  $a_{\text{fs}}^s$  already small BSM  $CP$  phases can enhance this quantity from its tiny SM prediction to a value accessible at experiment.

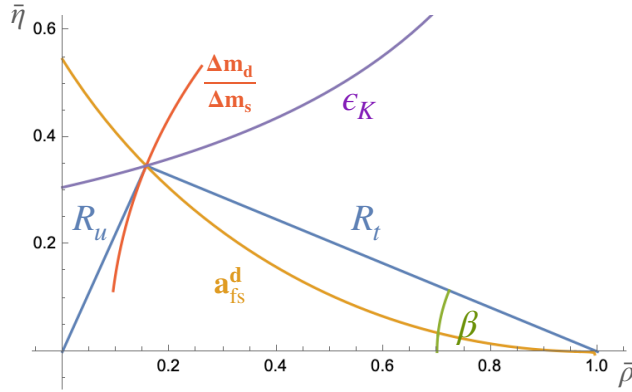


**Fig. 8** Constraints on the unitarity triangle from  $\Delta M_d/\Delta M_s$ ,  $\epsilon_K$ ,  $a_{fs}^d$ , and  $A_{CP}^{\text{mix}}(B_d \rightarrow J/\psi K_{\text{short}}) = -\sin(2\beta)$ , schematically for a hypothetical perfect agreement with the SM and no uncertainties.

#### 6.4 Effective hamiltonians for $K-\bar{K}$ mixing with predictions for $\epsilon_K$ and $\Delta M_K$ , overall picture of the UT

The formalism to describe  $CP$  violation in  $K-\bar{K}$  mixing and the relation of  $CP$  asymmetries to the  $CP$  phase  $\phi_K = \arg(-M_{12}^K/\Gamma_{12}^K)$  has been presented in Eqs. (120–136). The quantity  $\epsilon_K$  introduced in Eq. (121) encodes both  $CP$  violation in mixing and mixing-induced  $CP$  violation, while the semileptonic  $CP$  asymmetry  $A_L = a_{fs}^K/2$  of Eq. (133) is a measure of only the former type of  $CP$  violation.  $A_L$  and  $\text{Re } \epsilon_K$  provide the same information on  $\phi_K$ . In contrast to  $B-\bar{B}$  and  $D-\bar{D}$  mixing  $\text{Im } \epsilon_K$  encoding mixing-induced  $CP$  violation in the decay  $K \rightarrow (\pi\pi)_{l=0}$  does not provide new information compared to  $a_{fs}^K$  and also determines  $\phi_K$ , see Eq. (132). I will now show how  $\epsilon_K$  is calculated in the SM.

In  $K-\bar{K}$  mixing it is common practice to adopt the standard phase convention for the CKM matrix in which  $V_{us}V_{ud}^*$  is real and positive. Starting from Eq. (89), we write

$$\phi = \arg\left(-\frac{M_{12}^K}{\Gamma_{12}^K}\right) \simeq \frac{\text{Im } M_{12}^K}{|M_{12}^K|} - \arg(-\Gamma_{12}^K) = 2 \left[ \frac{\text{Im } M_{12}^K}{\Delta M_K^{\text{exp}}} + \xi_K \right] \quad (228)$$

where

$$2\xi_K \equiv -\arg(-\Gamma_{12}^K) \simeq -\arg\left(-\frac{\bar{A}_0}{A_0}\right). \quad (229)$$

In Eq. (228) I have used that the phases of both  $M_{12}^K$  and  $-\Gamma_{12}^K$  are small in the standard CKM phase convention and further traded  $|M_{12}^K|$  for the experimental  $\Delta M_K/2$ . Furthermore, in Eq. (229) the saturation of  $\Gamma_{12}$  by  $A_0^* \bar{A}_0$  in Eq. (126) has been used. Inserting Eq. (228) into our result for  $\epsilon_K$  in Eq. (132) gives

$$\epsilon_K \simeq \sin(\phi_\epsilon) e^{i\phi_\epsilon} \left[ \frac{\text{Im } M_{12}^K}{\Delta M_K^{\text{exp}}} + \xi_K \right]. \quad (230)$$

The term with  $\xi_K$  encodes the  $CP$ -odd phase in  $\bar{K} \rightarrow (\pi\pi)_{l=0}$ , which we expect to appear in a quantity measuring mixing-induced  $CP$  violation. It only contributes  $-6\%$  to  $\epsilon_K$  [177] (a recent lattice determination finds  $|\xi_K|$  slightly larger [178]) and will be briefly discussed below. The ballpark contribution to  $\epsilon_K$  stems from  $\text{Im } M_{12}^K$ , i.e. from the familiar  $K-\bar{K}$  box diagram.

The LO  $\Delta S = 2$  transition amplitude  $\mathcal{M}^{(0)}$  corresponding to the  $K-\bar{K}$  mixing box diagram in Fig. 1 is found from the corresponding  $\Delta B = 2$  expression in Eq. (175) by the substitutions  $b \rightarrow s$  and  $q \rightarrow d$  in the CKM elements. Everything else is unchanged, in particular we encounter the same Inami-Lim functions as in  $B-\bar{B}$  mixing. An important difference is the hierarchy among the three CKM combinations in Eq. (175), the smallness of  $(V_{ts}V_{td}^*)^2 \simeq A^4 \lambda^{10} (1 - \bar{\rho} - i\bar{\eta})^2$  compensates the large size of  $S(x_t)$  and the terms with  $S(x_c, x_t)$  and  $S(x_c)$  become important, where I recall the definition  $x_q \equiv m_q^2/M_W^2$ . For  $\epsilon_K$  in Eq. (230) we need the imaginary parts of the CKM factors. To lowest order in the Wolfenstein expansion one finds

$$\text{Im}(V_{ts}V_{td}^*)^2 \simeq 2(A\lambda^2)^4 \lambda^2 \bar{\eta} (1 - \bar{\rho}), \quad 2 \text{Im}(V_{ts}V_{td}^* V_{cs}V_{cd}^*) \simeq -\text{Im}(V_{cs}V_{cd}^*)^2 \simeq 2(A\lambda^2)^2 \lambda^2 \bar{\eta} \quad (231)$$

and the numerical hierarchy becomes evident from  $A\lambda^2 = |V_{cb}| = 0.04$ . Thus, in addition to  $S(x_t)$  in Eq. (178) we also need  $S(x_c) = x_c + O(x_c^2)$  and

$$S(x_c, x_t) = -x_c \ln x_c + x_c \left[ \frac{x_t^2 - 8x_t + 4}{4(1-x_t)^2} \ln x_t + \frac{3}{4} \frac{x_t}{x_t - 1} \right] + O(x_c^2 \ln x_c). \quad (232)$$

These three contributions require a very different treatment of their QCD corrections. The term with  $S(x_t)$  follows the pattern which we discussed for  $B-\bar{B}$  mixing, leading to the effective hamiltonian in Eq. (187). There is only one difference between the QCD correction

factor  $\eta_B b_B(\mu_b)$  in Eq. (187) and its counterpart  $\eta_{tt} b_K(\mu)$  in the  $|\Delta S| = 2$  hamiltonian: The RG evolution of the coefficient of the local operator

$$Q = \bar{d}_L \gamma_\nu s_L \bar{d}_L \gamma^\nu s_L. \quad (233)$$

must be carried to a lower scale  $\mu_K = O(1 \text{ GeV})$  and to this end one must match  $Q$  from five-flavour QCD to three-flavour QCD at an intermediate scale  $\mu_{bc} = O(m_c)$ . This requires to change  $f = 5$  to  $f = 3$  in the evolution of Eq. (184) for  $\mu_K \leq \mu \leq \mu_{bc}$ . Beyond LO there is also a threshold correction  $C^{|\Delta S|=2,f=3}(\mu_{bc})/C^{|\Delta S|=2,f=5}(\mu_{bc})$ , which is numerically very small.

The other two contributions, with light charm and up quarks on the internal lines, require the consideration of terms with two  $|\Delta S| = 1$  hamiltonians. We have encountered this piece as the second term of  $\Sigma_{12}$  in Eq. (207) in the discussion of  $|\Delta B| = 2$  transitions. This term does not only contribute to  $\Gamma_{12}$ , but also to  $M_{12}$  but is negligible in the case of  $|\Delta B| = 2$  transitions. In  $K - \bar{K}$  mixing the transition amplitude at intermediate scales  $\mu_{bc} \leq \mu \leq \mu_{tW}$  involves both a local  $|\Delta S| = 2$  hamiltonian and the bilocal matrix element with two copies of the  $|\Delta S| = 1$  hamiltonian, both of which are obtained from their  $|\Delta B| = 1, 2$  counterparts by appropriately replacing the quark fields in the operators and changing the CKM elements. When we arrive at the renormalization scale  $\mu_{bc}$ , we must match our  $\Delta S = 2$  amplitude of the five-flavour theory to an amplitude in a theory which only has  $u, d$ , and  $s$  as dynamical quark fields. For  $\mu \leq \mu_{bc}$  the  $\Delta S = 2$  transition solely involves the local  $\Delta S = 2$  operator of Eq. (233), just as in the case of the top quark contribution proportional to  $(V_{ts} V_{td}^*)^2$  discussed first. The two-step matching of the contributions with  $(V_{cs} V_{cd}^*)^2$  and  $V_{cs} V_{cd}^* V_{ts} V_{td}^*$  with the RG evolution between the scales  $\mu_{tW}$  and  $\mu_{bc}$  leads to a result in which the product of  $\alpha_s$  and the large logarithm  $\ln x_c$  is summed to all orders in perturbation theory. The final result for the effective hamiltonian reads

$$H^{|\Delta S|=2} = \frac{G_F^2}{4\pi^2} M_W^2 \left[ (V_{ts} V_{td}^*)^2 \eta_{tt} S(x_t) + 2V_{ts} V_{td}^* V_{cs} V_{cd}^* \eta_{ct} S(x_c, x_t) + (V_{cs} V_{cd}^*)^2 \eta_{cc} x_c \right] b_K(\mu_K) Q(\mu_K) + h.c. \quad (234)$$

with the QCD corrections encoded in  $\eta_{tt}$ ,  $\eta_{ct}$ , and  $\eta_{cc}$ , with a common factor  $b_K(\mu_K)$  factored out. The hadronic matrix elements is parametrized as

$$\langle K | Q(\mu_K) | \bar{K} \rangle = \frac{2}{3} M_K^2 f_K^2 \frac{\widehat{B}_K}{b_K(\mu_K)}, \quad (235)$$

where  $M_K = 497.6 \text{ MeV}$  [1] and  $f_K = 156 \text{ MeV}$  [179] are Kaon mass and decay constant, respectively. With  $M_{12}^K = \langle K | H^{|\Delta S|=2} | \bar{K} \rangle$  we can determine  $\text{Im } M_{12}^K$  in terms of  $\widehat{B}_K$  and write for  $\epsilon_K$  in Eq. (230):

$$1.21 \cdot 10^{-7} = \widehat{B}_K \left[ \text{Im} (V_{ts} V_{td}^*)^2 \eta_{tt} S(x_t) + 2 \text{Im} (V_{ts} V_{td}^* V_{cs} V_{cd}^*) \eta_{ct} S(x_c, x_t) + \text{Im} (V_{cs} V_{cd}^*)^2 \eta_{cc} x_c \right]. \quad (236)$$

Here the number on the LHS originates from

$$1.21 \cdot 10^{-7} = \frac{12\pi^2 \Delta M_K^{\text{exp}}}{G_F^2 f_K^2 M_K M_W^2 \sin \phi_\epsilon} (|\epsilon_K^{\text{exp}}| - \tilde{\xi}_K \sin \phi_\epsilon) \quad (237)$$

where I have used the numbers quoted in this report as well as  $G_F = 1.1663710^{-5} \text{ GeV}^{-2}$  and  $M_W = 80.370 \text{ GeV}$ . In Eq. (237)  $\tilde{\xi}_K \sim 0.6 \xi_K$  subsumes  $\xi_K$  in Eq. (230) and the bilocal contribution to  $\text{Im } M_{12}^K$  from two insertions of the  $|\Delta S| = 1$  hamiltonian [178, 180, 181], i.e. the bilocal “long-distance” matrix element  $\langle K | \int d^4x T[H^{|\Delta S|=1}(x) H^{|\Delta S|=1}(0)] | \bar{K} \rangle$  contributes to both  $\Gamma_{12}^K$  and  $M_{12}^K$ . The effect of the term with  $\tilde{\xi}_K$  in Eq. (237) can be implemented as a 3% reduction of the RHS via  $|\epsilon_K^{\text{exp}}| - \tilde{\xi}_K \sin \phi_\epsilon \simeq 0.97 |\epsilon_K^{\text{exp}}|$ . We can use Eq. (231) to express Eq. (236) in terms of  $\bar{\rho}$  and  $\bar{\eta}$ . Dividing Eq. (236) by  $2\lambda^2$  with  $\lambda = 0.225$  and trading  $A$  for  $|V_{cb}| = A\lambda^2$  one finds

$$1.20 \cdot 10^{-6} = \widehat{B}_K |V_{cb}|^2 \bar{\eta} \left[ |V_{cb}|^2 (1 - \bar{\rho}) \eta_{tt} S(x_t) + \eta_{ct} S(x_c, x_t) - \eta_{cc} x_c \right], \quad (238)$$

where a tiny term of order  $\lambda^2$  (to be found in Ref. [182]) has been neglected.

Since the perturbative calculation of  $\eta_{ct}$  and  $\eta_{cc}$  involves an expansion in  $\alpha_s(\mu_{bc}) \sim 0.3$ , we must calculate these coefficients to higher order than in the case of  $\eta_{tt}$ . The development of the effective-hamiltonian framework and the LO calculation of  $H^{|\Delta S|=2}$  was performed by Gilman and Wise [147] for the case of a top quark mass far below  $M_W$ . The calculation confirmed the results for  $\eta_{tt}$  and  $\eta_{cc}$  found before with other methods [183, 184]. Later the LO calculation was extended to the case of a heavy top quark [185].

The motivation for the NLO calculation of  $H^{|\Delta S|=2}$  was, in the first place, to find out whether RG-improved perturbation theory works at all in a non-leptonic process involving low scales with  $\alpha_s \gtrsim 0.3$ . While the NLO calculation of  $\eta_{tt}$ , which only involves  $\alpha_s(\mu_{tW})$ , showed a good behaviour of the perturbative series [130], the fate of a reliable prediction of  $\epsilon_K$  depended on the control over  $\eta_{ct}$ , and  $\eta_{cc}$ . The NLO calculation of  $\eta_{cc}$  indeed showed a disturbingly large positive correction of 65%, which, however, could be traced back to an accidental cancellation among different terms in the LO result which was weakened at NLO [127]. The NLO correction to  $\eta_{ct}$  implied an upward shift of 31% of this quantity [128, 131], which is of the expected size of a correction proportional to  $\alpha_s(m_c)$ . The NLO calculation further permits control over the definition of the quark masses, the numbers quoted below for  $\eta_{tt}$ ,  $\eta_{ct}$ , and  $\eta_{cc}$  correspond to the use of the  $\overline{\text{MS}}$  scheme, i.e.  $x_q \equiv (\bar{m}_q(\bar{m}_q)/M_W)^2$  is to be used in Eqs. (236) and (238).

To calculate  $\Delta M_K = 2|M_{12}^K| \cos \phi_K \simeq 2 \operatorname{Re} M_{12}^K$  we decompose  $\Delta M_K$  into a short-distance piece from the local contribution to  $M_{12}^K$  and a long-distance piece from the bilocal contribution with two  $|\Delta S| = 1$  hamiltonians:

$$\begin{aligned}\Delta M_K &= \Delta M_K^{\text{SD}} + \Delta M_K^{\text{LD}} \\ \Delta M_K^{\text{SD}} &\equiv \frac{1}{m_K} \operatorname{Re} \langle K | H^{|\Delta S|=2} | \bar{K} \rangle, \quad \Delta M_K^{\text{LD}} \equiv -\operatorname{Re} \frac{i}{2m_K} \int d^4x \langle K | H^{|\Delta S|=1}(x) H^{|\Delta S|=1}(0) | \bar{K} \rangle,\end{aligned}\quad (239)$$

which again is specific to the standard CKM phase convention, for which the dominant CKM combination  $(V_{us} V_{ud}^*)^2$  is real. While the tiny contribution proportional to  $(V_{ts} V_{td}^*)^2$  is relevant for  $\tilde{\xi}_K$  in Eq. (237), it is negligible for  $\Delta M_K$  and omitted in Eq. (239). Since the CKM factor is real, the dispersive part of the bilocal matrix element entering  $\Delta M_K^{\text{LD}}$  is identical to the real part. The dispersive part of the mixing amplitude has been explained after Eq. (73).

The values for the QCD coefficients in Eq. (234) are

$$\eta_{tt} = 0.5765 \pm 0.0065 \quad (\text{NLO}) [130], \quad \eta_{ct} = 0.496 \pm 0.047 \quad (\text{NNLO}) [133], \quad \eta_{cc} = 1.87 \pm 0.76 \quad (\text{NNLO}) [132]. \quad (240)$$

The value for  $\eta_{tt}$  is an update taken from Ref. [132] using  $\bar{m}_t(\bar{m}_t) = (163.7 \pm 1.1) \text{ GeV}$ . The  $\overline{\text{MS}}$  top mass is smaller than the pole mass quoted in the context of collider physics by roughly 8 GeV.  $\eta_{cc}$  depends steeply on  $m_c$ , the quoted value is for  $\bar{m}_c(\bar{m}_c) = (1.279 \pm 0.0013) \text{ GeV}$ , which should be kept in mind when comparing the NNLO value in Eq. (240) with the NLO values in Refs. [127, 128, 131]. With today's precise value of  $m_c$ , the uncertainties of  $m_c$  and other input parameters has no relevance. The uncertainties of  $\eta_{cc}$  and  $\eta_{ct}$  are dominated by the scale uncertainty, estimated by varying  $\mu_{bc}$  around  $\bar{m}_c$ . This uncertainty will diminish once perturbative calculations beyond NNLO will be performed. The NNLO result for  $\eta_{ct}$  in Eq. (240) is larger than the NLO result of Ref. [128] by just 8.5%, which testifies to a good behavior of the perturbative series. The NNLO result for  $\eta_{cc}$ , however, shows the same pathological situation as the NLO result of Ref. [127, 128]. The correction is large, increasing  $\eta_{cc}$  by 36% over the NLO value [132], which exceeds the LO value by 65%, so that  $\eta_{cc}$  more than doubled due to two-loop and three-loop QCD corrections.

This development has immediate consequences for  $\Delta M_K$ , as with Eqs. (234) and (235) we find from Eq. (239):

$$\Delta M_K^{\text{SD}} = \frac{G_F^2}{6\pi^2} f_K^2 M_K \widehat{B}_K \left( \operatorname{Re} (V_{cs} V_{cd}^*) \right)^2 \eta_{cc} m_c^2 \quad (241)$$

where  $M_W^2 x_c = m_c^2$  has been used. The contributions with other CKM factors amount to 1% and are negligible.

Using the values for  $M_K$  and  $f_K$  quoted below Eq. (235),  $\bar{m}_c(\bar{m}_c) = 1.279 \text{ GeV}$ , and  $\operatorname{Re} (V_{cs} V_{cd}^*) = -0.218$  we obtain

$$\frac{\Delta M_K^{\text{SD}}}{\Delta M_K^{\text{exp}}} = (1.16 \pm 0.47) \widehat{B}_K \quad (242)$$

where I further used the experimental value of Eq. (11). A full NNLO prediction further requires a two-loop lattice-continuum matching of the hadronic matrix element, i.e. of  $\widehat{B}_K$ , which involves the matching of the  $\overline{\text{MS}}$  result to a different renormalization scheme suited for a non-perturbative calculation. Ref. [186] presents this calculation for  $\widehat{B}_K$  and the application of the result to an average of different lattice computations to find  $\widehat{B}_K = 0.7627 \pm 0.0060$ . Thus Eq. (242) boils down to

$$\frac{\Delta M_K^{\text{SD}}}{\Delta M_K^{\text{exp}}} = (0.89 \pm 0.36), \quad (243)$$

implying short-distance dominance of  $\Delta M_K$ . The long-distance contribution lacks the prefactor  $m_c^2$  of Eq. (241) and should therefore be smaller by a factor of  $\Lambda_{\text{QCD}}^2/m_c^2 \sim 0.1$ . There are exploratory lattice calculations of  $\Delta M_K^{\text{LD}}$  plus certain terms contained in  $\Delta M_K^{\text{SD}}$ , employing the feature that this calculation is easier in QCD with four active flavours because the GIM cancellation between charm and up contributions improves the UV behaviour of the calculated quantity [187, 188].

$\epsilon_K$  in Eq. (238) defines a hyperbola in the  $\bar{\rho}$ - $\bar{\eta}$  plane characterized by  $\eta_{tt} S(x_t)$  and

$$\eta_{ct} S(x_c, x_t) - \eta_{cc} x_c \quad (244)$$

shown in Fig. 8. In Ref. [134] it has been observed that the pathological term in  $\eta_{cc} x_c$  drops out from this combination, so that the prediction of  $\epsilon_K$  does not inherit the uncertainty from the poor convergence of the perturbative series of  $\eta_{cc}$ . The first term  $\eta_{ct} S(x_c, x_t)$  is parametrically larger by a factor of the large logarithm  $\ln x_c$ , so that the term cancelling with  $\eta_{cc} x_c$  is numerically sub-leading and therefore has a smaller impact on  $\eta_{ct} S(x_c, x_t)$ . The cancellation can be understood by switching to a different form of Eq. (234) via the replacement  $V_{cs} V_{cd}^* \rightarrow -V_{us} V_{ud}^* - V_{ts} V_{td}^*$  [134]. The resulting prediction for  $\epsilon_K$  reads [134]

$$|\epsilon_K| = (2.16 \pm 0.18) \times 10^{-3} \frac{\widehat{B}_K}{0.7625} \quad (245)$$

for  $\bar{\rho} = 0.16$ ,  $\bar{\eta} = 0.38$ ,  $|V_{cb}| = (42.2 \pm 0.8) \cdot 10^{-3}$ , and the quark masses quoted above. The largest uncertainty in Eq. (245) stems from the input parameters, the perturbative uncertainty is down to 3%. The hyperbola of Eq. (238) reads with  $\eta_{tt}$  in Eq. (240) and  $\eta_{ct} S(x_c, x_t) - \eta_{cc} x_c = (7.98 \pm 0.18) \cdot 10^{-4}$  [134]:

$$1.20 \cdot 10^{-6} = \widehat{B}_K |V_{cb}|^2 \bar{\eta} \left[ |V_{cb}|^2 (1 - \bar{\rho})(1.36 \pm 0.02) + (7.98 \pm 0.18) \cdot 10^{-4} \right]. \quad (246)$$

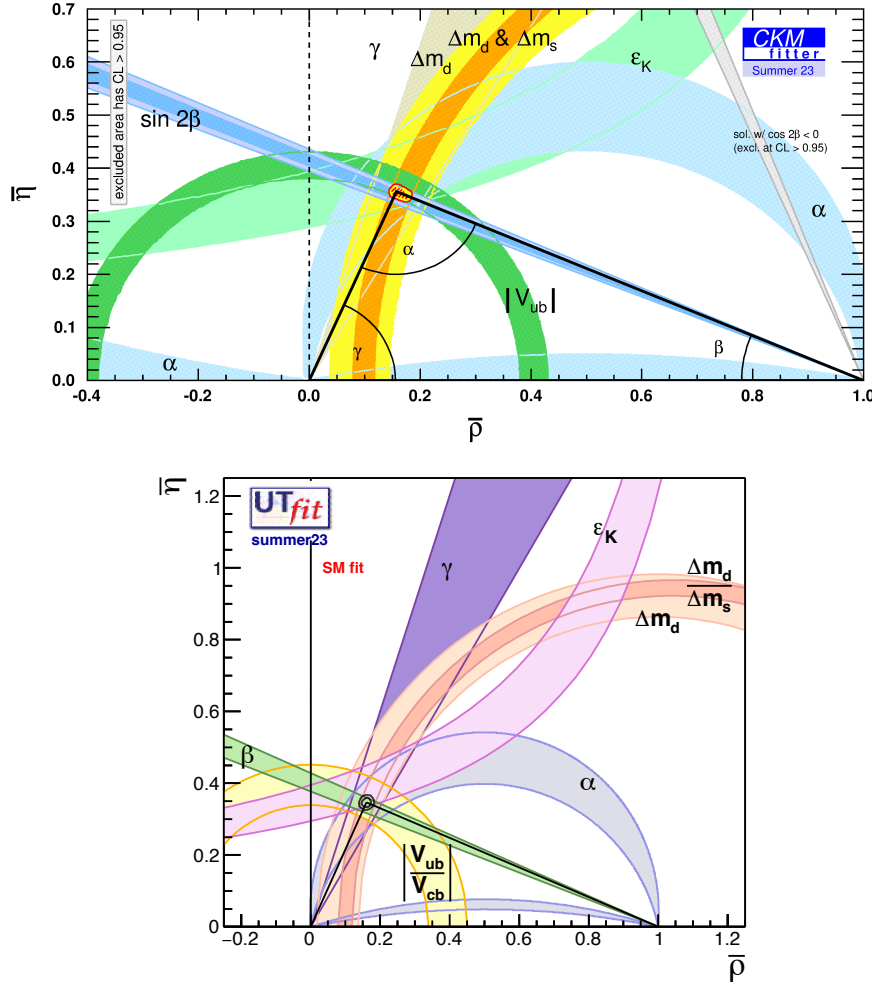


**Fig. 9** Constraints on the unitarity triangle from global fits to all quantities constraining  $(\bar{\rho}, \bar{\eta})$ . The upper and lower plots are from CKMfitter [189] and UTfit [74], respectively. The 68% C.L. contours for  $(\bar{\rho}, \bar{\eta})$  are indicated. CKMfitter uses a Frequentist approach in which systematic errors and theoretical uncertainties are scanned over, which results in a larger 68% C.L. region than the Bayesian approach of UTfit. The  $3\sigma$  regions found by both groups are similar.

The first term in the square bracket stemming from  $\eta_n S(x_t)$  contributes about  $3/4$  to  $|\epsilon_K|$ , so that  $|V_{cb}|$  essentially contributes to  $|\epsilon_K|$  with the fourth power. The value of  $|V_{cb}|$  is controversial, the determinations from exclusive and inclusive semileptonic  $B$  decays do not agree. For the lower value, found from exclusive decays, the hyperbola from  $\epsilon_K$  is not consistent with other constraints on the apex  $(\bar{\rho}, \bar{\eta})$  of the UT.

Finally,  $\Delta\Gamma_K$  in Eq. (10) has defied any calculation from first principles. For this we need  $\Gamma_{12}^K$ , which is completely dominated by the isospin-0 amplitude  $A_0$ , see Eq. (126). The experimental fact  $|A_0| \approx 22|A_2|$  is called “ $\Delta I = 1/2$  rule” and no analytical calculation could reproduce the value of  $|A_0/A_2|$ .

Fig. 8 shows the constraints on the apex of the unitarity triangle from the mixing-related observables discussed in this review. The actual situation from global fits to all measured quantities sensitive to  $\bar{\rho}$ ,  $\bar{\eta}$  is illustrated in Fig. 9, which shows the results from the two major groups performing such analyses, CKMfitter and UTfit.

To study BSM physics one may parameterize the BSM contributions in a model-independent way by foreseeing parameters modifying magnitude and phase of  $M_{12}^{d,s,K}$  and constrain these in conjunction with  $\bar{\rho}$  and  $\bar{\eta}$  in a global fit [72–74]. Ref. [74] find that  $O(20\%)$  BSM effects are allowed in  $|M_{12}^{d,s}|$  and  $\text{Im } M_{12}^K$ , while there is less space for new physics in the phases of  $M_{12}^{d,s}$ . With the result of the model-independent fit one can constrain any BSM model of interest, unless the model correlates different mixing observables.

BSM models addressing the gauge sector or Dark Matter are usually agnostic about the flavor structure, so that predictions rely on additional assumptions on the flavor sector. A widely studied approach is *minimal flavor violation (MFV)*, which organizes the flavour pattern of the SM Yukawa interactions in Eq. (161) in terms of small symmetry-breaking parameters called spurions [190, 191]. The MFV approach assumes that the same spurions governing Eq. (161) also determine the flavor structure of the studied BSM model, so that the new interaction involve the same CKM elements as the SM contributions. This reduces the BSM sensitivity of FCNC processes drastically and was originally motivated to permit lighter BSM particles in the reach of contemporary experiments. However, for instance in models

with more than one Higgs doublet, one even finds imprints on meson-antimeson mixing in the MFV case [192–199]. Some of the cited papers have considered the special case of the Minimal Supersymmetric Standard Model with decoupled heavy superpartners, resulting in a 2HDM in which a neutral heavy Higgs boson affects  $B_s - \bar{B}_s$  mixing in a critical way. If one relaxes the MFV hypothesis by adding a third spurion to the two spurions of the SM, one also finds large effects in meson-antimeson mixing observables [200].

## 7 Conclusions

This review article summarizes the theoretical formalism and the phenomenological methodology of  $K - \bar{K}$ ,  $D - \bar{D}$ ,  $B_d - \bar{B}_d$ , and  $B_s - \bar{B}_s$  mixing. All these meson-antimeson mixing systems involve  $|\Delta F| = 2$  transitions, in which the flavor quantum number  $F = S, C$  or  $B$  characterizing the meson changes by two units. The relevant  $2 \times 2$  matrix  $M - i\Gamma/2$  is composed of the hermitian mass and decay matrix and meson-antimeson mixing occurs because  $M_{12} - i\Gamma_{12}/2 \neq 0$ . Upon diagonalization of  $M - i\Gamma/2$  one finds the two mass eigenstates, which are superpositions of the particle state  $|M\rangle$  and the antiparticle state  $|\bar{M}\rangle$  and follow exponential decay laws. Meson-antimeson mixing is characterized by four quantities, the mass and width differences between the two mass eigenstates as well as the  $CP$  asymmetries in flavor-specific decays and a chosen exclusive decay. I have presented the formulae connecting these quantities to  $M_{12}$  and  $\Gamma_{12}$  and the Standard-Model (SM) predictions for them. While all four mixing complexes follow the same pattern, the numerical values of the corresponding quantities are very different with, for example,  $\langle \bar{B}_s \rangle$  mesons oscillating very rapidly while the very slow  $D - \bar{D}$  oscillations had impeded their discovery for a long time.

Another objective has been the recapitulation of the historical development of the field since the early 1950s, highlighting how the study of meson-antimeson mixing helped to shape the SM. The confirmation of the Kobayashi-Maskawa mechanism of  $CP$  violation needed a firm prediction of the size of mixing-induced  $CP$  violation in  $B_d - \bar{B}_d$  mixing from the  $CP$ -violating quantity  $\epsilon_K$  in  $K - \bar{K}$  mixing, the  $B_d - \bar{B}_d$  oscillation frequency, and the semileptonic  $B$  branching ratios for decays with and without charm in the final state. The needed predictions involved a rigorous theoretical basis and sophisticated calculational tools, which were developed in the late 1980s and early 1990s and proceeded along three avenues: (i) the establishment of a framework for perturbative calculations of short-distance QCD corrections, (ii) the advancement of lattice-QCD computations as a first-principle method to tackle long-distance QCD, and (iii) the identification of sizable theoretically clean mixing-induced  $CP$  asymmetries such as  $A_{CP}^{\text{mix}}(B_d \rightarrow J/\psi K_{\text{short}})$ . The theoretical progress was not only instrumental for the precise determination of CKM elements, which are fundamental parameters of the SM Yukawa sector, but also lead to the identification of “gold-mines” for the search for BSM physics, namely theoretically clean observables with sensitivity to new physics. With the exception of the width difference in the  $K - \bar{K}$  system, all above-mentioned observables could be calculated in  $K - \bar{K}$ ,  $B_d - \bar{B}_d$ , and  $B_s - \bar{B}_s$  mixing with good accuracy.  $D - \bar{D}$  mixing, however, has defied any calculation from first principles, with theory failing even at order-of-magnitude predictions for mass and width differences.

Meson-antimeson mixing processes are highly sensitive to BSM physics, with the potential to reveal virtual effects of new particles with masses far above 100 TeV. To disentangle BSM physics from SM contributions one must determine the CKM elements together with the parameters of the studied BSM model; especially  $(\bar{\rho}, \bar{\eta})$  determined from the global fit of Fig. 9 will be “contaminated” by BSM physics in the meson-antimeson mixing observables. At present, the identification of BSM physics in this way is impeded by the controversies on the values of  $|V_{cb}|$  and  $|V_{ub}|$  found from inclusive and exclusive decays. With better experimental possibilities for  $B$  physics at future runs of the LHC, with higher luminosity at Belle II, and further at the FCC-ee, mixing-induced  $CP$  asymmetries will become an important tool to discover or constrain BSM physics in rare decays. For example, if the flavor anomalies observed today in angular observables and branching fractions of  $B \rightarrow K\ell^+\ell^-$  and  $B_s \rightarrow \phi\ell^+\ell^-$  decays will manifest themselves also in the corresponding mixing-induced  $CP$  asymmetries, this will constitute an unambiguous discovery of BSM physics. On the theoretical side, continued effort is needed to keep up with the ever decreasing experimental error bars, especially better lattice-QCD predictions are highly desirable. Lattice QCD is further likely to emerge as the best avenue to address  $D - \bar{D}$  mixing. Finally, in the field of BSM physics flavor and collider observables will always go hand-in-hand to identify allowed parameter spaces and meson-antimeson mixing observables play an important role to this end.

## Acknowledgments

This research was supported by the Deutsche Forschungsgemeinschaft (DFG, German Research Foundation) under grant 396021762 - TRR 257 through project C1b of the Collaborative Research Center *Particle Physics after the Higgs Discovery (P3H)*.

## References

- [1] S. Navas, et al. (Particle Data Group), Review of particle physics, Phys. Rev. D 110 (3) (2024) 030001, doi:10.1103/PhysRevD.110.030001.
- [2] Murray Gell-Mann, A. Pais, Behavior of neutral particles under charge conjugation, Phys. Rev. 97 (1955) 1387–1389, doi:10.1103/PhysRev.97.1387.
- [3] W. F. Fry, J. Schneps, M. S. Swami, Evidence for a Long-Lived Neutral Unstable Particle, Phys. Rev. 103 (1956) 1904–1905, doi:10.1103/PhysRev.103.1904.
- [4] K. Lande, E. T. Booth, J. Impeduglia, L. M. Lederman, W. Chinowsky, Observation of Long-Lived Neutral V Particles, Phys. Rev. 103 (1956) 1901–1904, doi:10.1103/PhysRev.103.1901.

- [5] T. D. Lee, Chen-Ning Yang, Question of Parity Conservation in Weak Interactions, *Phys. Rev.* **104** (1956) 254–258, doi:10.1103/PhysRev.104.254.
- [6] T. D. Lee, R. Oehme, Chen-Ning Yang, Remarks on Possible Noninvariance Under Time Reversal and Charge Conjugation, *Phys. Rev.* **106** (1957) 340–345, doi:10.1103/PhysRev.106.340.
- [7] C. S. Wu, E. Ambler, R. W. Hayward, D. D. Hoppes, R. P. Hudson, Experimental Test of Parity Conservation in  $\beta$  Decay, *Phys. Rev.* **105** (1957) 1413–1414, doi:10.1103/PhysRev.105.1413.
- [8] Gerhart Lüders, On the Equivalence of Invariance under Time Reversal and under Particle-Antiparticle Conjugation for Relativistic Field Theories, *Kong. Dan. Vid. Sel. Mat. Fys. Medd.* **28N5** (5) (1954) 1–17.
- [9] W. Pauli, Exclusion principle, Lorentz group and reflexion of space-time and charge, in: W. Pauli (Ed.), *Niels Bohr and the Development of Physics*, MacGraw Hill 1955.
- [10] Gerhart Lüders, Proof of the TCP theorem, *Annals Phys.* **2** (1957) 1–15, doi:10.1016/0003-4916(57)90032-5.
- [11] E. Boldt, D. O. Caldwell, Y. Pal,  $\theta_1^0 - \theta_2^0$  Mass Difference, *Phys. Rev. Lett.* **1** (1958) 150, doi:10.1103/PhysRevLett.1.150.
- [12] F. Müller, R. W. Birge, W. B. Fowler, R. H. Good, W. Hirsch, R. P. Matsen, L. Oswald, W. M. Powell, H. S. White, O. Piccioni, Regeneration and Mass Difference of Neutral  $K$  Mesons, *Phys. Rev. Lett.* **4** (1960) 418–421, doi:10.1103/PhysRevLett.4.418.
- [13] Steven Weinberg, Time-Reversal Invariance and  $\theta_2^0$  Decay, *Phys. Rev.* **110** (1958) 782–784, doi:10.1103/PhysRev.110.782.
- [14] J. H. Christenson, J. W. Cronin, V. L. Fitch, R. Turlay, Evidence for the  $2\pi$  Decay of the  $K_2^0$  Meson, *Phys. Rev. Lett.* **13** (1964) 138–140, doi:10.1103/PhysRevLett.13.138.
- [15] R. G. Sachs, CP Violation in  $K_0$  Decays, *Phys. Rev. Lett.* **13** (1964) 286–288, doi:10.1103/PhysRevLett.13.286.
- [16] N. Cabibbo, Possibility of large CP and T violation in weak interactions, *Phys. Lett.* **12** (1964) 137–139, doi:10.1016/0031-9163(64)91138-2.
- [17] Tran N. Truong, Possibility of CP Violation in  $\Delta I = 3/2$  Decay of the  $K^0$  Meson, *Phys. Rev. Lett.* **13** (1964) 358–361, doi:10.1103/PhysRevLett.13.358.
- [18] J. Bernstein, G. Feinberg, T. D. Lee, Possible  $C$ ,  $T$  Noninvariance in the Electromagnetic Interaction, *Phys. Rev.* **139** (1965) B1650–B1659, doi:10.1103/PhysRev.139.B1650.
- [19] T. D. Lee, L. Wolfenstein, Analysis of CP Noninvariant Interactions and the  $K_1^0$ ,  $K_2^0$  System, *Phys. Rev.* **138** (1965) B1490–B1496, doi:10.1103/PhysRev.138.B1490.
- [20] G. D. Barr, et al. (NA31), A New measurement of direct CP violation in the neutral kaon system, *Phys. Lett. B* **317** (1993) 233–242, doi:10.1016/0370-2693(93)91599-I.
- [21] J. R. Batley, et al. (NA48), A Precision measurement of direct CP violation in the decay of neutral kaons into two pions, *Phys. Lett. B* **544** (2002) 97–112, doi:10.1016/S0370-2693(02)02476-0, hep-ex/0208009.
- [22] A. Alavi-Harati, et al. (KTeV), Measurements of Direct CP Violation, CPT Symmetry, and Other Parameters in the Neutral Kaon System, *Phys. Rev. D* **67** (2003) 012005, doi:10.1103/PhysRevD.70.079904, [Erratum: Phys. Rev. D 70, 079904 (2004)], hep-ex/0208007.
- [23] R. G. Moorhouse, A. E. Taylor, T. R. Walsh (Eds.), *Proceedings, Oxford International Conference on Elementary Particles*: Oxford, UK, September 19–25, 1965, Rutherford High Energy Laboratory 1966, <https://inspirehep.net/literature/1511181>.
- [24] S. L. Glashow, J. Iliopoulos, L. Maiani, Weak Interactions with Lepton-Hadron Symmetry, *Phys. Rev. D* **2** (1970) 1285–1292, doi:10.1103/PhysRevD.2.1285.
- [25] M. K. Gaillard, Benjamin W. Lee, Rare Decay Modes of the K-Mesons in Gauge Theories, *Phys. Rev. D* **10** (1974) 897, doi:10.1103/PhysRevD.10.897.
- [26] J. J. Aubert, et al. (E598), Experimental Observation of a Heavy Particle  $J$ , *Phys. Rev. Lett.* **33** (1974) 1404–1406, doi:10.1103/PhysRevLett.33.1404.
- [27] J. E. Augustin, et al. (SLAC-SP-017), Discovery of a Narrow Resonance in  $e^+e^-$  Annihilation, *Phys. Rev. Lett.* **33** (1974) 1406–1408, doi:10.1103/PhysRevLett.33.1406.
- [28] Nicola Cabibbo, Unitary Symmetry and Leptonic Decays, *Phys. Rev. Lett.* **10** (1963) 531–533, doi:10.1103/PhysRevLett.10.531.
- [29] Makoto Kobayashi, Toshihide Maskawa, CP Violation in the Renormalizable Theory of Weak Interaction, *Prog. Theor. Phys.* **49** (1973) 652–657, doi:10.1143/PTP.49.652.
- [30] Ling-Lie Chau, Wai-Yee Keung, Comments on the Parametrization of the Kobayashi-Maskawa Matrix, *Phys. Rev. Lett.* **53** (1984) 1802, doi:10.1103/PhysRevLett.53.1802.
- [31] Lincoln Wolfenstein, Parametrization of the Kobayashi-Maskawa Matrix, *Phys. Rev. Lett.* **51** (1983) 1945, doi:10.1103/PhysRevLett.51.1945.
- [32] CKMfitter Group (J. Charles et al.), Current status of the Standard Model CKM fit and constraints on  $\Delta F = 2$  New Physics, updated results and plots available at: <http://ckmfitter.in2p3.fr>, *Phys. Rev. D* **91** (7) (2015) 073007, doi:10.1103/PhysRevD.91.073007, 1501.05013.
- [33] T. D. Lee, A Theory of Spontaneous T Violation, *Phys. Rev. D* **8** (1973) 1226–1239, doi:10.1103/PhysRevD.8.1226.
- [34] Wolfgang Altmannshofer, Peter Stangl, Flavour Physics Beyond the Standard Model, in: Christian Fischer (Ed.), *Encyclopedia of Particle Physics*, Elsevier 2025, 2508 .03950.
- [35] H. Albrecht, et al. (ARGUS), Observation of  $B^0-\bar{B}^0$  Mixing, *Phys. Lett. B* **192** (1987) 245–252, doi:10.1016/0370-2693(87)91177-4.
- [36] C. Albajar, et al. (UA1), Search for  $B^0-\bar{B}^0$  oscillations at the CERN proton-antiproton collider, *Phys. Lett. B* **186** (2) (1987) 247–254, doi:10.1016/0370-2693(87)90288-7, [Erratum: Phys. Lett. B 197, 565 (1987)].
- [37] Swagato Banerjee, et al. (Heavy Flavor Averaging Group (HFLAV)), Averages of  $b$ -hadron,  $c$ -hadron, and  $\tau$ -lepton properties as of 2023, update at <https://hflav-eos.web.cern.ch/hflav-eos/triangle/summer2025> (2024), 2411.18639.
- [38] Roel Aaij, et al. (LHCb), A precise measurement of the  $B^0$  meson oscillation frequency, *Eur. Phys. J. C* **76** (7) (2016) 412, doi:10.1140/epjc/s10052-016-4250-2, 1604.03475.
- [39] D. Boutigny, et al. (BaBar), The BABAR physics book: Physics at an asymmetric  $B$  factory 1998, doi:10.2172/979931.
- [40] Marek Karliner, Harry J. Lipkin, About a Possible Nonstrange Cousin of the  $\Theta^+$  Pentaquark, in: *Narrow Nucleon Resonances: Predictions, Evidences, Perspectives* 2010, 1002.4149.
- [41] Dibyakrupa Sahoo, Rahul Sinha, N. G. Deshpande, Model independent method for a quantitative estimation of  $SU(3)$  flavor symmetry breaking using Dalitz plot distributions, *Phys. Rev. D* **91** (7) (2015) 076013, doi:10.1103/PhysRevD.91.076013, 1502.07089.
- [42] Lu Meng, Bo Wang, Guang-Juan Wang, Shi-Lin Zhu, Chiral perturbation theory for heavy hadrons and chiral effective field theory for heavy hadronic molecules, *Phys. Rept.* **1019** (2023) 1–149, doi:10.1016/j.physrep.2023.04.003, 2204.08716.
- [43] Carolina Bolognani, Ulrich Nierste, Stefan Schacht, K. Keri Vos, Anatomy of non-leptonic two-body decays of charmed mesons into final states with  $\eta'$ , *JHEP* **05** (2025) 148, doi:10.1007/JHEP05(2025)148, 2410.08138.
- [44] T. D. Lee, Chen-Ning Yang, Charge Conjugation, a New Quantum Number  $G$ , and Selection Rules Concerning a Nucleon Anti-nucleon System, *Nuovo Cim.* **10** (1956) 749–753, doi:10.1007/BF02744530.
- [45] Sarah Müller, Ulrich Nierste, Stefan Schacht, Topological amplitudes in  $D$  decays to two pseudoscalars: A global analysis with linear  $SU(3)_F$  breaking, *Phys. Rev. D* **92** (1) (2015) 014004, doi:10.1103/PhysRevD.92.014004, 1503.06759.

- [46] Michael Gronau, David London, Isospin analysis of CP asymmetries in B decays, Phys. Rev. Lett. 65 (1990) 3381–3384, doi:10.1103/PhysRevLett.65.3381.
- [47] Michael Gronau, David London, How to determine all the angles of the unitarity triangle from  $B_d^0 \rightarrow D K_S$  and  $B_s^0 \rightarrow D \phi$ , Phys. Lett. B 253 (1991) 483–488, doi:10.1016/0370-2693(91)91756-L.
- [48] Michael Gronau, Daniel Wyler, On determining a weak phase from CP asymmetries in charged B decays, Phys. Lett. B 265 (1991) 172–176, doi:10.1016/0370-2693(91)90034-N.
- [49] Ikaros I. Y. Bigi, A. I. Sanda, Notes on the Observability of CP Violations in B Decays, Nucl. Phys. B 193 (1981) 85–108, doi:10.1016/0550-3213(81)90519-8.
- [50] Ashton B. Carter, A. I. Sanda, CP Violation in Cascade Decays of B Mesons, Phys. Rev. Lett. 45 (1980) 952, doi:10.1103/PhysRevLett.45.952.
- [51] Ashton B. Carter, A. I. Sanda, CP Violation in B Meson Decays, Phys. Rev. D 23 (1981) 1567, doi:10.1103/PhysRevD.23.1567.
- [52] C. Jarlskog, Commutator of the Quark Mass Matrices in the Standard Electroweak Model and a Measure of Maximal CP Nonconservation, Phys. Rev. Lett. 55 (1985) 1039, doi:10.1103/PhysRevLett.55.1039.
- [53] Andrzej J. Buras, Markus E. Lautenbacher, Gaby Ostermaier, Waiting for the top quark mass,  $K^+ \rightarrow \pi^+ \nu \bar{\nu}$ ,  $B_s^0 - \bar{B}_s^0$  mixing and CP asymmetries in B decays, Phys. Rev. D 50 (1994) 3433–3446, doi:10.1103/PhysRevD.50.3433, hep-ph/9403384.
- [54] Ikaros I. Y. Bigi, Valery A. Khoze, N. G. Uraltsev, A. I. Sanda, The Question of CP Noninvariance - as Seen Through the Eyes of Neutral Beauty, Adv. Ser. Direct. High Energy Phys. 3 (1989) 175–248, doi:10.1142/9789814503280\_0004.
- [55] Alexander Lenz, Ulrich Nierste, Gaby Ostermaier, Determination of the CKM angle  $\gamma$  and  $|V_{ub}/V_{cb}|$  from inclusive direct CP asymmetries and branching ratios in charmless B decays, Phys. Rev. D 59 (1999) 034008, doi:10.1103/PhysRevD.59.034008, hep-ph/9802202.
- [56] Bernard Aubert, et al. (BaBar), Measurement of Time-Dependent CP Asymmetry in  $B^0 \rightarrow c\bar{c}K^{(*)0}$  Decays, Phys. Rev. D 79 (2009) 072009, doi:10.1103/PhysRevD.79.072009, 0902.1708.
- [57] I. Adachi, et al. (Belle), Precise measurement of the CP violation parameter  $\sin 2\phi_1$  in  $B^0 \rightarrow (c\bar{c})K^0$  decays, Phys. Rev. Lett. 108 (2012) 171802, doi:10.1103/PhysRevLett.108.171802, 1201.4643.
- [58] I. Adachi, et al. (Belle-II), New graph-neural-network flavor tagger for Belle II and measurement of  $\sin 2\phi_1$  in  $B^0 \rightarrow J/\psi K_S^0$  decays, Phys. Rev. D 110 (1) (2024) 012001, doi:10.1103/PhysRevD.110.012001, 2402.17260.
- [59] Roel Aaij, et al. (LHCb), Measurement of CP violation in  $B^0 \rightarrow J/\psi K_S^0$  and  $B^0 \rightarrow \psi(2S)K_S^0$  decays, JHEP 11 (2017) 170, doi:10.1007/JHEP11(2017)170, 1709.03944.
- [60] Roel Aaij, et al. (LHCb), Measurement of CP Violation in  $B^0 \rightarrow \psi[\rightarrow \ell^+ \ell^-]K_S^0[\rightarrow \pi^+ \pi^-]$  Decays, Phys. Rev. Lett. 132 (2) (2024) 021801, doi:10.1103/PhysRevLett.132.021801, 2309.09728.
- [61] Bernard Aubert, et al. (BaBar), Ambiguity-free measurement of  $\cos(2\beta)$ : Time-integrated and time-dependent angular analyses of  $B \rightarrow J/\psi K\pi$ , Phys. Rev. D 71 (2005) 032005, doi:10.1103/PhysRevD.71.032005, hep-ex/0411016.
- [62] Marten Z. Barel, Kristof De Bruyn, Robert Fleischer, Eleftheria Malami, In pursuit of new physics with  $B_d^0 \rightarrow J/\psi K^0$  and  $B_s^0 \rightarrow J/\psi \phi$  decays at the high-precision Frontier, J. Phys. G 48 (6) (2021) 065002, doi:10.1088/1361-6471/ab2a2, 2010.14423.
- [63] Roel Aaij, et al. (LHCb), Measurement of the time-dependent CP asymmetries in  $B_s^0 \rightarrow J/\psi K_S^0$ , JHEP 06 (2015) 131, doi:10.1007/JHEP06(2015)131, 1503.07055.
- [64] Philipp Frings, Ulrich Nierste, Martin Wiebusch, Penguin contributions to CP phases in  $B_{d,s}$  decays to charmonium, Phys. Rev. Lett. 115 (6) (2015) 061802, doi:10.1103/PhysRevLett.115.061802, 1503.00859.
- [65] Morad Aaboud, et al. (ATLAS), Measurement of the relative width difference of the  $B^0 - \bar{B}^0$  system with the ATLAS detector, JHEP 06 (2016) 081, doi:10.1007/JHEP06(2016)081, 1605.07485.
- [66] Albert M Sirunyan, et al. (CMS), Measurement of b hadron lifetimes in pp collisions at  $\sqrt{s} = 8$  TeV, Eur. Phys. J. C 78 (6) (2018) 457, doi:10.1140/epjc/s10052-018-5929-3, [Erratum: Eur.Phys.J.C 78, 561 (2018)], 1710.08949.
- [67] Roel Aaij, et al. (LHCb), Measurements of the  $B^+, B^0, B_s^0$  meson and  $\Lambda_b^0$  baryon lifetimes, JHEP 04 (2014) 114, doi:10.1007/JHEP04(2014)114, 1402.2554.
- [68] A. Abulencia, et al. (CDF), Measurement of the  $B_s^0 - \bar{B}_s^0$  Oscillation Frequency, Phys. Rev. Lett. 97 (2006) 062003, doi:10.1103/PhysRevLett.97.062003, hep-ex/0606027.
- [69] A. Abulencia, et al. (CDF), Observation of  $B_s^0 - \bar{B}_s^0$  Oscillations, Phys. Rev. Lett. 97 (2006) 242003, doi:10.1103/PhysRevLett.97.242003, hep-ex/0609040.
- [70] Roel Aaij, et al. (LHCb), Measurement of the CKM angle  $\gamma$  and  $B_s^0 - \bar{B}_s^0$  mixing frequency with  $B_s^0 \rightarrow D_s^+ h^\pm \pi^\mp \pi^\mp$  decays, JHEP 03 (2021) 137, doi:10.1007/JHEP03(2021)137, 2011.12041.
- [71] R. Aaij, et al. (LHCb), Precise determination of the  $B_s^0 - \bar{B}_s^0$  oscillation frequency, Nature Phys. 18 (1) (2022) 1–5, doi:10.1038/s41567-021-01394-x, 2104.04421.
- [72] A. Lenz, U. Nierste, J. Charles, S. Descotes-Genon, A. Jantsch, C. Kaufhold, H. Lacker, S. Monteil, V. Niess, S. T'Jampens, Anatomy of New Physics in  $B - \bar{B}$  mixing, Phys. Rev. D 83 (2011) 036004, doi:10.1103/PhysRevD.83.036004, 1008.1593.
- [73] A. Lenz, U. Nierste, J. Charles, S. Descotes-Genon, H. Lacker, S. Monteil, V. Niess, S. T'Jampens, Constraints on new physics in  $B - \bar{B}$  mixing in the light of recent LHCb data, Phys. Rev. D 86 (2012) 033008, doi:10.1103/PhysRevD.86.033008, 1203.0238.
- [74] Marcella Bona, et al. (UTfit), New UTfit Analysis of the Unitarity Triangle in the Cabibbo-Kobayashi-Maskawa scheme, Rend. Lincei Sci. Fis. Nat. 34 (2023) 37–57, doi:10.1007/s12210-023-01137-5, updated results and plots available at: <http://www.utfit.org>, 2212.03894.
- [75] Georges Aad, et al. (ATLAS), Measurement of the CP-violating phase  $\phi_s$  in  $B_s^0 \rightarrow J/\psi \phi$  decays in ATLAS at 13 TeV, Eur. Phys. J. C 81 (4) (2021) 342, doi:10.1140/epjc/s10052-021-09011-0, 2001.07115.
- [76] Vardan Khachatryan, et al. (CMS), Measurement of the CP-violating weak phase  $\phi_s$  and the decay width difference  $\Delta\Gamma_s$  using the  $B_s^0 \rightarrow J/\psi \phi(1020)$  decay channel in pp collisions at  $\sqrt{s} = 8$  TeV, Phys. Lett. B 757 (2016) 97–120, doi:10.1016/j.physletb.2016.03.046, 1507.07527.
- [77] Measurement of time-dependent CP violation in  $B_s^0 \rightarrow J/\psi \phi(1020)$  decays with the CMS detector (2024).
- [78] Roel Aaij, et al. (LHCb), Precision measurement of CP violation in  $B_s^0 \rightarrow J/\psi K^+ K^-$  decays, Phys. Rev. Lett. 114 (4) (2015) 041801, doi:10.1103/PhysRevLett.114.041801, 1411.3104.
- [79] Roel Aaij, et al. (LHCb), Resonances and CP violation in  $B_s^0$  and  $\bar{B}_s^0 \rightarrow J/\psi K^+ K^-$  decays in the mass region above the  $\phi(1020)$ , JHEP 08 (2017) 037, doi:10.1007/JHEP08(2017)037, 1704.08217.
- [80] Roel Aaij, et al. (LHCb), First study of the CP-violating phase and decay-width difference in  $B_s^0 \rightarrow \psi(2S)\phi$  decays, Phys. Lett. B 762 (2016) 253–262, doi:10.1016/j.physletb.2016.09.028, 1608.04855.
- [81] R. Aaij, et al. (LHCb), First measurement of the CP-violating phase in  $B_s^0 \rightarrow J/\psi(\rightarrow e^+ e^-)\phi$  decays, Eur. Phys. J. C 81 (11) (2021) 1026, doi:10.1140/epjc/s10052-021-09711-7, 2105.14738.
- [82] Ia. Bezshyiko, et al. (LHCb), Improved Measurement of CP Violation Parameters in  $B_s^0 \rightarrow J/\psi K^+ K^-$  Decays in the Vicinity of the  $\phi(1020)$  Resonance, Phys. Rev. Lett. 132 (5) (2024) 051802, doi:10.1103/PhysRevLett.132.051802, 2308.01468.

- [83] Roel Aaij, et al. (LHCb), A measurement of  $\Delta\Gamma_s$ , JHEP 05 (2024) 253, doi:10.1007/JHEP05(2024)253, 2310.12649.
- [84] Jonathan L. Rosner, Determination of pseudoscalar charmed meson decay constants from B meson decays, Phys. Rev. D 42 (1990) 3732–3740, doi:10.1103/PhysRevD.42.3732.
- [85] Amol S. Dighe, Isard Dunietz, Harry J. Lipkin, Jonathan L. Rosner, Angular Distributions and Lifetime Differences in  $B_s \rightarrow J/\psi\phi$  Decays, Phys. Lett. B 369 (1996) 144–150, doi:10.1016/0370-2693(95)01523-X, hep-ph/9511363.
- [86] Robert Fleischer, Isard Dunietz, CP violation and CKM phases from angular distributions for  $B_s$  decays into admixtures of CP eigenstates, Phys. Rev. D 55 (1997) 259–267, doi:10.1103/PhysRevD.55.259, hep-ph/9605220.
- [87] Amol S. Dighe, Isard Dunietz, Robert Fleischer, Extracting CKM phases and  $B_s - \bar{B}_s$  mixing parameters from angular distributions of nonleptonic B decays, Eur. Phys. J. C 6 (1999) 647–662, doi:10.1007/s100520050372, hep-ph/9804253.
- [88] Isard Dunietz, Robert Fleischer, Ulrich Nierste, In pursuit of new physics with  $B_s$  decays, Phys. Rev. D 63 (2001) 114015, doi:10.1103/PhysRevD.63.114015, hep-ph/0012219.
- [89] R. Aaij, et al. (LHCb), Determination of the sign of the decay width difference in the  $B_s$  system, Phys. Rev. Lett. 108 (2012) 241801, doi:10.1103/PhysRevLett.108.241801, 1202.4717.
- [90] Isard Dunietz,  $B_s - \bar{B}_s$  Mixing, CP Violation and Extraction of CKM Phases from Untagged  $B_s$  Data Samples, Phys. Rev. D 52 (1995) 3048–3064, doi:10.1103/PhysRevD.52.3048, hep-ph/9501287.
- [91] B physics at the Tevatron: Run II and beyond 2001, hep-ph/0201071.
- [92] Soumitra Nandi, Ulrich Nierste, Resolving the sign ambiguity in  $\Delta\Gamma_s$  with  $B_s \rightarrow D_s K$ , Phys. Rev. D 77 (2008) 054010, doi:10.1103/PhysRevD.77.054010, 0801.0143.
- [93] Kristof De Bruyn, Robert Fleischer, Robert Knegjens, Marcel Merk, Manuel Schiller, Niels Tuning, Exploring  $B_s \rightarrow D_s^{(*)\pm} K^\mp$  Decays in the Presence of a Sizable Width Difference  $\Delta\Gamma_s$ , Nucl. Phys. B 868 (2013) 351–367, doi:10.1016/j.nuclphysb.2012.11.012, 1208.6463.
- [94] M. Bobrowski, A. Lenz, J. Riedl, J. Rohrwild, How Large Can the SM Contribution to CP Violation in  $D^0 - \bar{D}^0$  Mixing Be?, JHEP 03 (2010) 009, doi:10.1007/JHEP03(2010)009, 1002.4794.
- [95] David Friday, Evelina Gersabeck, Alexander Lenz, Maria Laura Piscopo, Charm physics, in: Christian Fischer (Ed.), Encyclopedia of Particle Physics, Elsevier 2025, 2506.15584.
- [96] R. Aaij, et al. (LHCb), Observation of  $D^0 - \bar{D}^0$  oscillations, Phys. Rev. Lett. 110 (10) (2013) 101802, doi:10.1103/PhysRevLett.110.101802, 1211.1230.
- [97] Roel Aaij, et al. (LHCb), Observation of the Mass Difference Between Neutral Charm-Meson Eigenstates, Phys. Rev. Lett. 127 (11) (2021) 111801, doi:10.1103/PhysRevLett.127.111801, 2106.03744.
- [98] Howard Georgi,  $D - \bar{D}$  mixing in heavy quark effective field theory, Phys. Lett. B 297 (1992) 353–357, doi:10.1016/0370-2693(92)91274-D, hep-ph/9209291.
- [99] Thorsten Ohl, Giulia Ricciardi, Elizabeth H. Simmons,  $D - \bar{D}$  in heavy quark effective field theory: The Sequel, Nucl. Phys. B 403 (1993) 605–632, doi:10.1016/0550-3213(93)90364-U, hep-ph/9301212.
- [100] Paras Naik, Novel correlated  $D^0 \bar{D}^0$  systems for c/b physics and tests of T/CPT, JHEP 03 (2023) 038, doi:10.1007/JHEP03(2023)038, 2102.07729.
- [101] Ulrich Nierste, Three Lectures on Meson Mixing and CKM phenomenology, in: Helmholtz International Summer School on Heavy Quark Physics 2009, pp. 1–38, 0904.1869.
- [102] L. A. Khalfin, , Pisma Zh. Eksp. Teor. Fiz. 33 (1957) 1371.
- [103] V. Weisskopf, Eugene P. Wigner, Calculation of the natural brightness of spectral lines on the basis of Dirac's theory, Z. Phys. 63 (1930) 54–73, doi:10.1007/BF01336768.
- [104] C. B. Chiu, E. C. G. Sudarshan, Decay and evolution of the neutral kaon, Phys. Rev. D 42 (1990) 3712–3723, doi:10.1103/PhysRevD.42.3712.
- [105] Tim Gershon,  $\Delta\Gamma_d$ : A Forgotten Null Test of the Standard Model, J. Phys. G 38 (2011) 015007, doi:10.1088/0954-3899/38/1/015007, 1007.5135.
- [106] Ulrich Nierste, CP asymmetry in flavor-specific B decays, in: 39th Rencontres de Moriond on Electroweak Interactions and Unified Theories 2004, pp. 445–450, hep-ph/0406300.
- [107] Hitoshi Yamamoto, Lepton CP asymmetries in B decays, Phys. Lett. B 401 (1997) 91–99, doi:10.1016/S0370-2693(97)00388-2, hep-ph/9703336.
- [108] Roel Aaij, et al. (LHCb), Measurement of the CP asymmetry in  $B_s^0 - \bar{B}_s^0$  mixing, Phys. Rev. Lett. 117 (6) (2016) 061803, doi:10.1103/PhysRevLett.117.061803, [Addendum: Phys.Rev.Lett. 118, 129903 (2017)], 1605.09768.
- [109] Roel Aaij, et al. (LHCb), Measurement of CP asymmetry in  $B_s^0 \rightarrow D_s^\pm K^\mp$  decays, JHEP 03 (2025) 139, doi:10.1007/JHEP03(2025)139, 2412.14074.
- [110] J. P. Lees, et al. (BaBar), Study of CP Asymmetry in  $B^0 - \bar{B}^0$  Mixing with Inclusive Dilepton Events, Phys. Rev. Lett. 114 (8) (2015) 081801, doi:10.1103/PhysRevLett.114.081801, [Erratum: *ibid.*, 159901], 1411.1842.
- [111] E. Nakano, et al. (Belle), Charge asymmetry of same-sign dileptons in  $B^0 - \bar{B}^0$  mixing, Phys. Rev. D 73 (2006) 112002, doi:10.1103/PhysRevD.73.112002, hep-ex/0505017.
- [112] Roel Aaij, et al. (LHCb), Measurement of the semileptonic CP asymmetry in  $B^0 - \bar{B}^0$  mixing, Phys. Rev. Lett. 114 (2015) 041601, doi:10.1103/PhysRevLett.114.041601, 1409.8586.
- [113] Robert Fleischer, Joaquim Matias, Searching for new physics in nonleptonic B decays, Phys. Rev. D 61 (2000) 074004, doi:10.1103/PhysRevD.61.074004, hep-ph/9906274.
- [114] R. Aleksan, Isard Dunietz, Boris Kayser, F. Le Diberder, CP violation using non-CP eigenstate decays of neutral B mesons, Nucl. Phys. B 361 (1991) 141–165, doi:10.1016/0550-3213(91)90619-9.
- [115] Roy Aleksan, Isard Dunietz, Boris Kayser, Determining the CP Violating Phase  $\gamma$ , Z. Phys. C 54 (1992) 653–660, doi:10.1007/BF01559494.
- [116] Robert Fleischer, New strategies to obtain insights into CP violation through  $B_s \rightarrow D_s^\pm K^\mp$ ,  $D_s^{*\pm} K^\mp$ , and  $B_d \rightarrow D^\pm \pi^\mp$ ,  $D^{*\pm} \pi^\mp$  decays, Nucl. Phys. B 671 (2003) 459–482, doi:10.1016/j.nuclphysb.2003.08.010, hep-ph/0304027.
- [117] Yuval Grossman, Yosef Nir, CP Violation in  $\tau^\pm \rightarrow \pi^\pm K_S \nu$  and  $D^\pm \rightarrow \pi^\pm K_S$ : The Importance of  $K_S - K_L$  Interference, JHEP 04 (2012) 002, doi:10.1007/JHEP04(2012)002, 1110.3790.
- [118] Yuval Grossman, Paolo Leo, Alberto Martini, Guglielmo Papiri, Armine Rostomyan, CP violation in decays into states with neutral kaons (2025), 2509.07071.
- [119] K. Hartkorn, H. G. Moser, A new method of measuring  $\Delta\Gamma/\Gamma$  in the  $B_s^0 - \bar{B}_s^0$  system, Eur. Phys. J. C 8 (1999) 381–383, doi:10.1007/s100520050472.
- [120] Robert Fleischer, Isard Dunietz, CP violation and the CKM angle  $\gamma$  from angular distributions of untagged  $B_s$  decays governed by  $\bar{b} \rightarrow \bar{c} u \bar{s}$ , Phys. Lett. B 387 (1996) 361–370, doi:10.1016/0370-2693(96)01033-7, hep-ph/9605221.

- [121] Kristof De Bruyn, Robert Fleischer, Robert Kneijens, Patrick Koppenburg, Marcel Merk, Antonio Pellegrino, Niels Tuning, Probing New Physics via the  $B_s^0 \rightarrow \mu^+ \mu^-$  Effective Lifetime, Phys. Rev. Lett. 109 (2012) 041801, doi:10.1103/PhysRevLett.109.041801, 1204.1737.
- [122] G. Blaylock, A. Seiden, Y. Nir, The Role of CP violation in  $D^0$ - $\bar{D}^0$  mixing, Phys. Lett. B 355 (1995) 555–560, doi:10.1016/0370-2693(95)00787-L, hep-ph/9504306.
- [123] Andrzej J. Buras, Climbing NLO and NNLO Summits of Weak Decays: 1988-2023, Phys. Rept. 1025 (2023), doi:10.1016/j.physrep.2023.07.002, 1102.5650.
- [124] Gerhard Buchalla, Andrzej J. Buras, Markus E. Lautenbacher, Weak Decays beyond Leading Logarithms, Rev. Mod. Phys. 68 (1996) 1125–1144, doi:10.1103/RevModPhys.68.1125, hep-ph/9512380.
- [125] Andrzej J. Buras, Peter H. Weisz, QCD Nonleading Corrections to Weak Decays in Dimensional Regularization and 't Hooft-Veltman Schemes, Nucl. Phys. B 333 (1990) 66–99, doi:10.1016/0550-3213(90)90223-Z.
- [126] Gerhard Buchalla, Andrzej J. Buras, The rare decays  $K^+ \rightarrow \pi^+ \nu \bar{\nu}$  and  $K_L \rightarrow \mu^+ \mu^-$  beyond leading logarithms, Nucl. Phys. B 412 (1994) 106–142, doi:10.1016/0550-3213(94)90496-0, hep-ph/9308272.
- [127] Stefan Herrlich, Ulrich Nierste, Enhancement of the  $K_L$ - $K_S$  mass difference by short distance QCD corrections beyond leading logarithms, Nucl. Phys. B 419 (1994) 292–322, doi:10.1016/0550-3213(94)90044-2, hep-ph/9310311.
- [128] Stefan Herrlich, Ulrich Nierste, The Complete  $|\Delta S| = 2$  - Hamiltonian in the next-to-leading order, Nucl. Phys. B 476 (1996) 27–88, doi:10.1016/0550-3213(96)00324-0, hep-ph/9604330.
- [129] Stefan Herrlich, Ulrich Nierste, Evanescent operators, scheme dependences and double insertions, Nucl. Phys. B 455 (1995) 39–58, doi:10.1016/0550-3213(95)00474-7, hep-ph/9412375.
- [130] Andrzej J. Buras, Matthias Jamin, Peter H. Weisz, Leading and Next-to-leading QCD Corrections to  $\epsilon$  Parameter and  $B^0$ - $\bar{B}^0$  Mixing in the Presence of a Heavy Top Quark, Nucl. Phys. B 347 (1990) 491–536, doi:10.1016/0550-3213(90)90373-L.
- [131] Stefan Herrlich, Ulrich Nierste, Indirect CP violation in the neutral kaon system beyond leading logarithms, Phys. Rev. D 52 (1995) 6505–6518, doi:10.1103/PhysRevD.52.6505, hep-ph/9507262.
- [132] Joachim Brod, Martin Gorbahn, Next-to-Next-to-Leading-Order Charm-Quark Contribution to the CP Violation Parameter  $\epsilon_K$  and  $\Delta M_K$ , Phys. Rev. Lett. 108 (2012) 121801, doi:10.1103/PhysRevLett.108.121801, 1108.2036.
- [133] Joachim Brod, Martin Gorbahn,  $\epsilon_K$  at Next-to-Next-to-Leading Order: The Charm-Top-Quark Contribution, Phys. Rev. D 82 (2010) 094026, doi:10.1103/PhysRevD.82.094026, 1007.0684.
- [134] Joachim Brod, Martin Gorbahn, Emmanuel Stamou, Standard-Model Prediction of  $\epsilon_K$  with Manifest Quark-Mixing Unitarity, Phys. Rev. Lett. 125 (17) (2020) 171803, doi:10.1103/PhysRevLett.125.171803, 1911.06822.
- [135] Mikhail A. Shifman, A. I. Vainshtein, Valentin I. Zakharov, QCD and Resonance Physics. Theoretical Foundations, Nucl. Phys. B 147 (1979) 385–447, doi:10.1016/0550-3213(79)90022-1.
- [136] Mikhail A. Shifman, A. I. Vainshtein, Valentin I. Zakharov, QCD and Resonance Physics: Applications, Nucl. Phys. B 147 (1979) 448–518, doi:10.1016/0550-3213(79)90023-3.
- [137] William A. Bardeen, A. J. Buras, J. M. Gerard, The B Parameter Beyond the Leading Order of  $1/N$  Expansion, Phys. Lett. B 211 (1988) 343–349, doi:10.1016/0370-2693(88)90913-6.
- [138] Matthias Linster, Robert Ziegler, A Realistic  $U(2)$  Model of Flavor, JHEP 08 (2018) 058, doi:10.1007/JHEP08(2018)058, 1805.07341.
- [139] C. D. Froggatt, Holger Bech Nielsen, Hierarchy of Quark Masses, Cabibbo Angles and CP Violation, Nucl. Phys. B 147 (1979) 277–298, doi:10.1016/0550-3213(79)90316-X.
- [140] Paul H. Frampton, P. Q. Hung, Marc Sher, Quarks and leptons beyond the third generation, Phys. Rept. 330 (2000) 263, doi:10.1016/S0370-1573(99)00095-2, hep-ph/9903387.
- [141] Otto Eberhardt, Alexander Lenz, Jurgen Rohrwild, Less space for a new family of fermions, Phys. Rev. D 82 (2010) 095006, doi:10.1103/PhysRevD.82.095006, 1005.3505.
- [142] Otto Eberhardt, Geoffrey Herbert, Heiko Lacker, Alexander Lenz, Andreas Menzel, Ulrich Nierste, Martin Wiebusch, Joint analysis of Higgs decays and electroweak precision observables in the Standard Model with a sequential fourth generation, Phys. Rev. D 86 (2012) 013011, doi:10.1103/PhysRevD.86.013011, 1204.3872.
- [143] Otto Eberhardt, Geoffrey Herbert, Heiko Lacker, Alexander Lenz, Andreas Menzel, Ulrich Nierste, Martin Wiebusch, Impact of a Higgs boson at a mass of 126 GeV on the standard model with three and four fermion generations, Phys. Rev. Lett. 109 (2012) 241802, doi:10.1103/PhysRevLett.109.241802, 1209.1101.
- [144] T. Inami, C. S. Lim, Effects of Superheavy Quarks and Leptons in Low-Energy Weak Processes  $K_L \rightarrow \mu \bar{\mu}$ ,  $K^+ \rightarrow \pi^+ \nu \bar{\nu}$  and  $K^0 \rightarrow \bar{K}^0$ , Prog. Theor. Phys. 65 (1981) 297, doi:10.1143/PTP.65.297, [Erratum: Prog.Theor.Phys. 65, 1772 (1981)].
- [145] C. Hughes, C. T. H. Davies, C. J. Monahan, New methods for B meson decay constants and form factors from lattice NRQCD, Phys. Rev. D 97 (5) (2018) 054509, doi:10.1103/PhysRevD.97.054509, 1711.09981.
- [146] R. J. Dowdall, C. T. H. Davies, R. R. Horgan, G. P. Lepage, C. J. Monahan, J. Shigemitsu, M. Wingate, Neutral B-meson mixing from full lattice QCD at the physical point, Phys. Rev. D 100 (9) (2019) 094508, doi:10.1103/PhysRevD.100.094508, 1907.01025.
- [147] Frederick J. Gilman, Mark B. Wise,  $K^0$ - $\bar{K}^0$  Mixing in the Six Quark Model, Phys. Rev. D 27 (1983) 1128, doi:10.1103/PhysRevD.27.1128.
- [148] Andrzej J. Buras, Matthias Jamin, M. E. Lautenbacher, Peter H. Weisz, Effective Hamiltonians for  $|\Delta S| = 1$  and  $|\Delta B| = 1$  nonleptonic decays beyond the leading logarithmic approximation, Nucl. Phys. B 370 (1992) 69–104, doi:10.1016/0550-3213(92)90345-C, [Addendum: Nucl.Phys.B 375, 501 (1992)].
- [149] Andrzej J. Buras, Matthias Jamin, Markus E. Lautenbacher, Peter H. Weisz, Two loop anomalous dimension matrix for  $|\Delta S| = 1$  weak nonleptonic decays I:  $O(\alpha_s^2)$ , Nucl. Phys. B 400 (1993) 37–74, doi:10.1016/0550-3213(93)90397-8, hep-ph/9211304.
- [150] Andrzej J. Buras, Matthias Jamin, Markus E. Lautenbacher, Two loop anomalous dimension matrix for  $|\Delta S| = 1$  weak nonleptonic decays. 2.  $O(\alpha\alpha_s)$ , Nucl. Phys. B 400 (1993) 75–102, doi:10.1016/0550-3213(93)90398-9, hep-ph/9211321.
- [151] Marco Ciuchini, E. Franco, G. Martinelli, L. Reina, The  $|\Delta S| = 1$  effective Hamiltonian including next-to-leading order QCD and QED corrections, Nucl. Phys. B 415 (1994) 403–462, doi:10.1016/0550-3213(94)90118-X, hep-ph/9304257.
- [152] Martin Gorbahn, Ulrich Haisch, Effective Hamiltonian for non-leptonic  $|\Delta F| = 1$  decays at NNLO in QCD, Nucl. Phys. B 713 (2005) 291–332, doi:10.1016/j.nuclphysb.2005.01.047, hep-ph/0411071.
- [153] Mikhail A. Shifman, M. B. Voloshin, Preasymptotic Effects in Inclusive Weak Decays of Charmed Particles, Sov. J. Nucl. Phys. 41 (1985) 120.
- [154] Valery A. Khoze, Mikhail A. Shifman, N. G. Uraltsev, M. B. Voloshin, On Inclusive Hadronic Widths of Beautiful Particles, Sov. J. Nucl. Phys. 46 (1987) 112.
- [155] Alexander Lenz, Ulrich Nierste, Theoretical update of  $B_s$ - $\bar{B}_s$  mixing, JHEP 06 (2007) 072, doi:10.1088/1126-6708/2007/06/072, hep-ph/0612167.
- [156] M. Beneke, G. Buchalla, C. Greub, A. Lenz, U. Nierste, Next-to-leading order QCD corrections to the lifetime difference of  $B_s$  mesons, Phys. Lett. B 459 (1999) 631–640, doi:10.1016/S0370-2693(99)00684-X, hep-ph/9808385.

- [157] Martin Beneke, Gerhard Buchalla, Alexander Lenz, Ulrich Nierste, CP Asymmetry in Flavor Specific B Decays beyond Leading Logarithms, Phys. Lett. B 576 (2003) 173–183, doi:10.1016/j.physletb.2003.09.089, hep-ph/0307344.
- [158] J. S. Hagelin, Mass Mixing and CP Violation in the  $B^0 - \bar{B}^0$  system, Nucl. Phys. B 193 (1981) 123–149, doi:10.1016/0550-3213(81)90521-6.
- [159] E. Franco, Maurizio Lusignoli, A. Pugliese, Strong Interaction Corrections to CP Violation in  $B^0 - \bar{B}^0$  Mixing, Nucl. Phys. B 194 (1982) 403, doi:10.1016/0550-3213(82)90018-9.
- [160] Ling-Lie Chau, Quark Mixing in Weak Interactions, Phys. Rept. 95 (1983) 1–94, doi:10.1016/0370-1573(83)90043-1.
- [161] A. J. Buras, W. Slominski, H. Steger,  $B^0 - \bar{B}^0$  Mixing, CP Violation and the B Meson Decay, Nucl. Phys. B 245 (1984) 369–398, doi:10.1016/0550-3213(84)90437-1.
- [162] A. Datta, E. A. Paschos, U. Turke, Are There  $B_s$  Mesons With Two Different Lifetimes?, Phys. Lett. B 196 (1987) 382–386, doi:10.1016/0370-2693(87)90753-2.
- [163] A. Datta, E. A. Paschos, Y. L. Wu, On the Lifetime Difference of the  $B_s$  Mesons and Its Experimental Detection, Nucl. Phys. B 311 (1988) 35–45, doi:10.1016/0550-3213(88)90142-3.
- [164] M. Ciuchini, E. Franco, V. Lubicz, F. Mescia, C. Tarantino, Lifetime differences and CP violation parameters of neutral B mesons at the next-to-leading order in QCD, JHEP 08 (2003) 031, doi:10.1088/1126-6708/2003/08/031, hep-ph/0308029.
- [165] Marvin Gerlach, Ulrich Nierste, Vladyslav Shtabovenko, Matthias Steinhauser, Two-loop QCD penguin contribution to the width difference in  $B_s - \bar{B}_s$  mixing, JHEP 07 (2021) 043, doi:10.1007/JHEP07(2021)043, 2106.05979.
- [166] Marvin Gerlach, Ulrich Nierste, Vladyslav Shtabovenko, Matthias Steinhauser, The width difference in  $B - \bar{B}$  mixing at order  $\alpha_s$  and beyond, JHEP 04 (2022) 006, doi:10.1007/JHEP04(2022)006, 2202.12305.
- [167] H. M. Asatrian, Artyom Hovhannисyan, Ulrich Nierste, Arsen Yeghiazaryan, Towards next-to-next-to-leading-log accuracy for the width difference in the  $B_s - \bar{B}_s$  system: fermionic contributions to order  $(m_c/m_b)^0$  and  $(m_c/m_b)^1$ , JHEP 10 (2017) 191, doi:10.1007/JHEP10(2017)191, 1709.02160.
- [168] Hrachia M. Asatrian, Hrachya H. Asatryan, Artyom Hovhannисyan, Ulrich Nierste, Sergey Tumasyan, Arsen Yeghiazaryan, Penguin contribution to the width difference and CP asymmetry in  $B_q - \bar{B}_q$  mixing at order  $\alpha_s^2 N_f$ , Phys. Rev. D 102 (3) (2020) 033007, doi:10.1103/PhysRevD.102.033007, 2006.13227.
- [169] Artyom Hovhannисyan, Ulrich Nierste, Addendum to: Towards next-to-next-to-leading-log accuracy for the width difference in the  $B_s - \bar{B}_s$  system: fermionic contributions to order  $(m_c/m_b)^0$  and  $(m_c/m_b)^1$ , JHEP 06 (2022) 090, doi:10.1007/JHEP06(2022)090, 2204.11907.
- [170] Marvin Gerlach, Ulrich Nierste, Vladyslav Shtabovenko, Matthias Steinhauser, Width Difference in the  $B - \bar{B}$  System at Next-to-Next-to-Leading Order of QCD, Phys. Rev. Lett. 129 (10) (2022) 102001, doi:10.1103/PhysRevLett.129.102001, 2205.07907.
- [171] Marvin Gerlach, Ulrich Nierste, Pascal Reeck, Vladyslav Shtabovenko, Matthias Steinhauser, Current-current operator contribution to the decay matrix in  $B$ -meson mixing at next-to-next-to-leading order of QCD (2025), 2505.22740.
- [172] M. Beneke, G. Buchalla, I. Dunietz, Width Difference in the  $B_s - \bar{B}_s$  System, Phys. Rev. D 54 (1996) 4419–4431, doi:10.1103/PhysRevD.54.4419, [Erratum: Phys.Rev.D 83, 119902 (2011)], hep-ph/9605259.
- [173] CKMfitter Group (J. Charles et al.), updated results and plots available at: <http://ckmfitter.in2p3.fr>, Eur. Phys. J C41 (2005) 1–131, hep-ph/0406184.
- [174] Sandrine Laplace, Zoltan Ligeti, Yosef Nir, Gilad Perez, Implications of the CP asymmetry in semileptonic B decay, Phys. Rev. D 65 (2002) 094040, doi:10.1103/PhysRevD.65.094040, hep-ph/0202010.
- [175] Christoph Bobeth, Ulrich Haisch, New Physics in  $\Gamma_{12}^s$ : ( $\bar{s}b$ ) $(\bar{\tau}\tau)$  Operators, Acta Phys. Polon. B 44 (2013) 127–176, doi:10.5506/APhysPolB.44.127, 1109.1826.
- [176] Christoph Bobeth, Ulrich Haisch, Alexander Lenz, Ben Pecjak, Gilberto Tetlalmatzi-Xolocotzi, On new physics in  $\Delta\Gamma_d$ , JHEP 06 (2014) 040, doi:10.1007/JHEP06(2014)040, 1404.2531.
- [177] Andrzej J. Buras, Diego Guadagnoli, Correlations among new CP violating effects in  $\Delta F = 2$  observables, Phys. Rev. D 78 (2008) 033005, doi:10.1103/PhysRevD.78.033005, 0805.3887.
- [178] Seungyeob Jwa, Jeehun Kim, Sunghee Kim, Sunkyu Lee, Weonjong Lee, Sungwoo Park (SWME), 2025 update on  $\epsilon_K$  in the Standard Model with lattice QCD inputs (2025), 2503.00351.
- [179] Y. Aoki, et al. (Flavour Lattice Averaging Group (FLAG)), FLAG Review 2024 (2024), 2411.04268.
- [180] Andrzej J. Buras, Diego Guadagnoli, Gino Isidori, On  $\epsilon_K$  Beyond Lowest Order in the Operator Product Expansion, Phys. Lett. B 688 (2010) 309–313, doi:10.1016/j.physletb.2010.04.017, 1002.3612.
- [181] Ziyuan Bai, Norman H. Christ, Joseph M. Karpie, Christopher T. Sachrajda, Amarjit Soni, Bigeng Wang, Long-distance contribution to  $\epsilon_K$  from lattice QCD, Phys. Rev. D 109 (5) (2024) 054501, doi:10.1103/PhysRevD.109.054501, 2309.01193.
- [182] Ulrich Nierste, Phenomenology of epsilon(K) in the top era, in: Workshop on K Physics 1996, hep-ph/9609310.
- [183] A. I. Vainshtein, Valentin I. Zakharov, V. A. Novikov, Mikhail A. Shifman, Processes of the Second Order in the Weak Interaction in Asymptotically Free Strong Interaction Theories, Yad. Fiz. 23 (1976) 1024–1031.
- [184] M. I. Vysotsky,  $K^0 - \bar{K}^0$  transition in the standard  $SU(3) \times SU(2) \times U(1)$  model, Sov. J. Nucl. Phys. 31 (1980) 797.
- [185] Jonathan M. Flynn, QCD Correction Factors for  $K^0 \bar{K}^0$  Mixing for Large Top Quark Mass, Mod. Phys. Lett. A 5 (1990) 877, doi:10.1142/S0217732900000962.
- [186] Martin Gorbahn, Sebastian Jäger, Sandra Kvedaraité, RI-(S)MOM to  $\overline{\text{MS}}$  conversion for  $B_K$  at two-loop order, JHEP 09 (2025) 011, doi:10.1007/JHEP09(2025)011, 2411.19861.
- [187] N. H. Christ, T. Izubuchi, C. T. Sachrajda, A. Soni, J. Yu (RBC, UKQCD), Long distance contribution to the  $K_L - K_S$  mass difference, Phys. Rev. D 88 (2013) 014508, doi:10.1103/PhysRevD.88.014508, 1212.5931.
- [188] Z. Bai, N. H. Christ, T. Izubuchi, C. T. Sachrajda, A. Soni, J. Yu,  $K_L - K_S$  Mass Difference from Lattice QCD, Phys. Rev. Lett. 113 (2014) 112003, doi:10.1103/PhysRevLett.113.112003, 1406.0916.
- [189] J. Charles, Andreas Hocker, H. Lackner, S. Laplace, F. R. Le Diberder, J. Malcles, J. Ocariz, M. Pivk, L. Roos (CKMfitter Group), CP violation and the CKM matrix: Assessing the impact of the asymmetric B factories, Eur. Phys. J. C 41 (1) (2005) 1–131, doi:10.1140/epjc/s2005-02169-1, updated results and plots available at: <http://ckmfitter.in2p3.fr>, hep-ph/0406184.
- [190] R. Sekhar Chivukula, Howard Georgi, Composite Technicolor Standard Model, Phys. Lett. B 188 (1987) 99–104, doi:10.1016/0370-2693(87)90713-1.
- [191] G. D'Ambrosio, G. F. Giudice, G. Isidori, A. Strumia, Minimal flavor violation: An Effective field theory approach, Nucl. Phys. B 645 (2002) 155–187, doi:10.1016/S0550-3213(02)00836-2, hep-ph/0207036.
- [192] Andrzej J. Buras, Piotr H. Chankowski, Janusz Rosiek, Lucja Sławińska, Correlation between  $\Delta M_s$  and  $B_{s,d}^0 \rightarrow \mu^+ \mu^-$  in supersymmetry at large  $\tan\beta$ , Phys. Lett. B 546 (2002) 96–107, doi:10.1016/S0370-2693(02)02639-4, hep-ph/0207241.
- [193] Gino Isidori, Paride Paradisi, Hints of large  $\tan(\beta)$  in flavour physics, Phys. Lett. B 639 (2006) 499–507, doi:10.1016/j.physletb.2006.06.071, hep-ph/0605012.

## 50 Meson-antimeson mixing

- [194] Martin Gorbahn, Sebastian Jager, Ulrich Nierste, Stephanie Trine, The supersymmetric Higgs sector and  $B - \bar{B}$  mixing for large  $\tan\beta$ , Phys. Rev. D 84 (2011) 034030, doi:10.1103/PhysRevD.84.034030, 0901.2065.
- [195] Andrzej J. Buras, Jennifer Girrbach, Stringent tests of constrained Minimal Flavor Violation through  $\Delta F = 2$  transitions, Eur. Phys. J. C 73 (9) (2013) 2560, doi:10.1140/epjc/s10052-013-2560-1, 1304.6835.
- [196] Andrzej J. Buras, Fulvia De Fazio, Jennifer Girrbach, Robert Knegjens, Minoru Nagai, The Anatomy of Neutral Scalars with FCNCs in the Flavour Precision Era, JHEP 06 (2013) 111, doi:10.1007/JHEP06(2013)111, 1303.3723.
- [197] Otto Eberhardt, Ulrich Nierste, Martin Wiebusch, Status of the two-Higgs-doublet model of type II, JHEP 07 (2013) 118, doi:10.1007/JHEP07(2013)118, 1305.1649.
- [198] Tetsuya Enomoto, Ryoutaro Watanabe, Flavor constraints on the Two Higgs Doublet Models of  $Z_2$  symmetric and aligned types, JHEP 05 (2016) 002, doi:10.1007/JHEP05(2016)002, 1511.05066.
- [199] Oliver Atkinson, Matthew Black, Alexander Lenz, Aleksey Rusov, James Wynne, Cornering the Two Higgs Doublet Model Type II, JHEP 04 (2022) 172, doi:10.1007/JHEP04(2022)172, 2107.05650.
- [200] Martin S. Lang, Ulrich Nierste,  $B_s \rightarrow \mu^+ \mu^-$  in a two-Higgs-doublet model with flavour-changing up-type Yukawa couplings, JHEP 04 (2024) 047, doi:10.1007/JHEP04(2024)047, 2212.11086.